The Modeling and Analysis of the Apoptotic BAD/tBID/BAK Pathway as a Chemical Reaction Network

Christopher Corey Howells

Dissertation submitted to the faculty of the Virginia Polytechnic Institute and State University in partial fulfillment of the requirements for the degree of

Doctor of Philosophy
In
Electrical Engineering

William T. Baumann
Carla V. Finkielstein
Michael S. Hsiao
Douglas K. Lindner
Daniel J. Stilwell

April 14, 2010
Blacksburg, VA

Keywords: chemical reaction network, mass-action, complex-balanced, apoptosis

The Modeling and Analysis of the Apoptotic BAD/tBID/BAK Pathway as a Chemical Reaction Network

Christopher Corey Howells

ABSTRACT

Apoptosis, or programmed cell death, is an essential process in all multi-cellular organisms. It is indispensable to an organism's survival, preventing the malicious propagation of DNA damage and pathogenic alterations, through the clean disposal of afflicted cells. The BAD/tBID/BAK pathway is a portion of the apoptosis molecular pathway, albeit an important pathway since it is known to be deregulated and lead to pathological ailments such as cancer.

Using chemical kinetics the BAD/tBID/BAK signaling pathway is modeled as a set of (nonlinear) ordinary differential equations. A first-cut numerical analysis reveals a mechanism where BAD sensitizes a switch from tBID activation to BAK activation. The phosphorylation of BAD is shown to inhibit this sensitizing effect. All behaviors are supported by experimental data, thereby validating the model of the BAD/tBID/BAK pathway. Moreover, modeling the phosphorylation of BAD as one of two modes, some conflicting experimental data about BAD's phosphorylation can be studied.

Parameter values (in this case the kinetic rate constants) are prone to error or missing altogether. Chemical reaction network theory, however, provides a theoretical approach to complement the initial numerical analysis without having to specify rate constant values. We extend the global asymptotic stability and robustness results in [92] to include any complex-balanced mass-action network. This enables us to study the BAD/tBID/BAK signaling network by breaking it into two sub-networks: one with BAD and tBID, and the other with tBID and BAK.

The complex-balanced BAD/tBID sub-network is shown to possess a unique steady state which is globally asymptotically stable. This verifies the simple and dynamically well-behaved exchange of BAD for Bcl-2 proteins which guard against tBID activation. The second sub-network, tBID/BAK, is formulated as a complex-balanced network with a perturbation representing the reaction of tBID catalyzing the activation of BAK. Our theoretical results produce a non-conservative, though state-dependent, condition which can be used to prove global convergence to a neighborhood of the unperturbed steady state. We then illustrate the biological importance of the result for tBID/BAK sub-network with an example design for a drug delivery system.

TABLE OF CONTENTS

LIST OF FIGURES

LIST OF TABLES

1 Introduction

1.1 Introduction

Apoptosis, or programmed cell death, is an essential process in all multi-cellular organisms. It is indispensable to an organism's development, adaptation, and maintenance. In particular, apoptosis prevents the propagation of the malicious effects of damaged DNA, free radicals, growth-factor deprivation, and pathogens like viruses and bacteria, so that other cells may remain healthy. There are two main biological pathways in apoptosis: the intrinsic pathway and the extrinsic pathway. These are both illustrated in Fig. 1.1. Roughly speaking, the intrinsic pathway of apoptosis is mitochondria-dependent and the extrinsic pathway is not. Through the sequential release of proteins that are normally held sequestered or inactive in the cell, an apoptotic signal can flow downstream through one or both of these pathways. These pathways converge at a point where executioner proteins called caspases are activated (see Fig. 1.1). Activation of these caspases is considered the point-of-no-return for a cell. That is, if these caspases are activated, and no anti-apoptotic signals intervene, the cell will ultimately be destroyed.

Many of the molecules involved in the apoptosis pathway cannot be definitively labeled as pro- or anti-apoptotic since they are involved in several different reactions and/or undergo several property-changing modifications. Sometimes these changes occur at the transcriptional level and other times at the post-translational level [1-3]. For example, one of the earliest discovered apoptosis proteins, Bcl-2, an otherwise anti-apoptotic protein, becomes inert and no longer anti-apoptotic when it is cleaved by caspase-3 [4-6]. Furthermore, apoptosis proteins are frequently controlled by toxic organisms like viruses, bacteria, and parasitic protozoa, which can affect the concentrations of these proteins [9, 11-12]. In other cases apoptosis proteins are de-regulated by the cell itself, which is what happens when a cell turns cancerous [7, 8, 10].

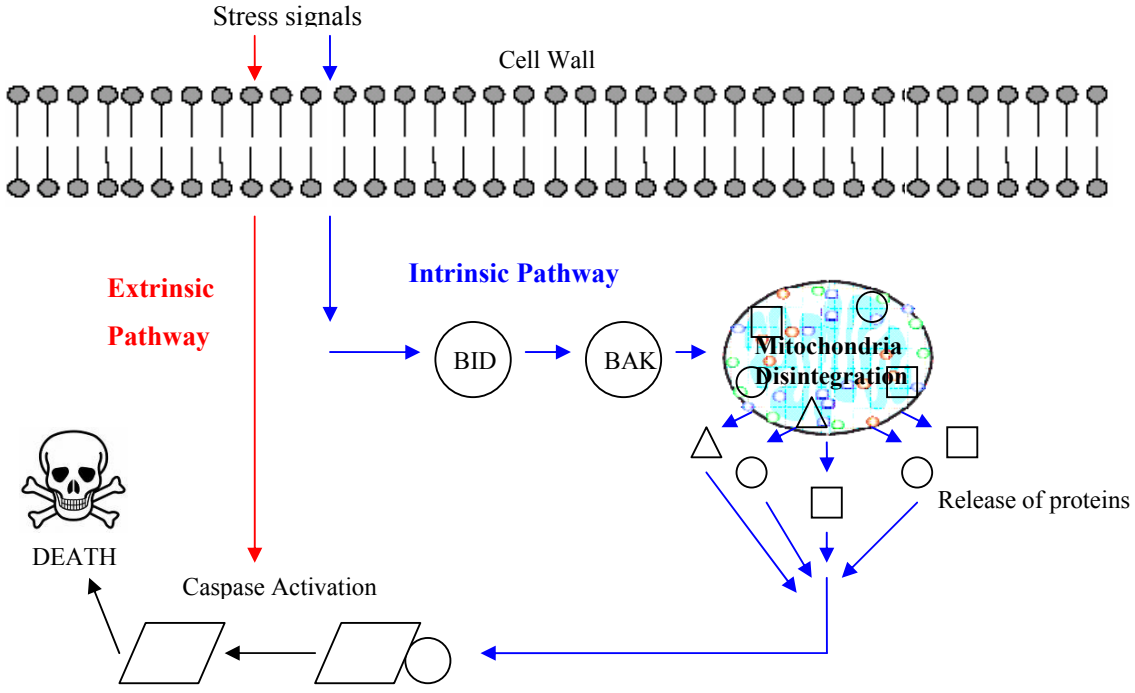

FIGURE 1.1 The apoptosis signaling network illustrating the intrinsic and extrinsic pathways

1.2 Motivation

The BH3-only proteins, well-known signaling molecules in the intrinsic pathway of apoptosis, quite often become pathological targets due to their ability to trigger apoptosis responses once certain thresholds of activation have been compromised. Notably, abnormally high levels of BAD (**B**cl-2-**a**ssociated **d**eath promoter) and BID (**B**H3-**i**nteracting **d**omain death agonist)—together or acting singly—can cause a healthy cell to become inappropriately apoptotic [9, 13-17]. This is because active BAD and BID can trigger the polymerization of BAK (**B**cl-2 **a**ntagonistic **k**iller) and BAX (**B**cl-2-**a**ssociated **x** protein) and lead to the disintegration of the mitochondria [12, 18-20]. As shown in Fig. 1.1, mitochondrial disintegration precedes the activation of the executioner caspases.

Due to the complexity of the apoptosis signaling pathway, as well as the potential therapeutic value that can be acquired through its disentanglement, it becomes important to introduce mathematical models. Many processes associated with BID [85-87] have been modeled in the past, but many of these models have neglected or abstracted the effects of BAD [85]. What is generally missing from these models is a description of how pro-survival signals (sometimes arriving from outside the cell) lead to the partial or complete inactivation of BAD. In this paper, we propose a novel model that includes this inactivation of BAD and how its inactivation is accomplished through phosphorylation processes and molecular chaperoning. Although experimental data about BAD is still lacking, an initial model can be developed and an assessment of the effects of BAD on BID, as well as on downstream events, can be undertaken. In particular, we investigate the interactions of BAD and BID in conjunction with the downstream events involving BAK. This model will be known as the BAD/tBID/BAK network model (where tBID, or **t**runcated BID, is the specific form of BID that must be incorporated into the model).

From a controls perspective, there are many ways biological systems resemble classical control systems, and likewise, there are many ways they differ, requiring adapted (and sometimes new) techniques. Techniques for the analysis of cellular processes are no different, often spanning from nonlinear optimization and numerical techniques to theoretical and graphical-dependent methods. After researching various methods of handling the BAD/tBID/BAK signaling network, always keeping in mind the current biological understanding of this particular network, we arrive to the conclusion that we require a biochemical method which exploits the network's graphical properties and stoichiometry, and which more loosely depends on the particular values of the chemical kinetic constants, which are a cellular network's system parameters. Mathematically, we will derive a set of differential equations which characterizes the static and dynamic behavior of the network, but these equations will include a set parameters which, according to the biological literature, are unknown or uncertain at best (again these are called the kinetic rate constants). Even for well-experimented and well-documented signaling networks this is often the case.

Hence, even though we would like to make an initial analysis of the BAD/tBID/BAK through selecting rate constant values and using familiar tools (simulation, bifurcation and sensitivity analysis), we require a more general approach to complement our work. Fortunately, certain chemical engineering techniques familiar to the design of chemical reactors can provide us with a way to do this. In fact, these techniques have already had recent success toward the analysis of several cellular signaling pathways [88-93]. Continuing along these lines, we are interested in knowing what these techniques can tell us about the BAD/tBID/BAK network.

Much of chemical reactor theory stems back to the works of Feinberg, Horn, and Jackson in the early 1970's [95-100]. Their work enables a chemical reaction network designer or analyst to conclude the existence, uniqueness, and stability of certain chemical reaction networks provided they satisfy certain graphical and stoichiometric constraints. More importantly, almost all of these conditions do not require selection of specific rate constant values. Interestingly, part of our network

will satisfy the graphical and stoichiometric constraints and hence will be a straightforward application. However, the remaining part of our network will not and so motivates us to extrapolate the theory to include this part. We will find that this is possible, so not only will be able to apply the result to our network but we will have developed theory which applies to *any* given network satisfying similar graphical and stoichiometric constraints.

1.3 Literature Review of Mathematical and Computer-aided Modeling of Biological Systems

1.3.1 Computer-aided approaches

Biological systems are usually large interconnected networks consisting of several species, which can include proteins, genes, and transcription factors. Because of the immensity of these networks a modeler or designer can be faced with multi-scale aspects in time and space. Complex networks, for example, can induce hundreds of differential equations (called kinetic equations) and system parameters (called kinetic rate constants) which span several orders of magnitude, and which can make systems stiff and difficult to integrate without extensive computational effort [57]. Many software packages have been created out of the need to handle these enormous sets of biologically-derived equations. Most of these packages share many similarities with more standard numerical packages, providing user-friendly environments for quick programming of simulations and sensitivity analyses. The biological-specific packages are generally faster, however, due to the additional customized programming, which can include modified integration techniques and inclusion of biological properties such as conservation and stoichiometry. For example, CellSim, a multi-analytic tool for the analysis of kinetic and spatio-temporal models, introduces automated computations of Jacobian and Hessian terms (as well as sparse linear algebraic computations for integration steps) to enhance its speed of integration [58-60]. In conclusion, biological systems can be tackled more efficiently and effectively, permitting a bio-analyst to focus more on functionality rather than numerical technique.

Biological networks often lack detailed specifications and consequently one must rely on a mixture of qualitative and quantitative data. In this instance, simulation and bifurcation analyses can provide a methodical approach to explore state and parameter spaces [61-62, 85-86]. Studies of the extrinsic pathway of apoptosis (depicted in Fig. 1.1) have lead [61] to investigate the mechanism with which extracellular signals lead directly to caspase activation. Using bifurcation and experimental data the work in [61] locate admissible regions of parameter space and identify a mathematical model which possesses the observed characteristics of the experimental model. Another example is a study on the intrinsic pathway, done in [85]. Again using bifurcation and experimental data, the work in [85] pinpoints a bistable toggle switch embedded within the BAX pathway. Many signaling pathways governing apoptosis have been experimentally and theoretically abstracted as bistable processes, generally incorporating a stable “life” steady state and a stable “death” steady state. In this case [85] uncovers the source of the bistability within the intrinsic pathway of apoptosis. Yet another example, sensitivity analysis is used to pinpoint system parameters which are responsible in deciding whether a cell moves predominantly along the intrinsic pathway or the extrinsic pathway shown in Fig. 1.1 [74]. What the researchers find is that the activation rate of caspase-8 (generally associated with the extrinsic pathway) in relation to the initial level of caspase-9 (generally associated with the intrinsic pathway) determines definitively whether the intrinsic or the extrinsic pathway of apoptosis is chosen.

Other numerical techniques to estimate biological system parameters rely on nonlinear optimization. Estimation is critical in study of biological system since many of the kinetic parameters (and even kinetic reaction rate laws) in any given biological system are uncertain or missing altogether. In [78], the cAMP pathway is analyzed. This pathway is an intracellular signaling pathway

which transmits the effects of hormones (glucagon, adrenaline) into the cell without penetrating the cell wall itself. One of the defining properties of the cAMP pathway is the presence of a stable limit cycle (when the state vector is assumed to be a vector of species' concentrations). The researchers identify sets of worst-case parameters (or kinetic rate constants), which, when perturbed, destabilize the limit cycle. This is done by minimizing a cost function with the help of hybrid optimization tools (combining local and global techniques). In turn, these parameters are compared to those given in experimental literature.

Sensitivity analyses, in particular, are also useful to quantify properties such as robustness. Essential cellular processes, such as apoptosis, must be robust against variations in the environment, against genetic mutations, as well as against other simultaneously occurring cellular processes. For example, [73] applies a direct finite-time Lyapunov exponent method to a caspase-8/caspase-3/XIAP pathway (a model for the extrinsic pathway of apoptosis) to delineate regions of phase space which exhibit high sensitivity to initial conditions. Roughly speaking, they do this by differentiating final trajectory positions with respect to initial conditions. In this manner, a separatrix is located which splits the set of feasible trajectories into two qualitatively different subsets -- one which is fundamentally pro-apoptotic and another which is fundamentally anti-apoptotic. Naturally, the network's definiteness toward one of two types of trajectories implicates a robust mechanism.

Stochastic approaches have also provided much aid in the numerical analysis of biological systems. External excitations through the employment of stochastic differential equations (SDEs). or Monte Carlo techniques, provide invaluable information regarding network structure and more qualitative attributes or as a way to include *in vivo* and *in vitro* statistical data (which can vary widely over cell lines) [66, 87]. In particular, stochastic chemical dynamics arise out of the randomness inherently associated with molecular collisions and the formation and destruction of chemical bonds. This is especially relevant in cellular networks where only a small number of molecules are known to exist (which is the case in many gene-transcription factor networks). The well-known Gillespie algorithm circumvents this problem [67]. In this method, each reaction has associated with it a probability that is proportional to the number of molecules of each reactant. Then discrete time trajectories are generated by randomly executing these reactions and randomly choosing time steps, where at each time step if a reaction is executed, molecules are exchanged according to the stoichiometry of the reaction. For example, if at some random time the reaction $A + B \to C$ is executed, then both species A and species B lose 1 molecule and species C gains 1 molecule.

1.3.2 Theoretical approaches

The mathematical treatment of biological networks has instinctively turned toward a systems approach -- that is, toward constructing cascades and feedbacks of elementary modules. Whereas simulation, bifurcation analyses, and nonlinear optimization techniques are certainly useful to explore the state and parameter spaces of biochemical networks, technology has not yet advanced to the point where we can experimentally validate the kinetic rate laws or even the values of kinetic rate constants. Hence, a "decomposition then reconnection" approach toward the study of biochemical networks has begun to emerge [79]. Attempts at creating elementary modules stem back to the Goldbeter-Koshland switch [77]. There, the researchers characterize and support phosphorylation processes as modular structures, arguing that these phosphorylation reactions are ubiquitous cascading signaling pathways within cells. From their analyses, they coined the concept of ultrasensitivity, which is a general term describing any robust switch process (which, in their case, was a consequence of the saturation of enzymes).

More recently, modularity in biological systems has taken the form of monotone systems (whose flows are characterized by preservation of a partial ordering) [80-81]. In these studies, a biological re-interpretation of the small-gain theorem has been derived using monotone theory. This can help gauge

the strength of naturally-occurring inhibitory feedbacks like the MAPK cascade (which is yet another cellular signaling pathway that uses phosphorylation to relay signals from outside the cell to inside the cell) [82-83]. Positive feedback connections of monotone systems can also be used to study bistability and bio-switches. For example, the λ phage lysis-lysogeny switch characterizes a virus which exhibits two distinct properties: it can either hijack a cell and burst it open (lysis), or it can lay hidden within the cell undetected to duplicate whenever the cell divides (lysogeny) [84]. Perhaps the most attractive feature of constructing cascades/feedbacks of biological systems is the theory that can be applied if the system comprises cascades/feedbacks of *monotone* subsystems. Roughly speaking, a kinetic system is monotone if an increasing input produces consistent increases or decreases in the states of the system. If a system consists of a cascade or a feedback of monotone subsystems, and there exist static input/output characteristics (steady state data) for each of these subsystems, then stability and robustness properties can be ascertained for the original system. For example, one can deduce the number of steady states, the stability of these steady states, and the robustness against perturbations from these steady states. In fact these conclusions can be made without even having to know the kinetic rate constants or internal kinetics.

System identification theory has become widely used in the bio-mathematical community. This theory can be used to identify kinetic mechanisms and interaction graphs, as well as validate numerical identification methods, when there is little a priori knowledge regarding internal kinetics. Many of these theoretical notions are adaptations of methods used for classical nonlinear control systems. For example, [71] considers how state accessibility conditions of nonlinear systems can be reinterpreted and applied to biochemical models. In situations where the exchange dynamics (the dynamics associated with the inputs and outputs) are known but the kinetic dynamics (the dynamics associated with the internal reaction network) are unknown, one can quickly infer the number of controllable states using the power of Lie algebras. This theory becomes important in the design of drug delivery systems as well as when the convergence of parameter identification algorithms needs to be ensured.

In situations where quantitative data is non-existent, approaches in chemical engineering as we mentioned earlier can provide a means to study qualitative properties of biochemical networks. The mathematical frameworks created out the works of Feinberg, Horn, and Jackson [95-100], known as chemical reaction network theory (CRNT), enable a bio-modeler or analyst to capitalize on graphical properties and stoichiometry of a biochemical network while being less dependent on the selection of specific kinetic rate constants (and in some cases even the kinetic rate laws). Although their work was originally applied to chemical reactors, recently, chemical reaction network theory has been extended to the study of cellular signaling pathways. For example, it is used (and adapted) to study the global asymptotical stability and robustness of a T-cell kinetic proofreading model [92]. T-cells respond more selectively and more quickly upon contact with an antigen-presenting cell in a lock-and-key manner. (Cells have a way of holding out infectious and hazardous pathogens, much like a flag, for T-cells.) Their binding initiates a chain of reactions which modifies the T-cell receptor complex (i.e. the lock). This chain is modeled as a chemical reaction network, and because it satisfies certain graphical and stoichiometric conditions, global asymptotic stability can be proven. In addition, [92] qualifies the extent to which such a network can be perturbed by unmodeled dynamics before stability is no longer guaranteed. Such work will be continually called upon when we consider a similar situation for the stability and robustness of our biological network.

More control concepts such as detectability and input-to-state stability have also begun to emerge from chemical reaction network theory -- in particular with applications to cellular receptor-ligand signaling (which propagate signals from outside to inside the cell) [88-91]. For example, variations in temperature or concentrations of enzymes can cause kinetic rate constants in cellular signaling networks to slowly vary over time (such as in receptor-ligand networks). Using nonlinear input-to-stability concepts, [90-91] sets up a formalism so that one may characterize the robustness against such perturbations, and applies it to a receptor-ligand network. This network, as a chemical reaction network, satisfies the same graphical and stoichiometric criteria as the above-mentioned T-cell kinetic proofreading model. Again, circumventing the troublesome problem associated with lack of

experimental data, the work in [91] is able to rule out bifurcations and describe the nice movement of steady states for these types of networks when kinetic rate "constants" vary in time.

These input-to-state stability concepts also lend themselves to extending control concepts like state estimation [88], which theoretically could be useful in biological experimentation and biomedical engineering. For example, the monitoring of proteins via fluorescent labeling of molecules could be considered to be a biological sensor which, at least theoretically, could be used to infer the concentrations of states (proteins, molecules, ions) of a kinetic signaling system. [88] looks at the stability of observers, and their robustness to sensor and process noise, for the same kind of chemical reaction networks which were mentioned above. The global stability properties inherent in such networks permit the design of an observer which responds significantly better than Kalman and Luenberger observer types.

1.4 Contributions

What separates our work from the analyses of many of the apoptotic pathways already studied is the novel inclusion of BAD. In addition to illustrating the well-established switch-like signaling behavior from tBID to BAK, we will show how BAD acts as a sensitizer, and how this sensitivity is modulated via phosphorylation of BAD. Our mathematical model will validate the experimental model where tBID is an "activator" and BAD is an "enabler" [21]. Another distinction is our concern with basal operating conditions, that is, we look at conditions for the BAD/tBID/BAK network when the cell is perfectly healthy and non-apoptotic. Many apoptotic studies disregard this important aspect of a network, which, for our purposes, can be used to delineate regions of parameter space which must be satisfied in order to maintain these basal conditions.

The modeling of BAD is significant since, for example, BAD has the capacity to restore a cancerous cell to one which responds normally to apoptotic stimuli. That is, cancer cells are generally defined by overexpression of anti-apoptotic proteins such as Bcl-2 [10, 22] and do not respond appropriately to apoptotic signaling. Technology today has reached the point where man-made BID and BAD molecules can be fabricated as parts of a drug delivery system which can eradicate cancer cells through apoptosis [28, 54]. Unfortunately, the targeting of cancerous versus normal healthy cells is an ongoing challenge. Targeting cells with BID can inadvertently lead to the destruction of healthy cells which do not exhibit Bcl-2-overexpresson. On the other hand, BAD-targeting might be more effective since, as we will demonstrate in this paper, BAD does *not* have the capacity to trigger apoptosis, but instead lowers the threshold at which cells respond to apoptotic stimuli. In this manner, cancer cells would become appropriately apoptotic and healthy cells would be less likely to die inappropriately, thereby minimizing the effect of misguided treatments.

Our initial analysis of the BAD/tBID/BAK network, by selecting specific rate constants and using tools such as simulation, bifurcation analysis, and sensitivity analysis, will reveal and support the sensitization of BAD on the tBID-induction of BAK. Such techniques will validate our model with respect to experimental data as well as provide a methodical way to pose hypotheses about the phosphorylation of BAD, on which experimental data remains fuzzy and entangled. With our model we will be able to disentangle some of these discrepancies and explain why some researchers ventured into some potentially contradictory findings. Finally, our initial analysis will be used in conjunction with assumptions about basal (non-apoptotic) static operating conditions. This will lead to a constraint on the kinetic rate constants necessary to ensure that such basal conditions are satisfied.

We prove a novel result in the study of chemical reaction network theory, generalizing the stability and robustness result in [92] to include *any* complex-balanced chemical reaction network (which would include any zero-deficiency mass-action network considered in [92]). This will come in the form of Theorem 1 (and Lemma 1) in Chapter 5. In particular, the result states that any complex-

balanced network is globally asymptotically stable (if there are no boundary equilibria) and furthermore this stability is retained against certain state-dependent perturbations which preserve the stoichiometric properties of the network. Moreover, the construction of the proof of Lemma 1 will provide an explicit formula to estimate stability-preserving perturbations.

We then apply our result to the two sub-networks of the BAD/tBID/BAK pathway, one which incorporates the reactions among the states of BAD and tBID (called the BAD/tBID network), and another which incorporates the reactions among the states of tBID and BAK (called the catalyzed tBID/BAK network). Straightforward application of our result will show that a complex-balanced BAD/tBID network is globally asymptotically stable. Application of our result to the catalyzed tBID/BAK network will generate a state-dependent condition under which we can also state global asymptotic stability. However, through further manipulation, we will be able to derive a more biologically-meaningful condition under which the activation of BAK, which directly activates the intrinsic pathway of apoptosis, is blocked. In either case, we will be able to make definitive claims regarding the static and dynamic behavior of the two sub-networks without actually specifying kinetic rate constants.

1.5 Plan of Attack

The plan of attack will 2-pronged. First, we shall explore the behavior of the BAD/tBID/BAK network using simulation, bifurcation analysis, sensitivity analysis, and explicit formulations derived from an approximate model known as the "skeleton" model. This will be done in Chapter 3 after we extract from the biology our full model of the BAD/tBID/BAK pathway in Chapter 2. Analysis of the full and skeleton models will give us a first-cut description of the basal and transient activities of the network, as well as a means for model verification.

Stripping this simplistic mechanism down to a skeleton model enables us to solve it explicitly in terms of symbolic rate constants and, subsequently, permits us to approximate the effects of BAD on tBID-induced activation of BAK. These equations will also be used to motivate hypotheses explaining some of the inconsistencies regarding the phosphorylation of BAD. Finally, these equations will provide us with a concrete means to delineate regions of parameter space in which it is possible to maintain basal (or non-apoptotic) conditions.

Second, we will turn toward chemical reactor theory, introduced in Chapter 4, to shed more light on the BAD/tBID/BAK network. Although the skeleton model provides a way to circumvent the problem of unknown rate constants, it lacks many of the nonlinear dependencies and detailed interactions inherent in the BAD/tBID/BAK network. Chemical reactor theory will enable us to include these nonlinearities without restricting attention to specific rate constants. This will lead to the development of our own theorem (and lemma) in Chapter 5 to handle the BAD/tBID/BAK network (or any network which satisfies the same graphical and stoichiometric constraints). In Chapter 6, we apply our theoretical results to the BAD/tBID/BAK by splitting it into two sub-networks: the BAD/tBID network and the catalyzed tBID/BAK network. Finally, in Chapter 7, we will consider what our results mean to the biologist and what could theoretically be done to treat pathological deregulations of the BAD/tBID/BAK network.

2 Biology and Derivation of Kinetic Equations for the BAD/tBID/BAK Network

2.1 Biological Network

Fig. 2.1 illustrates the biochemical reactions and processes among BAD, tBID, BAK, and Bcl-2 considered in this paper. Below, we give a detailed description of the current biological understanding of the signaling pathway. (The kinetic modeling of the reactions will be handled in the next section.) The network shown in Fig. 2.1 will be known as the BAD/tBID/BAK pathway. It is important to stress that even though Bcl-2 is a specific anti-apoptotic protein, in this paper we will assume that it represents either Bcl-2 or Bcl-x_L, the latter of which is another anti-apoptotic protein with only subtle differences from Bcl-2. In general, many of the behaviors of Bcl-2 and Bcl-x_L are very similar in regards to the BAD/tBID/BAK pathway, and reference to one or either of these proteins can be interchanged. This is what is usually done in many apoptosis models [85-87]. In our analysis, however, it will be useful to expand upon one of their subtle differences -- the qualitatively different impacts the proteins have upon the phosphorylation of BAD. We will make explicit reference to the specific protein under investigation when this is considered. In a much similar manner BAK is a specific protein but will be used to represent either BAK or BAX.

2.1.1 Bcl-2 heterodimerization and displacement process

In its free unbound form, the pro-apoptotic protein tBID is considered to be active since it can catalyze the activation of the pro-apoptotic protein BAK. tBID does this by directly inducing a conformational change in BAK, which drives its polymerization (that is, its formation into polymers) [19, 24-26]. BAK is considered to be active once the conformational change induced by tBID has taken place. However, Bcl-2 is an anti-apoptotic protein which prevents the activation of proteins like tBID and BAK through a process known as heterodimerization [22]. In heterodimerization, 1 molecule of Bcl-2 pairs up with 1 molecule of unbound tBID (or unbound BAK) to form one heterodimer molecule, which will be written tBID:Bcl-2 (or BAK:Bcl-2). This process is a sequestration process since as heterodimers, tBID can no longer catalyze BAK, and similarly, BAK can no longer oligomerize into polymers. Hence, tBID and BAK are no longer considered to be active once they become bound to Bcl-2.

Whereas tBID:Bcl-2 is considered to be the inactive form of tBID, BAD:Bcl-2 is considered to be the active form of the pro-apoptotic protein BAD [21-23]. This is because BAD, unlike tBID, cannot directly induce the activation of BAK but instead must steer the biological network toward apoptosis by displacing Bcl-2 from tBID [23, 27-28]. That is, BAD works in a pro-apoptotic manner by preventing Bcl-2 from inactivating tBID -- so that ultimately more tBID can be active. This is why BAD is often referred to as a "sensitizer" or an "enabler" [21, 85].

In Fig. 2.1, we observe the Bcl-2 heterodimerization reactions and displacement process occurring in the mitochondria. The former are indicated by the double-headed arrows between the Bcl-2-bound complex and the corresponding unbound pro-apoptotic protein (BAD, tBID, BAK) and a connecting arrow with free Bcl-2. This type of graphical representation is common in the description of reversible binding reactions. The displacement process is indicated by the intersection of two arrows emanating from BAD_m and tBID:Bcl-2, where at the intersection point we have two different arrows leaving and moving towards BAD:Bcl-2 and tBID. Although this process is assumed reversible as well (that is, Bcl-2 displaced by tBID), we have only indicated in Fig. 2.1 the dominant direction, which is the displacement of Bcl-2 by BAD.

2.1.2 The phosphorylation, dephosphorylation, and mitochondria-targeting of BAD

BAD is sequestered and deactivated by phosphorylation. The phosphorylation of BAD, and how growth and survival signals lead to its inactivation (that is, its removal from the complex BAD:Bcl-2), has been given recent attention in cellular biology but remains to be clarified. Below, we review some of the current biological understandings regarding the phosphorylation of BAD, keeping in mind that many of these findings are fragmented or contradictory.

Current research has established three critical sites of phosphorylation for BAD—Ser^{112}, Ser^{136}, and Ser^{155} [29-32]. Although phosphorylation at any of these sites results in BAD being phosphorylated, as we shall discuss, there are many differences to be noted. Phosphorylation of Ser^{112} or Ser^{136} is known to induce a conformational change in BAD such that a consensus binding site for 14-3-3, a kind of molecular chaperone, is made available [21, 33-34]. In such cases, 14-3-3 sequesters BAD to the cytoplasm, preventing BAD's interaction with Bcl-2 (who tends to be localized to the mitochondria). Ser^{155} kinases phosphorylate BAD within its BH3 domain, blocking the ability of BAD to effectively bind Bcl-2. In this case, the chaperoning via 14-3-3 is unnecessary since BAD is already secured from activation regardless of whether BAD remains in the mitochondria or not (though 14-3-3 binding and chaperoning can still occur if BAD is further phosphorylated at Ser^{112} or Ser^{136}).

There are also phosphatases which can dephosphorylate BAD once it is phosphorylated. The most well-known is the Ca^{2+}-stimulated phosphatase calcineurin, which can dephosphorylate any of the above-mentioned phosphorylation sites (as well as remove 14-3-3 from BAD) [14, 16, 34-35]. If left unphosphorylated, or has been recently dephosphorylated, BAD can target the mitochondria or cytoplasm without any help from chaperoning molecules [21].

Generally, phosphorylation of BAD occurs while BAD is in its free unbound form. However, it is recently suggested that whenever BAD is bound to Bcl-x_L (not Bcl-2) in the mitochondria, phosphorylation can induce the dissociation of the BAD:Bcl-x_L complex [21, 29, 31, 33, 36-37, 39]. However, it is unclear in what way(s) this is done. The experiments in [37] and [33] demonstrate the process as a simple consequence of Ser^{112} or Ser^{136} phosphorylation. On the other hand, experiments in [31] demonstrate the interesting experimental result that dissociation is still possible even when the Ser^{112} and Ser^{136} sites are replaced with unphosphorylatable mutations. In further contrast, experiments in [36] and [21] suggest that Ser^{155} phosphorylation must follow Ser^{136} phosphorylation to trigger dissociation (though, oddly in other experiments in [36], Ser^{155} phosphorylation is shown to work independently of Ser^{112} and Ser^{136} phosphorylations). Finally, at a completely different extreme, *in vitro* experiments in [40] indicate that Ser^{136} and Ser^{155} phosphorylations are not even possible when BAD is complexed with Bcl-x_L.

Fig. 2.1 graphically depicts our assumed three routes of phosphorylation (not to be mistaken with the three sites of phosphorylation). These are indicated by three arrows leaving BAD, BAD_m, and BAD:Bcl-2 and terminating at pBAD. We assume that these phosphorylations are irreversible in the sense that phosphorylated BAD (pBAD) must first bind 14-3-3 (to form pBAD:14-3-3) prior to any kind of dephosphorylation. This is consistent with the findings in [21], which demonstrate that once pBAD binds 14-3-3 (which they hypothesize to occur in the mitochondria as well as in the cytoplasm), the pBAD:14-3-3 complex must first reach the plasma membrane before dissociation, and therefore dephosphorylation, can occur. Even though 14-3-3 binding may not always be the reaction which immediately follows phosphorylation (as we said before, Ser^{155} phosphorylation may work independently of 14-3-3 chaperoning) our model does serve to illustrate how the phosphorylation of BAD provides a temporary removal (or prevention) of BAD activation in the mitochondria. Hence, we incorporate this chaperoning process into our network by assuming the arrow from pBAD to

pBAD:14-3-3 is a single-headed arrow, that is, we assume the reaction from pBAD to pBAD:14-3-3 is an irreversible process. Note that the reaction from pBAD:14-3-3 to cytoplasmic BAD is also assumed irreversible, since in a way we already incorporating the reverse reaction, which is phosphorylation. Finally, the cytoplasmic- and mitochondria-targeting of free unphosphorylated BAD is indicated with a double-headed arrow between BAD and BAD_m.

2.1.3 Activation and polymerization of BAK

Active tBID induces the activation and hence polymerization of BAK (e.g., into tetramers [20, 41]), forming pores through which lethal constituents are released into the cytosol [20, 18-19]. Since tBID, much like an enzyme, catalyzes the activation of BAK [19], we have drawn a dotted arrow leaving tBID and terminating at the double-headed arrow between BAK_{inac} and BAK (which is the active form of BAK). In other words, tBID drives the reaction of inactive BAK to active BAK but is not consumed in the process. This process is seen more explicitly in Table 2.1 which summarizes the reactions of the BAD/tBID/BAK network pictorially represented in Fig. 2.1. Like BAD, active BAK can associate with Bcl-2 as well as displace Bcl-2 from tBID [23, 42-46]. Fig. 2.1 illustrates this second displacement process in a manner similar to what was done for the first one involving BAD. Finally, the four lines connected to the double-headed arrow between BAK and BAK_{poly} are used to indicate the polymerization process where four molecules of active BAK cluster together to form one tetramer molecule, BAK_{poly}.

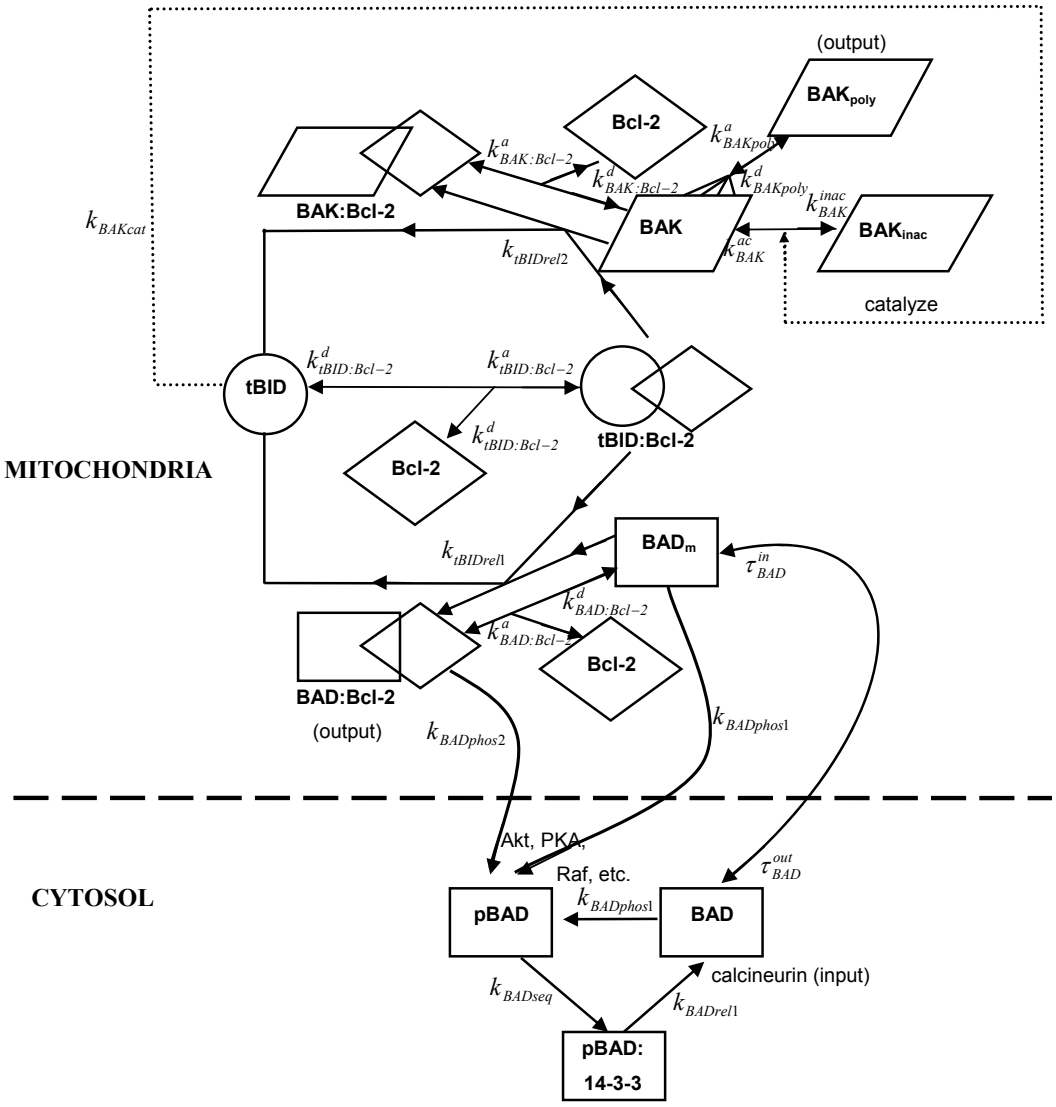

FIGURE 2.1 BAD/tBID/BAK network. Post-translational network showing the reactions and states among BAD (rectangles), tBID (circles), BAK (parallelograms), and Bcl-2 (diamonds). The dotted arrow refers to the up-regulation of BAK via tBID. Curved arrows indicate re-localization processes between the cytosol and mitochondria (lumped together as one big mitochondrion). Since calcineurin triggers the release of BAD from sequestration, it will sometimes be thought of as the "input". Likewise, since polymerized BAK leads to the disintegration of the mitochondria, it will be thought of as the "output".

TABLE 2.1 Summary of the reactions and rate constant assignments for the BAD/tBID/BAK network.

Reaction	Forward Rate Constant	Backward Rate Constant
$BAD \rightarrow pBAD$	$k_{BADphos1}$	
$BAD_m \rightarrow pBAD$	$k_{BADphos1}$	
$pBAD \rightarrow pBAD:14\text{-}3\text{-}3$	k_{BADseq}	
$pBAD:14\text{-}3\text{-}3 \rightarrow BAD$	$k_{BADrel1}$	
$BAD \leftrightarrow BAD_m$	τ_{BAD}^{in}	τ_{BAD}^{out}
$BAD_m + Bcl\text{-}2 \leftrightarrow BAD:Bcl\text{-}2$	$k_{BAD:Bcl-2}^{a}$	$k_{BAD:Bcl-2}^{d}$
$BAD:Bcl\text{-}2 \rightarrow pBAD + Bcl\text{-}2$	$k_{BADphos2}$	
$BAD_m + tBID:Bcl\text{-}2 \leftrightarrow tBID + BAD:Bcl\text{-}2$	$k_{tBIDrel1}$	$k_{BADrel2}$
$tBID + Bcl\text{-}2 \leftrightarrow tBID:Bcl\text{-}2$	$k_{tBID:Bcl-2}^{a}$	$k_{tBID:Bcl-2}^{d}$
$BAK_{inac} \leftrightarrow BAK$	k_{BAK}^{ac}	k_{BAK}^{inac}
$BAK_{inac} + tBID \rightarrow BAK + tBID$	k_{BAKcat}	
$BAK + Bcl\text{-}2 \leftrightarrow BAK:Bcl\text{-}2$	$k_{BAK:Bcl-2}^{a}$	$k_{BAK:Bcl-2}^{d}$
$BAK + tBID:Bcl\text{-}2 \leftrightarrow tBID + BAK:Bcl\text{-}2$	$k_{tBIDrel2}$	$k_{BAKrel1}$
$4\ BAK \leftrightarrow BAK_{poly}$	$k_{BAKpoly}^{a}$	$k_{BAKpoly}^{d}$

2.2 Kinetic Equations for the BAD/tBID/BAK Network

Since the (mass-action) kinetic modeling of the reactions between tBID and BAX has already been established in literature [85], we assimilate their kinetic equations into our BAD/tBID/BAK differential equations. What remains is the (mass-action) kinetics associated with the different states of BAD. Once defined, we will have a set of nonlinear ordinary differential equations, which by itself, completely defines the biochemical relationship of BAD, tBID, and BAK. This will be the model which is considered in this paper.

2.2.1 Kinetic rate laws for the different states of BAD

To keep our model simple yet capable of addressing some of the phosphorylation discrepancies in experimental literature, we model the overall phosphorylation of BAD with two kinetics: one for the phosphorylation of unbound BAD (which can occur either in the cytoplasm or mitochondria); and one for the phosphorylation of Bcl-2-bound BAD (which induces the dissociation of BAD from Bcl-2). This is why in Table 2.1 we have the kinetic rate constant $k_{BADphos1}$ appearing alongside two reactions and $k_{BADphos2}$ appearing alongside only one reaction.

We apply the law of mass-action to the set of reactions listed in Table 2.1. A network endowed with mass-action kinetics is one wherein each reaction has a reaction rate which is proportional to the product of the reactant species' concentrations. This is a common technique in biological model derivation and has origins in molecular collision theory (later when we consider the BAD/tBID/BAK network as a chemical reaction network, we will see exactly how our model is derived from the set of

reactions in Table 2.1). The result is shown in (Eqs. 1-12), which defines our BAD/tBID/BAK system. Note that the brackets are used to represent concentration levels.

$$\frac{d}{dt}[\mathrm{BAD}] = k_{BADrel1}[\mathrm{pBAD:14\text{-}3\text{-}3}] + \tau^{out}_{BAD}[\mathrm{BAD_m}] - (k_{BADphos1} + \tau^{in}_{BAD})[\mathrm{BAD}] \tag{1}$$

$$\frac{d}{dt}[\mathrm{pBAD}] = k_{BADphos1}[\mathrm{BAD}] + k_{BADphos1}[\mathrm{BAD_m}] + k_{BADphos2}[\mathrm{BAD:Bcl\text{-}2}] - k_{BADseq}[\mathrm{pBAD}] \tag{2}$$

$$\frac{d}{dt}[\mathrm{pBAD:14\text{-}3\text{-}3}] = k_{BADseq}[\mathrm{pBAD}] - k_{BADrel1}[\mathrm{pBAD:14\text{-}3\text{-}3}] \tag{3}$$

$$\begin{aligned}\frac{d}{dt}[\mathrm{BAD_m}] = {} & \tau^{in}_{BAD}[\mathrm{BAD}] + k^{d}_{BAD:Bcl-2}[\mathrm{BAD:Bcl\text{-}2}] + k_{BADrel2}[\mathrm{tBID}][\mathrm{BAD:Bcl\text{-}2}] \\ & - (k_{BADphos1} + \tau^{out}_{BAD})[\mathrm{BAD_m}] - k^{a}_{BAD:Bcl-2}[\mathrm{BAD_m}][\mathrm{Bcl\text{-}2}] - k_{tBIDrel1}[\mathrm{BAD_m}][\mathrm{tBID:Bcl\text{-}2}]\end{aligned} \tag{4}$$

$$\begin{aligned}\frac{d}{dt}[\mathrm{BAD:Bcl\text{-}2}] = {} & k^{a}_{BAD:Bcl-2}[\mathrm{BAD_m}][\mathrm{Bcl\text{-}2}] + k_{tBIDrel1}[\mathrm{BAD_m}][\mathrm{tBID:Bcl\text{-}2}] \\ & - (k_{BADphos2} + k^{d}_{BAD:Bcl-2})[\mathrm{BAD:Bcl\text{-}2}] - k_{BADrel2}[\mathrm{tBID}][\mathrm{BAD:Bcl\text{-}2}]\end{aligned} \tag{5}$$

$$\begin{aligned}\frac{d}{dt}[\mathrm{tBID}] = {} & k^{d}_{tBID:Bcl-2}[\mathrm{tBID:Bcl\text{-}2}] + k_{tBIDrel1}[\mathrm{BAD_m}][\mathrm{tBID:Bcl\text{-}2}] + k_{tBIDrel2}[\mathrm{BAK}][\mathrm{tBID:Bcl\text{-}2}] \\ & - k^{a}_{tBID:Bcl-2}[\mathrm{tBID}][\mathrm{Bcl\text{-}2}] - k_{BADrel2}[\mathrm{tBID}][\mathrm{BAD:Bcl\text{-}2}] - k_{BAKrel1}[\mathrm{tBID}][\mathrm{BAK:Bcl\text{-}2}]\end{aligned} \tag{6}$$

$$\begin{aligned}\frac{d}{dt}[\mathrm{tBID:Bcl\text{-}2}] = {} & k^{a}_{tBID:Bcl-2}[\mathrm{tBID}][\mathrm{Bcl\text{-}2}] + k_{BADrel2}[\mathrm{tBID}][\mathrm{BAD:Bcl\text{-}2}] \\ & + k_{BAKrel1}[\mathrm{tBID}][\mathrm{BAK:Bcl\text{-}2}] - k^{d}_{tBID:Bcl-2}[\mathrm{tBID:Bcl\text{-}2}] \\ & - k_{tBIDrel1}[\mathrm{BAD_m}][\mathrm{tBID:Bcl\text{-}2}] - k_{tBIDrel2}[\mathrm{BAK}][\mathrm{tBID:Bcl\text{-}2}]\end{aligned} \tag{7}$$

$$\begin{aligned}\frac{d}{dt}[\mathrm{Bcl\text{-}2}] = {} & (k_{BADphos2} + k^{d}_{BAD:Bcl-2})[\mathrm{BAD:Bcl\text{-}2}] + k^{d}_{tBID:Bcl-2}[\mathrm{tBID:Bcl\text{-}2}] + k^{d}_{BAK:Bcl-2}[\mathrm{BAK:Bcl\text{-}2}] \\ & - k^{a}_{BAD:Bcl-2}[\mathrm{BAD_m}][\mathrm{Bcl\text{-}2}] - k^{a}_{tBID:Bcl-2}[\mathrm{tBID}][\mathrm{Bcl\text{-}2}] - k^{a}_{BAK:Bcl-2}[\mathrm{BAK}][\mathrm{Bcl\text{-}2}]\end{aligned} \tag{8}$$

$$\frac{d}{dt}[\mathrm{BAK_{inac}}] = k^{inac}_{BAK}[\mathrm{BAK}] - k^{ac}_{BAK}[\mathrm{BAK_{inac}}] - k_{BAKcat}[\mathrm{tBID}][\mathrm{BAK_{inac}}] \tag{9}$$

$$\begin{aligned}\frac{d}{dt}[\mathrm{BAK}] = {} & k^{ac}_{BAK}[\mathrm{BAK_{inac}}] + k_{BAKcat}[\mathrm{tBID}][\mathrm{BAK_{inac}}] + k^{d}_{BAK:Bcl-2}[\mathrm{BAK:Bcl\text{-}2}] + 4k^{d}_{BAKpoly}[\mathrm{BAK_{poly}}] \\ & k_{BAKrel1}[\mathrm{tBID}][\mathrm{BAK:Bcl\text{-}2}] - k^{inac}_{BAK}[\mathrm{BAK}] - k^{a}_{BAK:Bcl-2}[\mathrm{BAK}][\mathrm{Bcl\text{-}2}] \\ & - k_{tBIDrel2}[\mathrm{BAK}][\mathrm{tBID:Bcl\text{-}2}] - 4k^{a}_{BAKpoly}[\mathrm{BAK}]^4\end{aligned} \tag{10}$$

$$\begin{aligned}\frac{d}{dt}[\mathrm{BAK:Bcl\text{-}2}] = {} & k^{a}_{BAK:Bcl-2}[\mathrm{BAK}][\mathrm{Bcl\text{-}2}] + k_{tBIDrel2}[\mathrm{BAK}][\mathrm{tBID:Bcl\text{-}2}] - k^{d}_{BAK:Bcl-2}[\mathrm{BAK:Bcl\text{-}2}] \\ & - k_{BAKrel1}[\mathrm{tBID}][\mathrm{BAK:Bcl\text{-}2}]\end{aligned} \tag{11}$$

$$\frac{d}{dt}[\mathrm{BAK_{poly}}] = k^{a}_{BAKpoly}[\mathrm{BAK}]^4 - k^{d}_{BAKpoly}[\mathrm{BAK_{poly}}] \tag{12}$$

EQUATIONS 1-12 Induced Differential Equations from BAD/tBID/BAK Network in Fig. 2.1 or chemical reaction network depicted in Table 2.1.

2.2.2 Kinetic rate constants and other system parameters

Although there is some published experimental data concerning some of the parameters involved in the BAD/tBID/BAK kinetic equations, most of these parameters are unknown or uncertain at best. This is the main reason we must consider a theoretical approach. However, we would first like to explore the behavior of this network with simulation and bifurcation technique based upon what is available. We may borrow values from the previous model of tBID and BAX as well as from another model incorporating tBID [85-86]. For the remaining, such as the reactions associated with BAD, we must estimate values from kinase and phosphatase assays, binding assays, and fluorescence polarization experiments in several various publications. Table 2.2 summarizes our chosen values alongside their references.

As (Eqs. 1-12) depict a conservative system, which frequently occurs in the modeling of biological systems, we define the following system parameters regarding total concentration levels:

$$[BAD_{total}] \triangleq [BAD]+[pBAD]+[pBAD:14-3-3]+[BAD_m]+[BAD:Bcl-2]$$
$$[tBID_{total}] \triangleq [tBID]+[tBID:Bcl-2]$$
$$[BAK_{total}] \triangleq [BAK_{inac}]+[BAK]+[BAK:Bcl-2]+4\cdot[BAK_{poly}]$$
$$[Bcl-2_{total}] \triangleq [Bcl-2]+[BAD:Bcl-2]+[tBID:Bcl-2]+[BAK:Bcl-2]$$

Inspection of equations (1-12) show that the total concentration levels will remain constant over time for any defined solution. With the kinetic equations in (1-12), the rate constant assignments in Table 2.2, and definitions of total concentrations, we are ready to simulate and proceed with an initial numerical analysis of the BAD/tBID/BAK network. This is done in the next chapter.

TABLE 2.2 Rate constant values

Rate constant values used for the BAD/tBID/BAK model. $k_{BADphos1}$ (unbound phosphorylation rate) and $k_{BADrel1}$ (dephosphorylation rate) are 1st-order estimations to the kinetic plots in [49] and [17], respectively. The value of $k_{BADphos2}$ (bound phosphorylation rate) is estimated to be an order of magnitude smaller than $k_{BADphos1}$ to account for unmodeled dynamics. Values of the Bcl-2 association rates for tBID and BAK, $k^a_{tBID:Bcl-2}$ and $k^a_{BAK:Bcl-2}$, respectively, were borrowed from [85]. It is assumed that bound Bcl-2 dissociates from BAD, tBID, or BAK at the same rate, .002s^{-1} (close to the value used in [85]). Association/dissociation rate constants also reflect a BAD/Bcl-x_L dissociation constant of less than 1 nM [53] and BAD's 5-times greater affinity for Bcl-2 than that of tBID [23]. The reaction rate for tBID displacement, $k_{tBIDrel1}$, was set to 25% of the association rate constant $k^a_{BAD:Bcl-2}$. $k^d_{BAKpoly}$ was assumed small to reflect the irreversibility property in [85] and then $k^a_{BAKpoly}$ was adjusted to match (qualitatively) the bifurcation plots of $r_{BAK} = ([\text{BAK}] + 4[\text{BAK}_{\text{poly}}])/[\text{BAK}_{\text{total}}]$ and time response curves in [85] for when there is no expression of BAD. The value of k_{BADseq} reflects the association constant between BAD and the 14-3-3ζ isoform in [21] for when 14-3-3ζ is assumed to have a fixed concentration of 10nM. Finally, the values of τ^{in}_{BAD} and τ^{out}_{BAD} were estimated to reflect the liposome-binding assay data in [21].

Rate constant	Value	Reference(s)
$k_{BADphos1}$	.001 s^{-1}	[48-50]
$k_{BADphos2}$	.0001 s^{-1}	Est.
k_{BADseq}	.001 s^{-1}	[21]
$k_{BADrel1}$	.00087 s^{-1}	[17, 51-52]
τ^{in}_{BAD}	.01 s^{-1}	[21]
τ^{out}_{BAD}	.002 s^{-1}	[21]
$k^a_{BAD:Bcl-2}$	15 $\mu M^{-1}s^{-1}$	[23]
$k^d_{BAD:Bcl-2}$	.002 s^{-1}	Est.
$k^a_{tBID:Bcl-2}$	3 $\mu M^{-1}s^{-1}$	[85]
$k^d_{tBID:Bcl-2}$	.002 s^{-1}	Est.
$k_{tBIDrel1}$	5 $\mu M^{-1}s^{-1}$	[23]
$k_{BADrel2}$	.001 $\mu M^{-1}s^{-1}$	[23]
k^{ac}_{BAK}	.001 s^{-1}	Est.
k_{BAKcat}	.5 $\mu M^{-1}s^{-1}$	[85]
k^{inac}_{BAK}	.1 s^{-1}	[85]
$k^a_{BAK:Bcl-2}$	2 $\mu M^{-1}s^{-1}$	[85]
$k^d_{BAK:Bcl-2}$	.002 s^{-1}	Est.
$k_{tBIDrel2}$	2 $\mu M^{-1}s^{-1}$	[85]
$k_{BAKrel1}$	.001 $\mu M^{-1}s^{-1}$	[85]
$k^a_{BAKpoly}$	2000 $\mu M^{-3}s^{-1}$	Est.
$k^d_{BAKpoly}$	5E-5s^{-1}	Est.

3 Initial Analysis of the BAD/tBID/BAK Network

In this chapter we provide a first-cut numerical analysis of the BAD/tBID/BAK network through simulation, sensitivity, and bifurcation analysis of the kinetic equations in (1-12). This analysis will validate the kinetic full model by comparison to experimental data. We will also design a "skeleton" model which captures the fundamental behavior of the BAD/tBID/BAK network and provide mathematical formulae to explore the state and kinetic parameter space.

What we find is that the tBID induction of BAK resembles a robust switch not unlike what is seen in many other cellular signaling pathways. The effect of BAD is one which sensitizes, and hence alters the robustness of, a switch from the activation of tBID to the activation of BAK. Roughly speaking, there is a simple one-to-one correspondence between the amount of BAD bound to Bcl-2 and the amount of Bcl-2 remaining to sequester tBID. Using this approximation in creating the skeleton model, we will be able to express the sensitizing and triggering relationship between BAD, tBID, and BAK as a simple bilinear function. Moreover, the skeleton model will be used in conjunction with basal (non-apoptotic) operating conditions to derive a necessary constraint on the kinetic rate constants. Finally, turning our attention to the novel kinetic modeling of BAD, the skeleton model (as well as further bifurcation and a sensitivity analysis) are used to qualify the behaviors of the two modes of phosphorylation of BAD (of Bcl-2-bound BAD or of unbound BAD), as well as decipher some of the experimental discrepancies concerning the phosphorylation of BAD.

3.1 Simulations and Bifurcation Analysis of tBID-induction of BAK

3.1.1 Simulations

Before we explain the sensitizing properties of BAD [21, 23, 28, 54], it is useful to first observe how tBID is an activator of BAK. Apoptosis signaling evolves through the BAD/tBID/BAK network as the activation of tBID provokes the activation of BAK. In particular, this signaling is enhanced by a positive feedback loop which exists between tBID and BAK since active BAK can displace tBID from the tBID:Bcl-2 complex (as well as drive down the level of free Bcl-2 through heterodimerization). Refer back to Figs. 2.1 and Table 2.1. Figs. 3.1a-b and 3.1c-d illustrate some example time response behaviors of the full model (1-12) for two different total concentrations of tBID—one that is too low to drive the auto-activation of BAK (Fig 3.1a-b) and another that is sufficiently high to drive the auto-activation (Fig. 3.1c-d). These simulations suggest that only when free Bcl-2 is nearly exhausted do we witness tBID activating BAK (that is, $[\mathrm{BAK}] > 0$). Moreover, we only observe polymerization of BAK (that is, $[\mathrm{BAK}_{\mathrm{poly}}] > 0$) after Bcl-2 exhaustion.

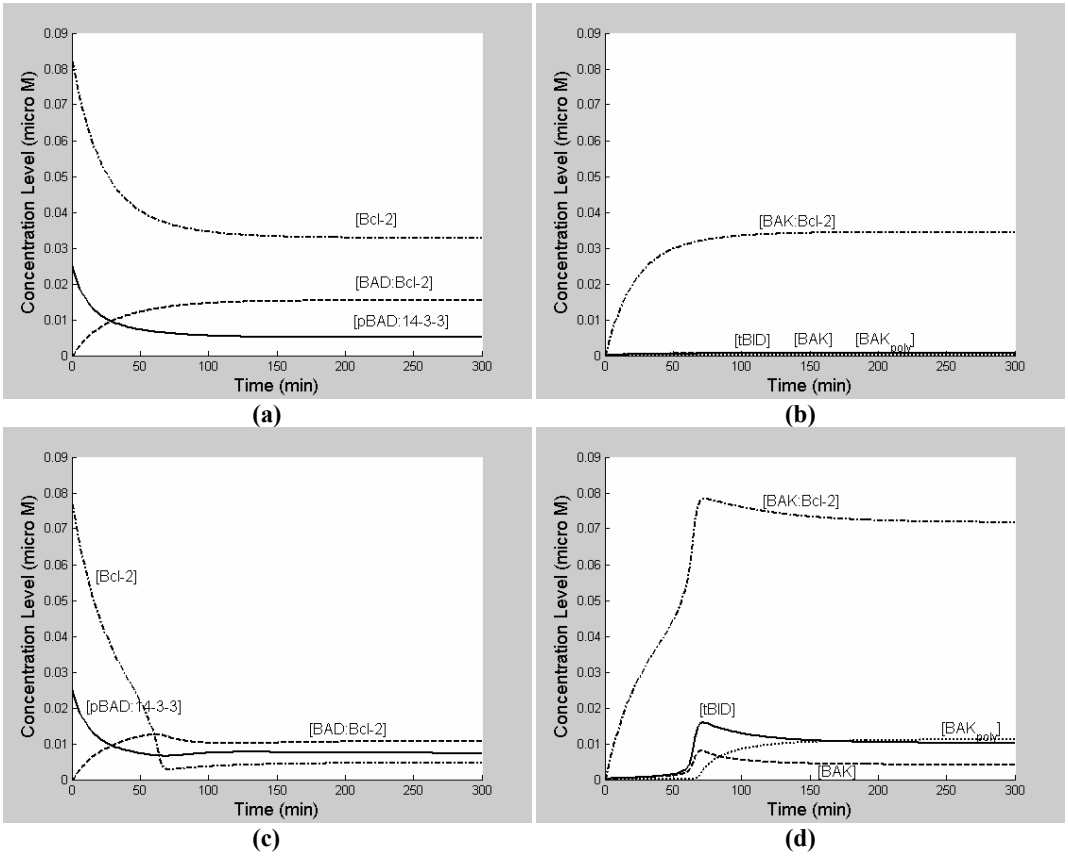

FIGURE 3.1 Representative time response curves for two different levels of total tBID. **(a)-(b)** BAK inactivation when $[\mathrm{tBID}_{\mathrm{total}}] = .018\ \mu\mathrm{M}$ and; **(c)-(d)** BAK activation when $[\mathrm{tBID}_{\mathrm{total}}] = .023\ \mu\mathrm{M}$. At time $t = 0$, the following constraints are assumed to be satisfied: $[\mathrm{pBAD:14\text{-}3\text{-}3}] = [\mathrm{BAD}_{\mathrm{total}}]$, $[\mathrm{tBID:Bcl\text{-}2}] = [\mathrm{tBID}_{\mathrm{total}}]$, $[\mathrm{Bcl\text{-}2}] = [\mathrm{Bcl\text{-}2}_{\mathrm{total}}] - [\mathrm{tBID}_{\mathrm{total}}]$, and $[\mathrm{BAK}_{\mathrm{inac}}] = [\mathrm{BAK}_{\mathrm{total}}]$, where $[\mathrm{BAD}_{\mathrm{total}}] = .025\ \mu\mathrm{M}$, $[\mathrm{Bcl\text{-}2}_{\mathrm{total}}] = .1\ \mu\mathrm{M}$, and $[\mathrm{BAK}_{\mathrm{total}}] = .2\ \mu\mathrm{M}$. All rate constants have been set to the values in Table 2.2.

3.1.2 Bifurcation analysis reveals BAD as a sensitizer to tBID-induced activation of BAK

Another way to observe the switch-like behavior between tBID and BAK is using bifurcation diagrams with $[\mathrm{tBID}_{\mathrm{total}}]$ as the bifurcation parameter. A bifurcation diagram of a given system $\dot{x} = f(x, p)$, where the scalar p is the bifurcation parameter, reveals important changes in the number and stability of equilibrium points as p is varied. Usually, the x-axis is the parameter p and y-axis is a particular state. Also, solid lines are usually used to indicate stable steady states, thinner (or dotted) lines are used to indicate unstable steady states, and big dots are used to indicate values of p where stability changes (known as bifurcation points). In particular, a saddle-node bifurcation point is a value of p where stability changes from that of a saddle point to a node (or vice versa). In the case below, a saddle-node bifurcation occurs whenever the number of steady states changes.

Fig. 3.2 is a bifurcation plot showing how steady state $[\mathrm{BAK}]$ varies with the bifurcation parameter $[\mathrm{tBID}_{\mathrm{total}}]$ for certain fixed levels of $[\mathrm{BAD}_{\mathrm{total}}]$. For each level of total BAD, our system exhibits bistability in a small interval between two saddle-node bifurcation points (with a maximum interval when there is no BAD), wherein two different stable steady state values of free BAK can be obtained

depending on where the system is initialized. A point on the smaller width line represents the third unstable steady state for that particular value of total tBID.

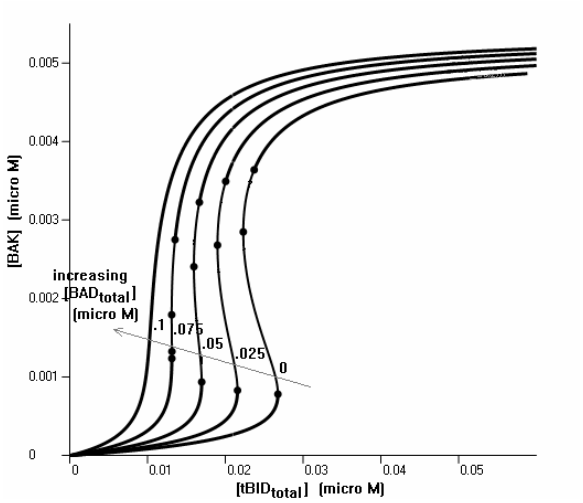

FIGURE 3.2 BAD sensitizes the activation of BAK induced by tBID. 1-parameter bifurcation diagram with total tBID as the bifurcation parameter for various fixed levels of total BAD. Here, we have set $[\text{Bcl-2}_{\text{total}}] = .1\ \mu\text{M}$ and $[\text{BAK}_{\text{total}}] = .2\ \mu\text{M}$.

For each level of total BAD, we take particular interest in the *rightmost* saddle-node bifurcation point in Fig. 3.2 since it represents the biologically meaningful threshold past which an initially inactive BAK is guaranteed to become active. That is, for any level of total tBID beyond this point, our system will move towards activation (or greater levels of active BAK), no matter what the initial condition is. We refer to this corresponding value of total tBID as the (total) tBID triggering level.

A 2-parameter bifurcation diagram of a system $\dot{x} = f(x, p_1, p_2)$, with parameters p_1 and p_2, is a a bifurcation diagram where both p_1 and p_2 are allowed to vary. However, instead of a 3-D plot, usually a 2-parameter bifurcation diagram shows only the evolution of the bifurcation points projected onto the p_1-p_2 plane.

The 2-parameter bifurcation diagram in Fig 3.3 illustrates how the tBID triggering level (rightmost line of each pair) evolves as a function of total BAD. Fig 4 also roughly depicts how it evolves as a function of total Bcl-2. Clearly, the tBID triggering level decreases in a nearly linear fashion as total BAD is increased. That is, an increase in total BAD corresponds to a proportional decrease in the total tBID triggering level. Thus, BAD sensitizes tBID-induction of BAK by lowering the threshold at which tBID can activate BAK.

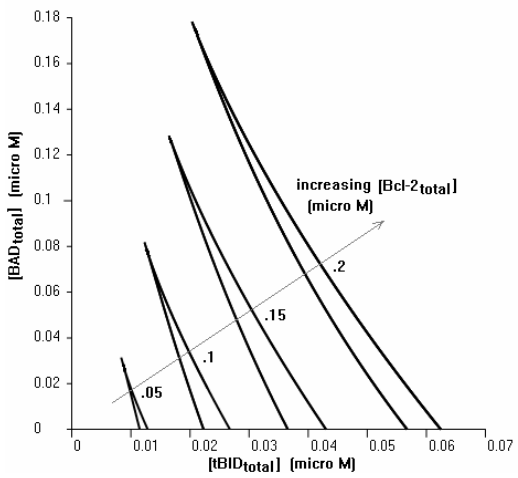

FIGURE 3.3 BAD lowering the threshold mechanism between tBID and BAK. This 2-parameter diagram shows the evolution of both saddle-node bifurcation points as a function of total tBID and total BAD for various fixed values of total Bcl-2. The rightmost line of each pair is the triggering threshold for BAK activation in response to increasing tBID.

3.2 Validating the Effects of BAD on tBID-induction of BAK with Experimental Data

We consider studies that have analyzed the impact of various synthetic peptides derived from the BH3 domains (the pro-apoptotic parts) of BAD and BID. These are usually called BADBH3 and BIDBH3, respectively. In these studies, the peptides are injected into cells or isolated mitochondria and their effects compared in regards to how well they induce apoptosis. Naturally, these studies are used to hypothesize the behaviors of endogenous BAD and tBID. For our purposes, however, we will use these studies to validate the bifurcation results in Fig. 3.3 concerning the effects of BAD on tBID-induced activation of BAK.

These studies demonstrate three basic facts about BAD and tBID. First, BAD is incapable of triggering apoptosis by itself [23, 28, 54]. Second, the presence of both peptides, even at sublethal doses, are shown to behave synergistically, affecting cells more than would be predicted through additive stoichiometry [28, 54]. Stated another way, these two findings indicate that BAD can only lower the threshold at which tBID can activate BAK. And third, without some form of Bcl-2-like expression (e.g., Bcl-2 or Bcl-x_L), this synergy between BAD and BID is absent [23, 54]. The first and third facts are simple consequences of the network structure itself (refer back to Fig. 2.1), since the primary activity of BAD is to displace Bcl-2 and not directly activate tBID or BAK. Indeed, the absence of tBID or Bcl-2 would preclude the activation of BAD having any downstream impact on this network.

The "synergy" recognized between BAD and tBID is easily seen in Fig. 3.3. Consider any point on any of the rightmost lines in Fig. 3.3, such that total BAD and total tBID are non-zero. Then consider this point's projection on the x - and y - axes. The former corresponds to a level of total tBID which is incapable of triggering BAK since it would be to the left of the line. The latter corresponds to a level of total BAD which is incapable of triggering BAK because, again, it would be to the left of the line. (In fact, even if total BAD was increased significantly, triggering would still not occur.) On the other hand, the point itself corresponds to a combining of those same levels of total BAD and total tBID, and hence corresponds to a situation where the activation of BAK is triggered.

3.3 Designing a Skeleton Mechanism to Model the BAD/tBID/BAK Network

In Figure 3.3 we see that the relation between tBID, BAD and Bcl-2 required to trigger BAK activation is approximately linear. Therefore, we propose a skeleton description of the effects of BAD on the tBID-induced activation of BAK. In this manner we will be able to derive formulae which are functions of the rate constants and dispense with the cumbersome challenges associated with selecting specific rate constant values.

At the coarsest level of approximation, we could assume that *all* BAD gets sequestered by Bcl-2, whether it was previously bound or unbound (e.g., bound to tBID or BAK). Any remaining Bcl-2 would then bind tBID to prevent it from activating BAK. Hence, with this approximation, only when $[\text{tBID}_{\text{total}}]$ becomes greater than $[\text{Bcl-2}_{\text{total}}] - [\text{BAD}_{\text{total}}]$ would we see tBID activating BAK.

The high affinity of BAD for Bcl-2 justifies the approximation that any BAD in the mitochondria would bind Bcl-2 (refer back to parameter values in Table 2.2), but the lower affinity of tBID for Bcl-2 requires a somewhat finer approximation than the one above to determine the amount of free tBID needed to trigger BAK activation. We consider this below.

3.3.1 Model derivation

Consider the simple binding reaction between tBID and Bcl-2.

$$\text{tBID} + \text{Bcl-2} \leftrightarrow \text{tBID:Bcl-2} \tag{3.1}$$

If no other reactions are considered, the steady state level of free tBID can be computed as a function of the three parameters

$$[\text{tBID}_{\text{total}}] = [\text{tBID}] + [\text{tBID:Bcl-2}]$$
$$[\text{Bcl-2}_{\text{total}}] = [\text{Bcl-2}] + [\text{tBID:Bcl-2}]$$
$$K_{D.tBID} = k^{d}_{tBID:Bcl-2} / k^{a}_{tBID:Bcl-2}$$

the latter parameter being the ratio of the association and dissociation rate constants. From (3.1) the steady state level of free tBID is constrained to the quadratic equation,

$$[\text{tBID}]^2 + \left(K_{D.tBID} + [\text{Bcl-2}_{\text{total}}] - [\text{tBID}_{\text{total}}]\right)[\text{tBID}] - K_{D.tBID}[\text{tBID}_{\text{total}}] = 0 \tag{3.2}$$

(3.2) has only one positive root which is the unique steady state level of free tBID. Setting the level of free tBID to the level required for BAK activation, say this is denoted $[\text{tBID}_{\text{act}}]$ (which will be assumed constant), we can solve for the level of total tBID necessary to trigger the activation of BAK:

$$[\text{tBID}_{\text{total}}] = [\text{tBID}_{\text{act}}] + \frac{[\text{tBID}_{\text{act}}]}{K_{D.tBID} + [\text{tBID}_{\text{act}}]}[\text{Bcl-2}_{\text{total}}] \tag{3.3}$$

To account for the fact that total available Bcl-2 is reduced by the amount of BAD in the mitochondria we replace $[\text{Bcl-2}_{\text{total}}]$ with $[\text{Bcl-2}_{\text{total}}] - r_{BAD:Bcl-2}[\text{BAD}_{\text{total}}]$, resulting in

$$[\mathrm{tBID}_{\mathrm{total}}] = [\mathrm{tBID}_{\mathrm{act}}] + \frac{[\mathrm{tBID}_{\mathrm{act}}]}{K_{D.tBID} + [\mathrm{tBID}_{\mathrm{act}}]}\left([\mathrm{Bcl\text{-}2}_{\mathrm{total}}] - r_{BAD:Bcl-2}[\mathrm{BAD}_{\mathrm{total}}]\right) \tag{3.4}$$

The coefficient $r_{BAD:Bcl-2} \in [0, 1]$ accounts for the percentage of total BAD which is BAD:Bcl-2. Shown in Appendix A, we can find an expression for $r_{BAD:Bcl-2}$ by setting a portion of the kinetic equations (Eqs. 1-5) to zero and solving for

$$r_{BAD:Bcl-2} \triangleq \frac{[\mathrm{BAD:Bcl\text{-}2}]}{[\mathrm{BAD}_{\mathrm{total}}]} = \frac{1}{1 + \alpha_2 + (1 + \alpha_1)\beta_2 + (1 + \alpha_1)(1 + \beta_1)\gamma} \tag{3.5}$$

where

$$\alpha_1 \triangleq \frac{k_{BADphos1}}{k_{BADseq}} + \frac{k_{BADphos1}}{k_{BADrel1}}$$

$$\alpha_2 \triangleq \frac{k_{BADphos2}}{k_{BADseq}} + \frac{k_{BADphos2}}{k_{BADrel1}}$$

$$\beta_1 \triangleq \frac{k_{BADphos1} + \tau_{BAD}^{out}}{\tau_{BAD}^{in}}$$

$$\beta_2 \triangleq \frac{k_{BADphos2}}{\tau_{BAD}^{in}}$$

and where

$$\gamma \triangleq \frac{k_{BADphos2} + k_{BAD:Bcl-2}^{d} + k_{BADrel2}[\mathrm{tBID}]}{k_{BAD:Bcl-2}^{a}[\mathrm{Bcl\text{-}2}] + k_{tBIDrel1}[\mathrm{tBID:Bcl\text{-}2}]}$$

The assumption that γ is small is reasonable when the level of total tBID has yet to *surpass* the triggering level. This is because we do not expect to see much free tBID until this occurs, making $[\mathrm{tBID:Bcl\text{-}2}]$ relatively large. Consequently, we make the approximation that

$$r_{BAD:Bcl-2} = \frac{1}{1 + \alpha_2 + (1 + \alpha_1)\beta_2} \tag{3.6}$$

which makes the ratio $r_{BAD:Bcl-2}$ a function of kinetic rate constants only. Finally, substituting this value of $r_{BAD:Bcl-2}$ back into (3.4) we arrive to the skeleton approximation of the tBID triggering levels:

$$[\mathrm{tBID}_{\mathrm{total}}] = [\mathrm{tBID}_{\mathrm{act}}] + \frac{[\mathrm{tBID}_{\mathrm{act}}]}{K_{D.tBID} + [\mathrm{tBID}_{\mathrm{act}}]}[\mathrm{Bcl\text{-}2}_{\mathrm{total}}] - \frac{[\mathrm{tBID}_{\mathrm{act}}]}{K_{D.tBID} + [\mathrm{tBID}_{\mathrm{act}}]}\frac{1}{1 + \alpha_2 + (1 + \alpha_1)\beta_2}[\mathrm{BAD}_{\mathrm{total}}] \tag{3.7}$$

3.3.2 Comparison of triggering mechanisms between skeleton model and full Model

We check the accuracy of our skeleton approximation in (3.7) to the triggering mechanism of the BAD/tBID/BAK network depicted in Fig. 3.3. To do this, we first need to compute the coefficients

for $[\text{Bcl-2}_{\text{total}}]$ and $[\text{BAD}_{\text{total}}]$ in (3.7). Using one of the x-intercepts in Fig. 3.3 (e.g., $[\text{tBID}_{\text{total}}] = .0267$ μM and $[\text{Bcl-2}_{\text{total}}] = .1$ μM) we can use (3.2) to solve for $[\text{tBID}_{\text{act}}]$, which in this case comes out to be $[\text{tBID}_{\text{act}}] = 2.4 \times 10^{-4}$ μM. Other x-intercepts in Fig. 3.3 produced similar values for $[\text{tBID}_{\text{act}}]$ (verifying our assumption that it remains approximately constant). With the set of rate constant values in Table 2.2 we can compute $K_{D.tBID}$, α_1, α_2, and β_2. Finally, substituting all values into (3.7), we obtain our approximation specific to the triggering levels in Fig. 3.3:

$$[\text{tBID}_{\text{total}}] = 0.00024\mu\text{M} + 0.26[\text{Bcl-2}_{\text{total}}] - 0.18[\text{BAD}_{\text{total}}] \tag{3.8}$$

We first take note of the coefficient 0.26. According to (3.7), this coefficient is dependent on the values of the dissociation constant $K_{D.tBID}$ and the free triggering level $[\text{tBID}_{\text{act}}]$ and can range anywhere from zero to unity. The stronger the affinity between tBID and Bcl-2, the larger the coefficient and the greater the amount of tBID that is needed to induce triggering. In particular, a coefficient of unity implies that total tBID must reach at least the same level of total Bcl-2 before triggering can ensue. So a coefficient of 0.26 means that tBID need only reach approximately a quarter of total Bcl-2 to trigger BAK (of course this is assuming no BAD is present).

According to (3.7) the magnitude of the second coefficient is the same as that of the first coefficient but off by a factor of $r_{BAD:Bcl-2}$. For our example $r_{BAD:Bcl-2} \approx 0.70$, meaning approximately 70% of total BAD makes it into the mitochondria as the complex BAD:Bcl-2. Note that if all BAD were to make it into the mitochondria, then we would expect to see the second coefficient be the negative of the first coefficient.

We replot the bifurcation curves from Fig. 3.3 but now include with them our linear approximations predicted by (3.8) (shown in red). Note that each red line approximates the evolution of the rightmost saddle-node (or tBID triggering level) for some fixed level of total Bcl-2. The approximation is accurate with one exception. If total BAD is small and total Bcl-2 is large, then triggering will occur for a larger level of total tBID than what is predicted by our skeleton model. This is because, with a smaller amount of BAD, a surplus of Bcl-2 has the capacity to target BAK upon any attempted activation by tBID. Hence, this necessitates a slightly larger level of tBID. Of course, modeling of the dynamics of BAK was not factored into the skeleton model.

Recapitulating, our approximation demonstrates two important facts of the BAD/tBID/BAK network: first, the impact of BAD on the tBID-induction of BAK is much like a titration process where the activation of BAD reflects the amount of Bcl-2 which is sequestered away from tBID; and second, the level of BAD activation, interpreted as a ratio of Bcl-2-bound BAD to total BAD, is a function of rate constants only.

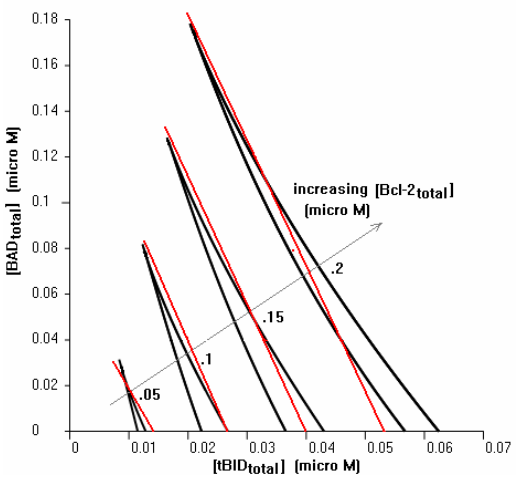

FIGURE 3.4 Approximation (3.8) to the rightmost saddle-nodes in Fig. 3.3 (shown in red).

3.4 Using Bifurcation Analysis to Decipher the Role of Phosphorylation and Experimental Data

The phosphorylation and dephosphorylation processes determine the proportion of BAD that is available to displace Bcl-2, and hence drive the sensitization of tBID-induced activation of BAK. Phosphatases like calcineurin drive the activation of BAD through the release of BAD from cytoplasmic sequestration while kinases inhibit this activation through phosphorylation (refer back to Fig. 2.1).

In order to address how phosphorylation and dephosphorylation affect the activation of BAK, 2-parameter bifurcation diagrams will once again be generated but this time we will be using the phosphorylation and dephosphorylation rates as the parameters. Furthermore, two specific cases will be considered: one where the phosphorylation rate associated with the bound form of BAD (that is, $k_{BADphos2}$) is nonzero; and another where $k_{BADphos2}$ is instead zero. One of the reasons for doing this is the observed experimental differences between the phosphorylation of Bcl-2-bound BAD and the phosphorylation of Bcl-x_L-bound BAD (where now we are distinguishing between the proteins Bcl-2 and Bcl-x_L). Whereas the latter generally results in the dissociation of BAD from the anti-apoptotic protein, the former generally does not [27, 33, 37]. We can study these two cases by letting $k_{BADphos2}$ be non-zero and then zero, respectively.

The first case is motivated by the experimental data in [27, 33, 37], which show that the extracellular survival factor, interleukin-3 (IL-3), can stimulate the phosphorylation-induced dissociation of BAD:Bcl-x_L in Bcl-x_L-expressing FL5.12 cells. The way we analyze such behavior with our model is to use a single phosphorylation parameter, $k_{BADphos}$, where

$$k_{BADphos} = k_{BADphos1} = 100 \times k_{BADphos2},$$

as one of our bifurcation parameters. The remaining bifurcation parameter is chosen to be $k_{BADrel1}$, which is the rate constant associated with the dephosphorylation rate (refer back to Table 2.1). The results of the bifurcation analysis are shown in Fig. 3.5. Like Fig. 3.3, Fig. 3.5 shows bistability and a

threshold mechanism. In general, sufficiently low phosphorylation rates ($k_{BADphos} < .02\ s^{-1}$) are seen to activate BAK (brought on, of course, by the accumulation of mitochondrial BAD); and sufficiently high phosphorylation rates ($k_{BADphos} > .06\ s^{-1}$) are seen to keep BAK inactivated. The former is consistent with some studies that have shown that growth-factor-withdrawal can cause cells to become apoptotic merely from *lack* of BAD phosphorylation [27, 29-30, 33-34, 37]. The latter is consistent with studies which show that the pathological upregulation of BAD phosphorylation can lead to the survival and proliferation of several types of pre-cancerous and cancerous cells by shutting off the apoptosis mechanism [7, 32, 39, 55].

Of particular interest in Fig. 3.5 are the saddle-node lines partitioning the bistable and monostable regions. They are relatively vertical for dephosphorylation rates above $.005 s^{-1}$. (Recall in our previous bifurcations we were operating near $k_{BADrel1} = .01\ s^{-1}$). This means that for certain phosphorylation rates, no matter how strongly we drive the release of BAD through dephosphorylation, we can never activate BAK. In other words, there is a certain maximum impact that dephosphorylation can impart to the network. Inspection of the network in Fig. 2.1 reveals that because we modeled the phosphorylation and sequestration processes of BAD such that phosphorylated BAD must first be sequestered by 14-3-3 before it can be dephosphorylated, 14-3-3 sequestration becomes a rate-limiting step. In particular, because $k_{BADseq} = .001\ s^{-1}$, it is clear that dephosphorylation loses its incremental effectiveness at approximately 5 times the sequestration rate.

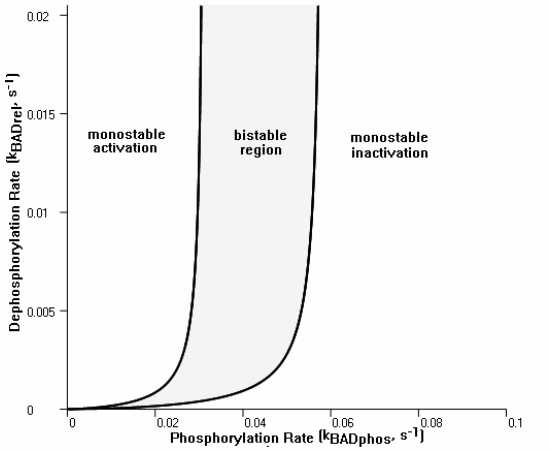

FIGURE 3.5 Effect of simultaneous unbound and bound forms of phosphorylation on the stability of BAK activation. Here, we have set $[BAD_{total}] = .05\ \mu M$, $[Bcl\text{-}2_{total}] = .1\ \mu M$, $[BAK_{total}] = .2\ \mu M$, and $[tBID_{total}] = .015\ \mu M$ (chosen close to a triggering point). Other rate constants have been set to the values in Table 2.2.

There is also a large amount of experimental data that would suggest the absence of phosphorylation-induced dissociation of the BAD complex. For example, [37] shows that IL-3-stimulated Bcl-2-expressing FL5.12 cells are incapable of dissociating the BAD:Bcl-2 complex (where, in this case, Bcl-2 denotes the actual protein Bcl-2 and not Bcl-x_L). Moreover, the experiments in [36] would suggest that it is necessary Ser^{136} and Ser^{155} phosphorylations work concomitantly to dissociate the BAD complex. If this is the case, then any survival signals relying solely on stimulation via Akt, predominantly a Ser^{136} kinase (and not a Ser^{155} kinase), would be limited to the unbound form of phosphorylation only.

We can use our model to address these situations by assuming

$$k_{BADphos} = k_{BADphos1}, \quad k_{BADphos2} = 0$$

Producing bifurcation plots for this second case (Fig. 3.6) much like we did for the previous case, we see the plot shifting to the right. This means that a higher demand upon the phosphorylation rate is required to prevent triggering. Nonetheless, sufficient phosphorylation is still capable of inhibiting the dephosphorylation signaling of BAD to activation, despite the absence of the capacity for phosphorylation-induced dissociation of BAD:Bcl-2. This could explain why in some cells, certain kinases (such as Akt), without any evidence of inducing dissociation, can still inhibit the activation of BAD and apoptosis [29-32, 34, 39].

Because of the shifting to the right, we can say the dephosphorylation rate becomes more effective in triggering BAK. That is, there exist more phosphorylation rates where dephosphorylation could still potentially trigger BAK. Conversely, given a certain dephosphorylation rate, the demand upon phosphorylation for cell viability has increased approximately two-fold. Since kinase levels may vary from experiment to experiment, this may explain why Akt works as an inhibitor in one case but fails to do so in another. That is, unlike the experiments just mentioned in which Akt restores cell viability, [36] argues in their mutation experiments that Akt restoration of cell viability when phosphorylation-induced dissociation of BAD:Bcl-x_L is blocked is impossible.

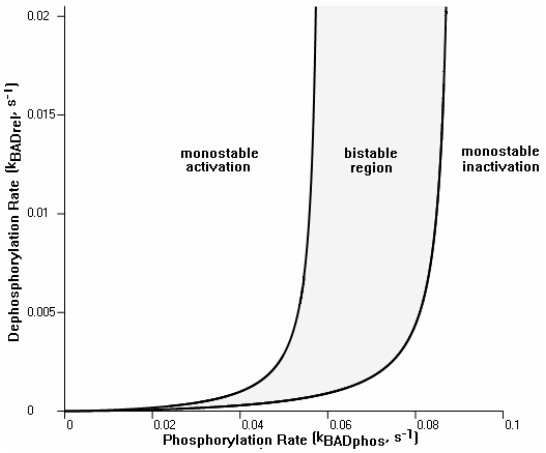

FIGURE 3.6 Increased demand upon phosphorylation when phosphorylation-induced dissociation of BAD:Bcl-2 is blocked. Like before, $[BAD_{total}] = .05\,\mu M$, $[Bcl\text{-}2_{total}] = .1\,\mu M$, $[BAK]_{m.total} = .2\,\mu M$, and $[tBID_{total}] = .015\,\mu M$. Other rate constants have been set to the values in Table 2.2.

3.5 Assumptions of Basal Operating Conditions Place Constraints on Kinetic Rate Constants

In most healthy cells, we do not expect to see any expression of BAD or tBID. This would be equivalent to assuming $[BAD_{total}] = 0$ and $[tBID_{total}] = 0$. This is trivial and not at all interesting. However, there might be certain situations where we find the expression of one or the other (or both) and yet their presence still does not admit an apoptotic response. Such "basal" situations are certainly interesting from a biological standpoint since they impose certain necessary constraints on the kinetic rate constants which must be satisfied in order to maintain a non-apoptotic response. One of particular interest is when it is presumed

$$[BAD:Bcl\text{-}2] << [BAD_{total}]$$

and

$$[\text{tBID}] << [\text{tBID}_{\text{total}}]$$

at steady state. Such would be the case if there was a presence of tBID (bound to Bcl-2) but in amounts less than the tBID triggering level and a presence of BAD not in its active state (that is, not bound to Bcl-2). Such a situation is certainly observed in experimental data [13, 19, 34], observed in our model in the previous sections, and is expected to occur since otherwise the BAD/tBID/BAK network would not be robust (and every cell would lose their mitochondria!).

Using the skeleton model equations (3.7), it is shown in Appendix A that in order for $[\text{BAD} : \text{Bcl-2}] << [\text{BAD}_{\text{total}}]$ and $[\text{tBID}] << [\text{tBID}_{\text{total}}]$ to be satisfied, we necessarily must have

$$\alpha_2 + (1+\alpha_1)\beta_2 >> \max\left\{0,\ \frac{[\text{BAD}_{\text{total}}]}{[\text{Bcl-2}_{\text{total}}]} - 1\right\} \tag{3.9}$$

where, like before, $\alpha_1 = \frac{k_{BADphos1}}{k_{BADseq}} + \frac{k_{BADphos1}}{k_{BADrel1}}$, $\alpha_2 = \frac{k_{BADphos2}}{k_{BADseq}} + \frac{k_{BADphos2}}{k_{BADrel1}}$, and $\beta_2 = \frac{k_{BADphos2}}{\tau_{BAD}^{in}}$.

One way we can interpret (3.9) is that in order for the BAD/tBID/BAK network to be operating under the assumed conditions, it is necessary that one or both of the phosphorylation rate constants be sufficiently large compared to one or more of the rate constants associated with 14-3-3 sequestration (k_{BADseq}), dephosphorylation ($k_{BADrel1}$), and translocation (τ_{BAD}^{in}). Clearly, the Bcl-2-bound form of phosphorylation ($k_{BADphos2}$) is *independently* more effective towards the removal of BAD from the mitochondria than the unbound form of phosphorylation ($k_{BADphos1}$), which seems to require cooperation from the other form of phosphorylation or a significant reduction in translocation. In addition, (3.9) implies that if there is a larger presence of BAD than Bcl-2, then this puts a larger demand on the phosphorylation rate constants. This is obvious since with little Bcl-2 safeguarding tBID, it is necessary that almost all free BAD be removed from the cytoplasm, lest it move to the mitochondria and displace tBID.

3.6 Sensitivity of Trajectories with Respect to Variations in the Phosphorylation Rate Constants

We extend our study on the phosphorylation of BAD by studying the effects of variations in the phosphorylation rate constants. To do this, we calculate the partial derivative of $[\text{BAD} : \text{Bcl-2}](t)$ with respect to the two phosphorylation rate constants and evaluate these derivatives along the two reference solutions simulated and depicted in Figs. 3.1a-b and 3.1c-d (the former being a trajectory which does not trigger BAK and the latter being a trajectory which triggers BAK).

Suppose that

$$\dot{x} = f(x, p)$$

represents a set of biochemical kinetic equations and which models some biological network (such as the BAD/tBID/BAK network). Here, $x = \begin{bmatrix} x_1 & x_2 & \dots & x_m \end{bmatrix}'$ is a vector of species' concentrations and $p = \begin{bmatrix} p_1 & p_2 & \dots & p_r \end{bmatrix}'$ is a vector of kinetic rate constants. Then the set of sensitivity coefficients,

$\frac{\partial x_i}{\partial p_j}$ for $i = 1,\ 2,\ ...,\ m$, with respect to some parameter p_j, evaluated on some reference solution $x^*(t; p^*)$, and at some reference p^*, satisfies the set of linear time-varying differential equations

$$\frac{d}{dt}\frac{\partial x_i}{\partial p_j}(t) = \sum_{k=1}^{m} \frac{\partial f_i}{\partial x_k}(x^*(t; p^*), p^*)\frac{\partial x_k}{\partial p_j}(t) + \frac{\partial f_i}{\partial p_j}(x^*(t; p^*), p^*) \tag{3.10}$$

for $i = 1,\ 2,\ ...,\ m$. Each set of partial derivatives, $\frac{\partial x_i}{\partial p_j}(t)$ for $i = 1,\ 2,\ ...,\ m$, represents the difference in nearby trajectories from the reference solution $x^*(t; p^*)$ at time t whenever a small change is made in the parameter p_j. (3.10) has initial conditions given by $\frac{\partial x_i}{\partial p_j}(0) = 0$ for $i = 1,\ 2,\ ...,\ m$.

For the BAD/tBID/BAK network we assume $p = \begin{bmatrix} k_{BADphos1} & k_{BADphos2} \end{bmatrix}^T$, $x^*(t; p^*)$ is one of the two reference solutions depicted in Fig. 3.1, and p^* is given by the values of $k_{BADphos1}$ and $k_{BADphos2}$ in Table 2.2. We simulate the set (3.10), concomitantly with the kinetic equations (1-12), to compute the log-normalized sensitivity coefficients

$$\frac{\partial[\text{BAD}:\text{Bcl}-2]}{[\text{BAD}:\text{Bcl}-2]} \Big/ \frac{\partial k_{BADphos1}}{k_{BADphos1}}$$
$$\frac{\partial[\text{BAD}:\text{Bcl}-2]}{[\text{BAD}:\text{Bcl}-2]} \Big/ \frac{\partial k_{BADphos2}}{k_{BADphos2}}$$

Fig. 3.7a shows the evolutions of these two coefficients when the reference solution is a non-triggering response. For at least an hour the trajectory is more sensitive to a variation in unbound phosphorylation ($k_{BADphos1}$) than Bcl-2-bound phosphorylation ($k_{BADphos2}$), while for subsequent times we have the opposite behavior. Looking back at Figs. 3.1 we see that it takes a little over an hour for any transient signaling to die down and hence any species' concentrations to be stationary. Therefore, whereas Bcl-2-bound phosphorylation is more effective toward the removal of BAD from the mitochondria at steady state (which was concluded with the skeleton model), the unbound form of phosphorylation is more effective during the transient.

Fig. 3.7b shows the evolutions of these coefficients when the reference solution is a triggering response. Up to the time of the activation of tBID (which is about an hour again), we see little difference in Fig. 3.7a and 3.7b. However, at activation, we see sharp decreases in the magnitude of the sensitivity coefficients. This is especially true for the unbound form of phosphorylation. Such a behavior is explained by γ below (3.5). This is because the value of γ is no longer negligible once tBID is released from Bcl-2 sequestration. As a result of Bcl-2 binding to *both* tBID and BAK, naturally we should find more unbound BAD, making the unbound mode of phosphorylation more effective than usual. However, the inactivation of BAD becomes pointless if the level of tBID moves beyond its triggering level.

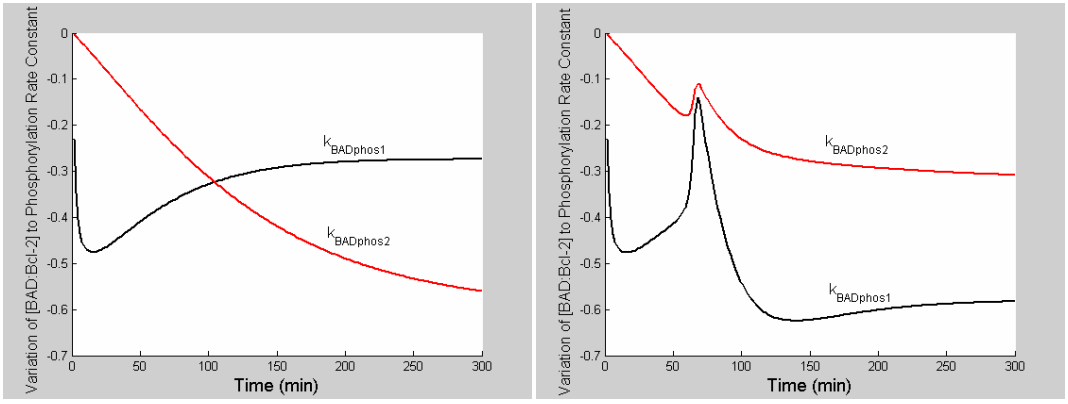

FIGURE 3.7 Evolution of log-normalized sensitivity coefficients $\frac{\partial[\text{BAD}:\text{Bcl}-2]}{[\text{BAD}:\text{Bcl}-2]} \Big/ \frac{\partial k_{BADphos1}}{k_{BADphos1}}$ (black) and $\frac{\partial[\text{BAD}:\text{Bcl}-2]}{[\text{BAD}:\text{Bcl}-2]} \Big/ \frac{\partial k_{BADphos2}}{k_{BADphos2}}$ (red) with respect to: **(a)** a trajectory which does not trigger BAK; and **(b)** a trajectory which triggers BAK.

3.7 Concluding Thoughts Regarding Simulation, Bifurcation, Sensitivity, and Skeleton Studies

BAD acts as a sensitizer by displacing Bcl-2 from tBID. This lowers the threshold amount of tBID guaranteed to induce the activation of BAK. In a sense, the addition of BAD can be thought of a titration system, in which BAD molecules pick off Bcl-2 molecules one-by-one until activation of BAK occurs.

It should be noted that whereas bistability of BAK as a function of tBID occurs within a subset of the parameter space, weaker affinities between Bcl-2 and the three pro-apoptotic proteins (BAD, tBID, or BAK) in our model suffice to entirely remove the bistable region (similarly in the case of [85]'s BAX activation module). In this analysis, the affinities of tBID/Bcl-2 and BAK/Bcl-2 were set relative to a rather tight BAD/Bcl-x_L affinity which was less than 1nM [53]; however, there is experimental data which support looser binding affinities by up to two orders of magnitude [23, 87]. Fortunately, even though the bistable region disappears, the highly sigmoidal behavior from an initially inactive BAK to an active BAK induced by tBID still remains; and the sensitization due to BAD (and its inhibition by phosphorylation) still remains. So despite the apparent uncertainty in our parameters, our results remain qualitatively correct.

An important question to ask is if the bifurcation plots in Figs. 3.2 and 3.3 tell us everything we need to know about the dynamic behavior of this network. From a nonlinear systems perspective, making general statements about the behavior of the BAD/tBID/BAK model, based upon specific rate constants, is insufficient. Our bifurcation diagrams cannot, for example, preclude the existence of nonlinear behaviors such as periodic orbits. And even though the skeleton model was independent of selecting specific kinetic rate constants, it neglected several nonlinearities, particularly in the BAK pathway, and does not tell us everything about the dynamic behavior of the BAD/tBID/BAK network. Therefore, in the next chapters we call upon the works of Feinberg, Horn, and Jackson to make more definitive claims regarding the existence and uniqueness of steady states, and stability, with less approximation.

4 Introduction to Chemical Reaction Network Theory

This chapter is an introduction to the theory of chemical reaction networks, invented by Feinberg, Horn, Jackson, et al [95-100]. We do not claim any novelty in this chapter whatsoever but the theoretical formulations and some of the main results will be useful for our theoretical contributions in the next chapter. Our aim in the next chapter, which will dictate the discussion in this chapter, is to prove the global asymptotic stability and study the robustness of *any* given mass-action network which satisfies a property known as "complex-balancing". In particular, this will enable us to study the stability and robustness of the BAD/tBID/BAK network without having to specify rate constants.

In Chapter 6, we will break up our analysis of the BAD/tBID/BAK network into two sub-networks: one with BAD and tBID and the other with tBID and BAK. The BAD/tBID sub-network possesses a graphical property known as "weak reversibility". From the theory developed in the next chapter, it will be straightforward to make claims about the global asymptotic stability of the BAD/tBID sub-network. The tBID/BAK sub-network is not weakly reversible, and, in fact, we should not expect global asymptotic stability (as we observed multiple steady states and/or bistability in the tBID induction of BAK in the previous chapter). However, we will be able to re-organize the tBID/BAK network as a weakly reversible network operating under a certain dynamic perturbation. Then, we will be able to apply our theoretical results to the tBID/BAK network and assess dynamic features such as robustness against apoptotic stimuli.

Throughout the chapter we will continually refer to two sub-networks (known as the BAD/tBID network and the un-catalyzed tBID/BAK network, which is the tBID/BAK network without the perturbation) as illustrative examples. These are depicted in Figs. 4.1 and 4.2, respectively. Note that the union of the two sub-networks contain every reaction in the BAD/tBID/BAK network listed in Table 2.1 with the exception of one: the catalyzing reaction of tBID on BAK.

In this chapter we formally define a "chemical reaction network endowed with mass-action kinetics". Roughly, a chemical reaction network consists of 3 sets: a set of reacting species, a set of "complexes" (which are linear combinations of species which appear before and after each reaction arrow), and a set of reactions. A chemical reaction network endowed with mass-action kinetics is one in which every reaction rate is proportional to the product of its reactant species' concentrations. With such a rule, a set of differential equations (like (Eqs. 1-12)) is induced that governs the dynamic behavior of a mass-action network.

4.1 Looking at a Biological Network as a Biochemical Network

Suppose in some volume we have a mixture of chemical species. This mixture could be any ensemble of atoms, molecules, ions, or molecular fragments, in which each species is chemically different from the others. We presume that this mixture remains spatially homogeneous for all time. In general, the chemical composition of this mixture will not remain constant, but rather species will be consumed and generated. We wish to describe how this composition evolves over time. We will denote the instantaneous molar concentrations of the species by the vector $x(t)$. The chemical reactions within this mixture are what change the chemical composition over time.

It is generally accepted that the rate of reactions in this chemical network are dependent on the concentrations of its contents, that is, $x(t)$. We presume there exists a non-negative real-valued rate function for each reaction which characterizes the reaction rate. A collection of reactions endowed with a certain kinetics means that each reaction has been assigned a rate function. Quite often, chemical networks are assumed to be endowed with mass-action kinetics, where each rate function is

the product of the concentrations of the reactants multiplied by a constant of proportionality called the rate constant.

What we just assumed for a chemical network is similar to what we said about the BAD/tBID/BAK network in Chapter 2. That is, the BAD/tBID/BAK network, though a biological system, is also a mass-action *chemical* network which comprises a mixture of molecules (usually proteins), which are assumed to be spatially homogeneous, and whose concentrations we wish to track over time. The only difference is that we do not necessarily know the values of the rate constants. Fortunately, the same problems with rate constants appear in the study of chemical networks. In fact, much of the theory revolving around chemical reaction networks is based on the assumption that these rate constants are fixed, but arbitrary, values.

4.2 Defining a Chemical Reaction Network

Now, we review the formal definition of a chemical reaction network, which consists of 3 sets describing the topology. A chemical reaction network is defined by the triple $\{\mathcal{S},\ \mathcal{C},\ \mathcal{R}\}$, where

(1) $\mathcal{S}$ is a set of species
(2) $\mathcal{C}$ is a set of complexes
(3) $\mathcal{R}$ is a set of reactions

$\mathcal{S}$ is a set of m species which comprise the chemical composition, and whose concentrations we wish to track over time. For example, the set of species for the BAD/tBID network in Fig. 4.1 is

$$\mathcal{S} = \{\text{BAD},\ \text{pBAD},\ \text{pBAD}:14\text{-}3\text{-}3,\ \text{BAD}_{\text{m}},\ \text{BAD}:\text{Bcl-2},\ \text{tBID},\ \text{tBID}:\text{Bcl-2},\ \text{Bcl-2}\}$$

For analysis we will assume $\mathcal{S} = \{1,\ 2,\ ...,\ m\}$, that is, we will assume that the species are labeled species 1, species 2, up to species m. Let $x_1(t),\ x_2(t),\ ...\ ,\ x_m(t)$ denote the instantaneous concentration levels of species 1, species 2, … , up to species m, respectively, and denote the full concentration vector as $x(t) \triangleq [x_1(t)\quad x_2(t)\quad ...\quad x_m(t)]'$. Naturally, we can associate the vector space $\mathbb{R}^m$ with $\mathcal{S}$ by letting $x(t) \in \mathbb{R}^m$ wherever it is defined and letting the elements of $\mathcal{S} = \{1,\ 2,\ ...,\ m\}$ index the components of x in the obvious manner.

$\mathcal{C}$ is the set of "complexes", or the non-negative combinations of species appearing before and after reaction arrows. For example, in the BAD/tBID network the displacement reaction

$$\text{BAD}_{\text{m}} + \text{tBID}:\text{Bcl-2} \rightarrow \text{tBID} + \text{BAD}:\text{Bcl-2}$$

is a reaction from the complex $\text{BAD}_{\text{m}} + \text{tBID}:\text{Bcl-2}$, a combination of the species BAD_{m} and $\text{tBID}:\text{Bcl-2}$, to the complex $\text{tBID} + \text{BAD}:\text{Bcl-2}$, a combination of the species tBID and $\text{BAD}:\text{Bcl-2}$. In other instances we may find more than one of the same species. For example, in the un-catalyzed tBID/BAK network in Fig. 4.2, the reaction

$$4\ \text{BAK} \rightarrow \text{BAK}_{\text{poly}}$$

necessitates that we have the complex $4\ \mathrm{BAK}$, a combination of 4 of the species BAK. Because complexes comprise combinations of species, another definition for a complex will be a vector y in the non-negative orthant $\mathbb{R}^m_{\geq 0}$ where the k^{th} component is the number of molecules of species k needed to create the complex. In other words, y is a vector representing the stoichiometry of a complex. For example, if we label the species in $\mathcal{S}$ for the BAD/tBID network as species 1 to species $m = 8$ (according to the order in which the species are shown above), then the vector $y = [0 \quad 0 \quad 0 \quad 1 \quad 0 \quad 0 \quad 1 \quad 0]'$ is another way to represent the complex $\mathrm{BAD_m} + \mathrm{tBID} : \mathrm{Bcl\text{-}2}$ and the vector $y = [0 \quad 0 \quad 0 \quad 0 \quad 1 \quad 1 \quad 0 \quad 0]'$ is another way to represent the complex $\mathrm{tBID} + \mathrm{BAD} : \mathrm{Bcl\text{-}2}$. It is assumed that the components of the complexes are always non-negative integers (but there may be situations where non-integer values are of use in chemical reaction network theory, e.g., see [95]).

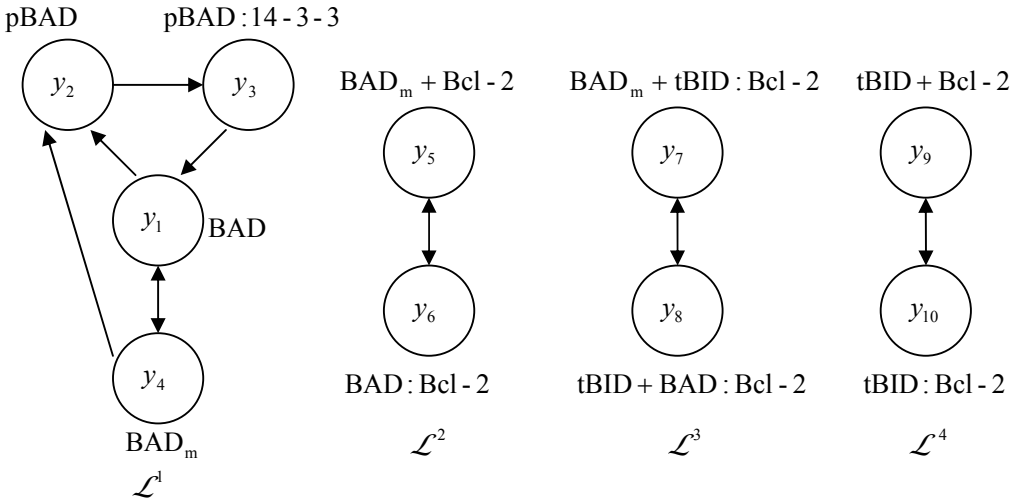

FIGURE 4.1 BAD/tBID Chemical Reaction Network

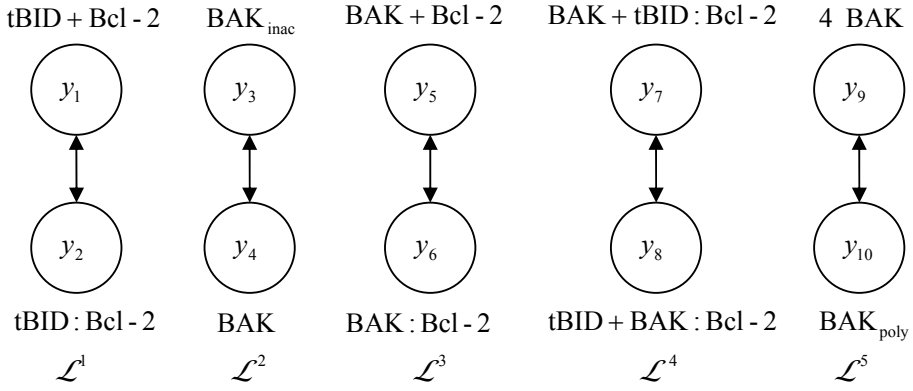

FIGURE 4.2 Un-catalyzed tBID/BAK Chemical Reaction Network

For analysis we will suppose that there are a total of n complexes. We arbitrarily label the complexes $y_1, y_2, \ldots, y_n$, so $\mathcal{C} = \{y_1, y_2, \ldots, y_n\}$. In order to maintain consistency with the notation in [92], we label the components of each complex in the following manner: if y_j is some complex in $\mathcal{C}$, then $y_j = [y_{1j} \quad y_{2j} \quad \ldots \quad y_{mj}]'$. Here, y_{kj} is the number of species k needed to

create complex y_j. This is done with the intention of creating a matrix $Y = [y_1 \quad y_2 \quad \ldots \quad y_n]'$, a matrix whose columns are the complexes and which satisfies $(Y)_{kj} = y_{kj}$.

Much like we did for the species set, we can associate the vector space $\mathbb{R}^n$ with $\mathcal{C}$. Similar to that for the species set, where a point in $\mathbb{R}^m$ can have the meaning of a concentration vector $x(t) \in \mathbb{R}^m$ or a complex $y_j \in \mathbb{R}^m$, a point in $\mathbb{R}^n$ can represent a vector of "total currents", that is, a vector where the component associated with complex y_j is the sum of all reaction rates going to and leaving y_j, or the total current at y_j. This will be made clearer below. In order to also maintain some consistency with Feinberg's notation (which avoids issues with the artificial ordering of species, complexes, and reactions), the complexes in $\mathcal{C}$ will be used to index the components of a given vector $g \in \mathbb{R}^n$. That is, the complexes y_1, y_2, ..., y_n themselves will be used as the subscripts. For example, g_{y_j} represents that component of g associated with complex y_j (which may or may not be the j^{th} component depending on one's choice of ordering).

$\mathcal{R} = \{y_j \to y_i : \; y_i, y_j \in \mathcal{C}\}$ is the set of reactions defined among the complexes. In a similar manner, we will associate the vector space $\mathbb{R}^r$ with the set of r reactions in $\mathcal{R}$. For example, each reaction has associated with it precisely one rate constant, so we can think of $k \in \mathbb{R}^r_+$ (positive orthant) as a vector of rate constants. Like $\mathcal{C}$, the elements in the reaction set $\mathcal{R}$ will be used as subscripts to represent components of vectors in $\mathbb{R}^r$. For example, $k_{y_j \to y_i}$ is the component of $k \in \mathbb{R}^r_+$ which is associated with $y_j \to y_i$, the reaction of complex y_j reacting to complex y_i.

4.3 Preliminary Notation

It will be useful to introduce some preliminary notation. First, define the exponential and logarithm functions to be functions of vectors in the following component-wise manner: Let $p > 1$ be an integer and $x \in \mathbb{R}^p$ where $[x_1 \quad x_2 \quad \ldots \quad x_p]'$. Then, define

$$e^x \triangleq [e^{x_1} \quad e^{x_2} \quad \ldots \quad e^{x_p}]'$$

If $x \in \mathbb{R}^p_+$, define

$$\ln x \triangleq [\ln x_1 \quad \ln x_2 \quad \ldots \quad \ln x_p]'$$

We also define multiplication and division of two vectors in a component-wise manner: Let $w, z \in \mathbb{R}^p$. Then, define

$$wz \triangleq [w_1 z_1 \quad w_2 z_2 \quad \ldots \quad w_p z_p]'$$
$$w/z \triangleq [w_1/z_1 \quad w_2/z_2 \quad \ldots \quad w_p/z_p]'$$

the latter of which is defined as long as no component of z is zero. Finally, we define a "vector raised to another vector" in a component-wise manner: Let $w, z \in \mathbb{R}^p_{\geq 0}$. Then define

$$w^z \triangleq w_1^{z_1} w_2^{z_2} \cdots w_p^{z_p}$$

Consider a collection of complexes denoted $\mathcal{L}$. Define $\omega_{\mathcal{L}} \in \mathbb{R}^n_{\geq 0}$ to be the characteristic vector whose components have 1's in the entries corresponding to complexes in $\mathcal{L}$ and 0's in all remaining entries. That is, for all $y_j \in \mathcal{C}$ such that $y_j \in \mathcal{L}$, $(\omega_{\mathcal{L}})_{y_j} = 1$, and for all $y_j \in \mathcal{C}$ such that $y_j \notin \mathcal{L}$, $(\omega_{\mathcal{L}})_{y_j} = 0$. In the special case that $\mathcal{L} = \{y_j\}$ is a singleton, we write ω_{y_j} instead of $\omega_{\{y_j\}}$ for simplicity. In this manner, the set $\{\omega_{y_j}\}_{y_j \in \mathcal{C}}$ becomes the standard basis for $\mathbb{R}^n$.

4.4 A Chemical Reaction Network Endowed with Mass-Action Kinetics

The law of mass-action originates from collision theories, with the understanding that the probability of a reaction taking place in some small interval about a time t is proportional to the product of the reactant concentrations, and is proportional to the length of the interval. Hence, a reaction which abides by the law of mass-action has the property that the reaction rate is the product of the concentrations of the reactants times a constant of proportionality called the rate constant. For example, if in the BAD/tBID network the reaction

$$\mathrm{BAD_m} + \mathrm{tBID:Bcl\text{-}2} \rightarrow \mathrm{tBID} + \mathrm{BAD:Bcl\text{-}2}$$

abides to the law of mass-action, then its reaction rate would be

$$k_{\mathrm{BAD_m+tBID:Bcl-2 \rightarrow tBID+BAD:Bcl-2}}[\mathrm{BAD_m}][\mathrm{tBID:Bcl-2}]$$

where $k_{\mathrm{BAD_m+tBID:Bcl-2 \rightarrow tBID+BAD:Bcl-2}}$ is the rate constant.

A chemical reaction network endowed with mass-action kinetics is defined by the quadruple $\{\mathcal{S}, \mathcal{C}, \mathcal{R}, k\}$ where $\{\mathcal{S}, \mathcal{C}, \mathcal{R}\}$ is a chemical reaction network, $k \in \mathbb{R}^r_+$ is the vector of rate constants, and where it is understood that for each reaction $y_j \rightarrow y_i \in \mathcal{R}$, the reaction rate is given by $k_{y_j \rightarrow y_i} x(t)^{y_j} = k_{y_j \rightarrow y_i} x_1(t)^{y_{1j}} x_2(t)^{y_{2j}} \cdots x_m(t)^{y_{mj}}$.

.

4.5 Induced Differential Equations of a Chemical Reaction Network

We are now ready to define the differential equations induced by a network endowed with mass-action kinetics. For the vector, $x \in \mathbb{R}^m_{\geq 0}$, of all species concentrations we can write

$$\begin{aligned} \dot{x}(t) &= f(x(t)) \\ &\triangleq \sum_{y_j \rightarrow y_i \in \mathcal{R}} k_{y_j \rightarrow y_i} x^{y_j} (y_i - y_j) \end{aligned} \tag{4.1}$$

Using this we can also express the rate of change for species k as

$$\begin{aligned}\dot{x}_k(t) &= f_k(x(t)) \\ &\triangleq \sum_{y_j \to y_i \in \mathcal{R}} k_{y_j \to y_i} x^{y_j} (y_{ki} - y_{kj})\end{aligned} \tag{4.2}$$

Example 4.5.1

The sum in the right-hand-side of (4.1) is indexed over the set of reactions $\mathcal{R}$ in which each term, e.g., the reaction $y_j \to y_i$, is given by the product of the scalar $k_{y_j \to y_i} x^{y_j}$ with the vector $y_i - y_j$. The scalar $k_{y_j \to y_i} x^{y_j}$, that is $k_{y_j \to y_i} x_1^{y_{1j}} x_2^{y_{2j}} \cdots x_m^{y_{mj}}$, is the reaction rate (or rate function) assumed by the law of mass-action and the vector $y_i - y_j$ provides the information as to how this reaction rate enters into the differential equations. So consider the BAD/tBID network as an example. The term in (4.1) which would correspond to the reaction

$$\mathrm{BAD_m} + \mathrm{tBID:Bcl\text{-}2} \to \mathrm{tBID} + \mathrm{BAD:Bcl\text{-}2}$$

is

$$k_{\mathrm{BAD_m+tBID:Bcl-2 \to tBID+BAD:Bcl-2}}[\mathrm{BAD_m}][\mathrm{tBID:Bcl-2}][0 \quad 0 \quad 0 \quad -1 \quad 1 \quad 1 \quad -1 \quad 0]'$$

(Note according to Fig 4.1 this can also be written as $k_{y_7 \to y_8} x_4 x_7 [0 \quad 0 \quad 0 \quad -1 \quad 1 \quad 1 \quad -1 \quad 0]'$.) Looking back at (Eqs. 1-12), our kinetic equations for the BAD/tBID/BAK network, we see that the reaction rate

$$k_{tBIDrel1}[\mathrm{BAD_m}][\mathrm{tBID:Bcl-2}]$$

(in this case, $k_{tBIDrel1} = k_{\mathrm{BAD_m+tBID:Bcl-2 \to tBID+BAD:Bcl-2}}$) appears in four different locations. The reaction vector $[0 \quad 0 \quad 0 \quad -1 \quad 1 \quad 1 \quad -1 \quad 0]'$ indicates in which state derivative this reaction rate appears and how it is introduced (e.g., positively or negatively). In particular, one molecule of species 4 ($\mathrm{BAD_m}$) combines with one molecule of species 7 ($\mathrm{tBID:Bcl\text{-}2}$) to form one molecule of species 5 ($\mathrm{BAD:Bcl\text{-}2}$) and one molecule of species 6 (tBID). Hence, according to the definition of the induced differential equations for a chemical reaction network, the reaction rate $k_{y_7 \to y_8} x_4 x_7$, that is, $k_{\mathrm{BAD_m+tBID:Bcl-2 \to tBID+BAD:Bcl-2}}[\mathrm{BAD_m}][\mathrm{tBID:Bcl-2}]$, is defined to appear negatively (with a scale of unity) in the rates of change of the concentrations for species 4 and 7, and positively (with a scale of unity) in the rates of change of the concentrations for species 5 and 6. Clearly this is shown in (Eqs. 1-12), and this is how the kinetic equations for the BAD/tBID/BAK network were derived.

Remark 4.5.2

$f: \mathbb{R}^m_{\geq 0} \to \mathbb{R}^m$ is defined as a polynomial vector field, and hence is locally Lipschitz. According to [94], this means that there exists a maximal forward trajectory $x(\cdot)$ in some maximal interval $[0, \sigma)$ when $x(0) \in \mathbb{R}^m_{\geq 0}$. Note that (4.1) is only defined for $x \in \mathbb{R}^m_{\geq 0}$ since concentrations must remain non-negative. However, it can be shown that $\mathbb{R}^m_{\geq 0}$ is forward-invariant for system (4.1). To see this, consider any reaction $y_j \to y_i \in \mathcal{R}$. If there exists $k \in \{l: \ y_{lj} \neq 0\}$ such that $x_k = 0$, then

the reaction rate $k_{y_j \to y_i} x^{y_j} = k_{y_j \to y_i} x_1^{y_{1j}} x_2^{y_{2j}} \cdots x_m^{y_{mj}} = 0$. From repetitive use of this property, it is immediate that whenever $x_k = 0$, we must have $\dot{x}_k \geq 0$. Therefore, the solution $x(\cdot)$, with $x(0) \in \mathbb{R}^m_{\geq 0}$, remains in the nonnegative orthant as long as it is defined there.

Definition 4.5.3

For any chemical reaction network $\{\mathcal{S}, \mathcal{C}, \mathcal{R}\}$, the stoichiometric subspace $D \subset \mathbb{R}^m$ is defined by

$$D \triangleq \text{span } \{y_i - y_j \in \mathbb{R}^m : \ y_j \to y_i \in \mathcal{R}\}$$

Remark 4.5.4

(4.1) depicts f as a non-negative linear combination of all vectors $y_i - y_j$ such that $y_j \to y_i \in \mathcal{R}$. Observe that any composition $x(t)$, which exists on some interval $[t_1, t_2]$, must satisfy $x(t_2) - x(t_1) \in D$. That is, $x(t_2) \in (x(t_1) + D) \bigcap \mathbb{R}^m_{\geq 0}$, where the coset $x + D \triangleq \{x + \gamma : \ \gamma \in D\}$. In fact, any maximal solution $x(\cdot)$ with $x(0) \in \mathbb{R}^m_{\geq 0}$ is forced to reside in its coset $x(0) + D$ for all time in its interval of existence $[0, \sigma)$. These cosets, which will generally be denoted with the letter S, partition the non-negative orthant $\mathbb{R}^m_{\geq 0}$ into stoichiometric classes. That is, for each $x \in \mathbb{R}^m_{\geq 0}$, $(x + D) \bigcap \mathbb{R}^m_{\geq 0}$ is the stoichiometric class which contains x. Of course, any other $x' \in \mathbb{R}^m_{\geq 0}$ such that $x' - x \in D$ is "compatible" with x, and hence $x' \in (x + D) \bigcap \mathbb{R}^m_{\geq 0}$. If there is no particular value of x in mind, $(x + D) \bigcap \mathbb{R}^m_{\geq 0}$ will be denoted $S \bigcap \mathbb{R}^m_{\geq 0}$, where S is some coset $x + D$. We define a positive stoichiometric class to be a stoichiometric class whose intersection with the positive orthant is non-empty, that is, $S \bigcap \mathbb{R}^m_{+} \neq \phi$. There may exist stoichiometric classes which are not positive (these, of course are restricted to the boundary $\partial \mathbb{R}^m_{\geq 0}$), and there may also exist positive stoichiometric classes which may intersect the boundary $\partial \mathbb{R}^m_{\geq 0}$.

4.6 Interpreting Network Structure and Stoichiometry

We are interested in what happens to $x(\cdot)$ in each stoichiometric class. We presume that the vector $k \in \mathbb{R}^r_{+}$ is fixed but unknown and we would like to describe the qualitative behavior of $x(\cdot)$ relying on the network structure and stoichiometry.

The network structure, such as those in Figs. 4.1 and 4.2, suggests a partition of $\mathcal{C}$ into linkage classes $\mathcal{L}^1$, $\mathcal{L}^2$, ..., $\mathcal{L}^l$ where each $\mathcal{L}^\theta$ consists of complexes which are "linked" together but which are not "linked" to complexes in other linkage classes. In other words, y_j and y_i are directly linked together if either $y_j \to y_i \in \mathcal{R}$ or $y_i \to y_j \in \mathcal{R}$ (or both). This rule can be thought of as an equivalence relation, and applying it repetitively results in the linkage classes for a chemical reaction network. For example, the BAD/tBID network consists of four linkage classes as shown in Fig. 4.1,

which we have labeled $\mathcal{L}^1$, $\mathcal{L}^2$, $\mathcal{L}^3$, and $\mathcal{L}^4$. Similarly, the un-catalyzed tBID/BAK network in Fig. 4.2 consists of five linkage classes. We reserve the symbol ℓ for the number of linkage classes.

A complex y_j is said to ultimately react to another complex y_i if their exists a directed path from y_j to y_i, that is, if there exists a sequence of complexes $\{y_{h_1}, y_{h_2}, ..., y_{h_N}\}$ with $y_{h_1} = y_j$ and $y_{h_N} = y_i$ such that $y_{h_1} \to y_{h_2} \to \cdots \to y_{h_N}$. Two complexes, y_j and y_i, are strongly linked if both y_j ultimately reacts to y_i, and y_i ultimately reacts to y_j. Once again, repetitive use of this "strong linking" operation creates another equivalence relation on $\mathcal{C}$, partitioning the set of complexes into strong linkage classes. Finally, a terminal strong linkage class Λ is a strong linkage class such that no member of Λ reacts to a complex outside of Λ. For example, each of the linkage classes in both the BAD/tBID network and the un-catalyzed tBID/BAK network are terminal strong linkage classes.

Definition 4.6.1

A chemical reaction network is said to be weakly reversible if for each $\theta \in \{1, 2, ..., \ell\}$ and each $y_j, y_i \in \mathcal{L}^\theta$, with $y_j \neq y_i$, there exists a set of complexes $\{y_{h_1}, y_{h_2}, ..., y_{h_N}\}$ with $y_{h_1} = y_j$ and $y_{h_N} = y_i$ such that $y_{h_1} \to y_{h_2} \to \cdots \to y_{h_N}$. In other words, we can travel in any linkage class $\mathcal{L}^\theta$, and in a directed manner, from any complex in $\mathcal{L}^\theta$ to any other complex in $\mathcal{L}^\theta$.

Definition 4.6.2

A network is said to be a $t = \ell$ network if the number of terminal strong linkage classes (we reserve the symbol t for this number), is equal to the number of linkage classes, ℓ. Equivalently, a $t = \ell$ network is one in which there exists precisely one terminal strong linkage class in each linkage class.

Remark 4.6.3

In the terminology above, a weakly reversible network is one where each linkage class is a terminal strong linkage class (and hence a $t = \ell$ network). In other words, a weakly reversible is a network in which each terminal linkage class coincides with the linkage class itself. Looking at the networks in Figs. 4.1 and 4.2, we see that both the BAD/tBID and un-catalyzed tBID/BAK networks are not only $t = \ell$ networks but also weakly reversible networks.

4.7 Three Useful Mappings

It will be useful in several instances to reformulate (4.1). This will give us the ability to segregate the differential equations' dependency on $k \in \mathbb{R}^r_+$ from the dependency on its graphical structure and stoichiometry. Reformulation requires the introduction of three mappings from [95]. First, $Y: \mathbb{R}^n \to \mathbb{R}^m$ is the linear transformation defined by the left-multiplication of the matrix of complexes Y discussed earlier. Second, $\psi: \mathbb{R}^m_{\geq 0} \to \mathbb{R}^n_{\geq 0}$ is defined by $\psi(x) \triangleq \sum_{y_j \in \mathcal{C}} x^{y_j} \omega_{y_j}$, which is

a vector of "reaction rates without the rate constants". $\psi(x)$ is clearly dependent on the stoichiometry. Second, for each $k \in \mathbb{R}_+^r$, we let $A_k : \mathbb{R}^n \to \mathbb{R}^n$ be the linear transformation defined by $A_k(p) \triangleq \sum_{y_j \to y_i \in \mathcal{R}} k_{y_j \to y_i} p_{y_j} (\omega_{y_i} - \omega_{y_j})$. Using these three mappings, we see that a network endowed with mass-action kinetics can be written more compactly as

$$\dot{x} = YA_k\psi(x) \tag{4.3}$$

4.8 Equilibrium Points and their Relationship with kerYA_k

Relying exclusively on the network structure and stoichiometry, we would like to extract as much information as possible about the equilibrium points in mass-action kinetic networks. In the next couple of sections we will see that a lot can be derived based on the fact that the network is either $t = \ell$ or weakly reversible. As discussed earlier, the two networks in Figs. 4.1 and 4.2, the BAD/tBID network and the un-catalyzed tBID/BAK network, are weakly reversible. Furthermore, because any weakly reversible network is also a $t = \ell$ network, we will be able to be utilize all these properties in our analyses of these networks.

Define

$$E_+ \triangleq \{x \in \mathbb{R}_+^m : \ f(x) = 0\}$$

and

$$E_0 \triangleq \{x \in \partial\mathbb{R}_{\geq 0}^m : \ f(x) = 0\}$$

to be the set of interior and boundary equilibrium points for system (4.1), respectively.

Remark 4.8.1

Because (4.3) is equivalent to (4.1), and because we wish to seek information about equilibrium points, we are interested in $\ker YA_k \bigcap \mathbb{R}_{\geq 0}^n$ and $\ker A_k \bigcap \mathbb{R}_{\geq 0}^n$. That is, any equilibrium point $x^* \in \mathbb{R}_{\geq 0}^m$ must satisfy $\psi(x^*) \in \ker YA_k$. The stronger inclusion, that is $\psi(x^*) \in \ker A_k$, which may or may not be the case for any given equilibrium point, represents what will soon be defined as a complex-balanced point.

We first examine what it means for an equilibrium point $x^* \in \mathbb{R}_{\geq 0}^m$ to satisfy $\psi(x^*) \in \ker YA_k \bigcap \mathbb{R}_{\geq 0}^n$. To aid in this analysis, it is useful to define the set

$$\Delta \triangleq \{\omega_{y_i} - \omega_{y_j} : \ y_j \to y_i \in \mathcal{R}\}$$

Remark 4.8.2

It can be shown that $\text{image} A_k = \text{span}\Delta$ for any $t = \ell$ network [95]. Hence, we see a potential complication associated with the value of k for mass-action networks being removed once $t = \ell$. Because any equilibrium point $x^* \in \mathbb{R}_{\geq 0}^m$ must satisfy $\psi(x^*) \in \ker YA_k$, we must have

$A_k\psi(x^*) \in \ker Y \bigcap \text{image} A_k$. Hence, whenever $t = \ell$, we must have $g^* \in \ker Y \bigcap \text{span}\Delta$, where $g^* = A_k\psi(x^*)$. This gives us the following two constraints on the vector g^*, which can be thought of as a vector of "total currents":

$$\sum_{y_j \in \mathcal{C}} g^*_{y_j} y_j = 0 \tag{4.4}$$

$$\sum_{y_j \in \mathcal{L}^\theta} g^*_{y_j} = 0 \tag{4.5}$$

Another, but more meaningful, way to derive the first condition (4.4) above is to re-group the mass-action system (4.3) at an equilibrium point as

$$\sum_{y_j \in \mathcal{C}} (\kappa^*_{\to y_j} - \kappa^*_{y_j \to}) y_j = 0 \tag{4.6}$$

where $\kappa^*_{\to y_j} \triangleq \sum_{y_k \in \mathcal{C}} k_{y_k \to y_j} \psi_{y_k}(x^*)$ and $\kappa^*_{y_j \to} \triangleq \sum_{y_k \in \mathcal{C}} k_{y_j \to y_k} \psi_{y_j}(x^*)$ are the "currents" flowing into and out of each complex y_j at $x = x^*$. The "total current" for a complex is simply the current flowing in minus the current flowing out, that is, $g^*_{y_j} = \kappa^*_{\to y_j} - \kappa^*_{y_j \to}$. Consequently (4.6) becomes $\sum_{y_j \in \mathcal{C}} g^*_{y_j} y_j = 0$, like before.

4.9 Complex-balanced Points and Relationship with Weakly Reversible Networks

A lot more can be said about an equilibrium point $x^* \in \mathbb{R}^m_{\geq 0}$ which satisfies $\psi(x^*) \in \ker A_k \bigcap \mathbb{R}^n_{\geq 0}$ (which because $\ker A_k \subset \ker YA_k$ must also satisfy $\psi(x^*) \in \ker YA_k \bigcap \mathbb{R}^n_{\geq 0}$). From the terminology in [100], such a point will be called "complex-balanced". As we shall see, a network must be weakly reversible in order to admit any complex-balanced point in the positive orthant $\mathbb{R}^m_+$. In fact, the BAD/tBID and un-catalyzed tBID/BAK, endowed with certain mass-action kinetics, will not only admit a complex-balanced equilibrium point but will *only* have complex-balanced equilibria. It turns out that complex-balanced points have nice dynamic properties, which will be furthered explored in the next section. For now, however, we provide the theory which will enable us to prove the existence of complex-balanced points in any given weakly reversible network.

Definition 4.9.1

A chemical reaction network, endowed with mass-action kinetics, is said to be complex-balanced at a point $x^* \in \mathbb{R}^m_{\geq 0}$ if $\psi(x^*) \in \ker A_k$.

Remark 4.9.2

We can derive a more physical understanding of what a complex-balanced point is by doing the same thing we did in Remark 4.8.2 with the more general equilibrium point. To do this, consider $A_k\psi(x^*) = 0$. This is the same as

$$\sum_{y_j \to y_i \in \mathcal{R}} k_{y_j \to y_i} \psi(x^*)_{y_j} (\omega_{y_i} - \omega_{y_j}) = 0$$

The left-hand-side can be re-grouped so that

$$\sum_{y_j \in \mathcal{C}} (\kappa^*_{\to y_j} - \kappa^*_{y_j \to}) \omega_{y_j} = 0 \tag{4.7}$$

where $\kappa^*_{\to y_j} = \sum_{y_k \in \mathcal{C}} k_{y_k \to y_j} \psi_{y_k}(x^*)$ and $\kappa^*_{y_j \to} = \sum_{y_k \in \mathcal{C}} k_{y_j \to y_k} \psi_{y_j}(x^*)$, again, are the sum of all reaction rates entering and leaving complex y_j, respectively. Once again, these sums can be thought of as currents entering and leaving each complex. Hence, in order for (4.7) to be satisfied, each term in the summand must be zero. Hence, $\kappa^*_{\to y_j} = \kappa^*_{y_j \to}$ for all $y_j \in \mathcal{C}$. Therefore, an equilibrium point $x^* \in \mathbb{R}^m_{\geq 0}$ at which $\psi(x^*) \in \ker A_k$, that is, a complex-balanced point, must be such that the current flowing into each complex is "balanced" by the current flowing out of the complex. This is the same as saying that every component of g^* in (4.4) and (4.5) is zero.

To make further progress toward what it means for an equilibrium point to be complex-balanced, we will need the following useful result regarding $\ker A_k$:

Theorem 4.9.3

For $t = \ell$ (and hence for weakly reversible) networks, $\ker A_k = \text{span}\ \{p^1,\ p^2,\ ...,\ p^\ell\}$ where $\{p^1,\ p^2,\ ...,\ p^\ell\}$ is a particular basis satisfying the following property: $p^\theta_{y_j} > 0$ for all $y_j \in \Lambda^\theta$ and $p^\theta_{y_j} = 0$ for all $y_j \notin \Lambda^\theta$, for each $\theta \in \{1,\ 2,\ ...,\ \ell\}$, where Λ^θ is the unique terminal strong linkage class within the linkage class $\mathcal{L}^\theta$.

Proof:
See [100]

Corollary 4.9.4

Because of Theorem 4.9.3 and the coincidence of the terminal strong linkage classes with the linkage classes in a weakly reversible network, it is easily shown that $\ker A_k \bigcap \mathbb{R}^n_+$ is non-empty if and only if the network is weakly reversible [95].

A more meaningful (and interesting) corollary to Theorem 4.9.3 is stated and proved below as Corollary 4.9.5 (taken from [95]). Unlike Remark 4.9.2, κ in this corollary is not a function of some equilibrium point, though it still possess the interpretation of "currents". However, the result will

enable us to tie together our first relationship between weakly reversible networks and complex-balanced points.

Corollary 4.9.5

A chemical reaction network is weakly reversible if and only if there exists $\kappa \in \mathbb{R}^r_+$ such that

$$\sum_{y_j \to y_i \in \mathcal{R}} \kappa_{y_j \to y_i} (\omega_{y_i} - \omega_{y_j}) = 0 \tag{4.8}$$

Proof:

Suppose a network is weakly-reversible. Then for any $k \in \mathbb{R}^r_+$ there exists a $p \in \mathbb{R}^n_+$ such that $A_k p = 0$ (simply use $p = \sum_\theta p^\theta$, where $\{p^\theta\}$ is the basis described in Theorem 4.9.1). Then,

$$\sum_{y_j \to y_i \in \mathcal{R}} k_{y_j \to y_i} p_{y_j} (\omega_{y_i} - \omega_{y_j}) = 0$$

Set $\kappa_{y_j \to y_i} = k_{y_j \to y_i} p_{y_j}$ and the first half follows.

Now suppose that there exists $\kappa \in \mathbb{R}^r_+$ such that $\sum_{y_j \to y_i \in \mathcal{R}} \kappa_{y_j \to y_i} (\omega_{y_i} - \omega_{y_j}) = 0$. Then, $A_\kappa \vec{1} = 0$ (where $\vec{1} \in \mathbb{R}^n_{\geq 0}$ is the vector of all ones) since

$$\sum_{y_j \to y_i \in \mathcal{R}} \kappa_{y_j \to y_i} \vec{1}_{y_j} (\omega_{y_i} - \omega_{y_j}) = \sum_{y_j \to y_i \in \mathcal{R}} \kappa_{y_j \to y_i} (\omega_{y_i} - \omega_{y_j}) = 0$$

Hence, there exists a positive vector, in this case $\vec{1}$, which resides in $\ker A_\kappa$. Hence we have found a value of $k \in \mathbb{R}^r_+$, in this case $k = \kappa$, such that $\ker A_k \bigcap \mathbb{R}^n_+$ is non-empty. According to Remark 4.9.2, this means that the network must be weakly reversible.

□

Remark 4.9.6

The above property suggests that for weakly reversible networks any $x \in \mathbb{R}^m_+$ can be made a complex-balanced equilibrium point by proper choice of the mass-action kinetics (to see this, choose $k_{y_j \to y_i} = \kappa_{y_j \to y_i} / \psi_{y_j}(x)$, where $\kappa \in \mathbb{R}^r_+$ is the vector which satisfies (4.8)). Conversely, it can be shown that for weakly reversible networks (as long as $\dim(\ker Y \bigcap \text{span}\Delta) > 0$) there exists a value of $k \in \mathbb{R}^r_+$ such that the corresponding mass-action network is nowhere complex-balanced in the positive orthant [100]. Fortunately, there is a condition derived in [95] and repeated in Appendix B, which will help us distinguish those kinetics which admit complex-balanced points from those kinetics which do not.

Theorem 4.9.7

Consider any weakly-reversible network endowed with mass-action kinetics. Let $\{p^1, p^2, ..., p^\ell\} \subset \mathbb{R}^n_{\geq 0}$ be a basis for $\ker A_k$ which satisfies the following property: for each $\theta = 1, 2, ..., \ell$, $p^\theta_{y_j} > 0$ for all $y_j \in \mathcal{L}^\theta$ and $p^\theta_{y_j} = 0$ for all $y_j \notin \mathcal{L}^\theta$. Then, there exists an $x^* \in \mathbb{R}^m_+$ such that $\psi(x^*) \in \ker A_k$ if and only if

$$\ln\left(\sum_{\theta=1}^{\ell} p^\theta\right) \in \text{image } Y^T + \mathcal{U} \tag{4.9}$$

where Y^T is the transpose of Y and $\mathcal{U} \triangleq \text{span}\{\omega_{\mathcal{L}^1}, \omega_{\mathcal{L}^2}, ..., \omega_{\mathcal{L}^\ell}\}$.

Proof: See Appendix B or [95].

□

Remark 4.9.8

The condition (4.9) in Theorem 4.9.7 will be used to prove the existence of complex-balanced points in the BAD/tBID and un-catalyzed mass-action networks. As the next section will reveal, the existence of one complex-balanced point for a given mass-action network is sufficient to ensure that all other interior equilibrium points in the same mass-action network are complex-balanced.

4.10 Stability of Equilibrium Points

In this section we introduce the concepts of quasi-thermostatic (QTS) and quasi-thermodynamic (QTD), from the works of [98-99] to study the stability of complex-balanced points (as well as more general equilibrium points). We will find that a QTD mass-action network is a network in which each positive stoichiometric class has a unique interior equilibrium point that is locally asymptotically stable relative to its class (and globally if there are no boundary equilibria). That is, any solution of a QTD mass-action network which is initialized sufficiently close to some unique (and stable) equilibrium point will converge to that point. In fact, in the next chapter we will show that any mass-action network which contains a complex-balanced point is also a QTD mass-action network and therefore exhibits the same well-behaved dynamic behavior. Hence, many of the concepts below regarding QTS and QTD networks will be fundamental to how we must approach the stability and robustness of the BAD/tBID and un-catalyzed tBID/BAK networks.

Definition 4.10.1

A network endowed with mass-action kinetics exhibits normal statics (NS) if there exists one and only one interior equilibrium point $x^* \in \mathbb{R}^m_+$ in each positive stoichiometric class $S \cap \mathbb{R}^m_{\geq 0}$.

Definition 4.10.2

A network endowed with mass-action kinetics exhibits normal dynamics (ND) if the mass-action network exhibits NS, and additionally, each interior equilibrium point $x^* \in S \cap \mathbb{R}^m_+$ is asymptotically stable within its positive stoichiometric class (that is, for all $\varepsilon > 0$ there exists $\delta > 0$ such that

$|x(t)-x^*|<\varepsilon$ for all $t\geq 0$ whenever $|x(0)-x^*|<\delta$, with $x(0)\in S\bigcap\mathbb{R}^m_{\geq 0}$, and $x(t)\to x^*$ as $t\to\infty$.

Remark 4.10.3

We shall see that normal statics and dynamics can be obtained globally for a mass-action network which is quasi-thermodynamic and does not possess any boundary equilibria. Quasi-thermostaticity (QTS) and Quasi-thermodynamicity (QTD) are defined below:

Definition 4.10.4

A network endowed with mass-action kinetics is quasi-thermostatic (QTS) with respect to $x^*\in\mathbb{R}^m_+$ if

$$E_+=\{x\in\mathbb{R}^m_+:\ \ln x-\ln x^*\in D^\perp\}$$

where E_+ is the set of interior equilibrium points defined in Section 4.8.

Definition 4.10.5

A network endowed with mass-action kinetics is quasi-thermodynamic (QTD) if there exists an $x^*\in\mathbb{R}^m_+$ such that

$$\left[\sum_{y_j\to y_i\in\mathcal{R}}k_{y_j\to y_i}x^{y_j}(y_i-y_j)\right]\cdot(\ln x-\ln x^*)\ \leq\ 0 \tag{4.10}$$

for all $x\in\mathbb{R}^m_+$ with equality holding if and only if $\mu\triangleq\ln x-\ln x^*\in D^\perp$.

Remark 4.10.6

In general, for each $x^*\in\mathbb{R}^m_+$, the set $\{x\in\mathbb{R}^m_+:\ \ln x-\ln x^*\in D^\perp\}$ meets each positive stoichiometric class in the interior (i.e. $\mathbb{R}^m_+$) at precisely one point [97]. Such a result is proven in [101], whose proof amounts to exploiting the strictly monotonic nature of the $\ln(\cdot)$ function and the following property: for any $a,b\in\mathbb{R}^m_+$, there exists a unique $\mu\in D^\perp$ such that $ae^\mu-b\in D$. (This is similar to the fact that each vector v in any inner product space $V=W\oplus W^\perp$, with respect to some subspace $W\subset V$, has the unique representation $v=w+w_\perp$ where $w\in W$ and $w_\perp\in W^\perp$.) Nonetheless, a mass-action network which is QTS with respect to some x^* has the property that each positive stoichiometric class contains precisely one interior equilibrium point, and hence exhibits normal statics. Moreover, it is immediate that x^* is an equilibrium point and the mass-action network is QTS with respect to any other interior equilibrium point. Hence we may talk of a network which is QTS without respect to any particular point.

Remark 4.10.7

There exists a very nice relationship between the set $Z_1 = \{x \in \mathbb{R}^m_+ : \ \ln x - \ln x^* \in D^\perp\}$ and the set $Z_2 = \{x \in \mathbb{R}^m_+ : \ A_k \psi(x) = 0\}$ of interior complex-balanced points whenever $Z_2 \neq \phi$ and $x^* \in Z_2$, where x^* is the point used to create Z_1. In fact, we must have $Z_1 = Z_2$. That is, given some mass-action network, if there exists at least one complex-balanced point, then $\{x \in \mathbb{R}^m_+ : \ \ln x - \ln x^* \in D^\perp\}$ is equivalent to the set of all complex-balanced points and furthermore, because $\{x \in \mathbb{R}^m_+ : \ \ln x - \ln x^* \in D^\perp\}$ meets each positive stoichiometric class in precisely one point, there exists precisely one *complex-balanced* point in each positive stoichiometric class. This is thoroughly proven in [101], but the reasoning is as follows: Let $x^{**} \in \mathbb{R}^m_+$ be any point in Z_1. Then, we must have $(\ln x^{**} - \ln x^*) \cdot (y_i - y_j) = 0$ for all $y_j \to y_i \in \mathcal{R}$, that is,

$$y_j \cdot \ln\left(\frac{x^{**}}{x^*}\right) = y_i \cdot \ln\left(\frac{x^{**}}{x^*}\right)$$

or

$$\left(\frac{x^{**}}{x^*}\right)^{y_j} = \left(\frac{x^{**}}{x^*}\right)^{y_i}$$

for all $y_j \to y_i \in \mathcal{R}$. In particular, this means that $\frac{(x^{**})^{y_j}}{(x^*)^{y_j}}$ is constant on each linkage class $\mathcal{L}^\theta$. More precisely, for each $\theta = 1, \ldots, \ell$ there exists a constant $\eta_\theta > 0$ such that $\frac{(x^{**})^{y_j}}{(x^*)^{y_j}} = \eta_\theta$ for all $y_j \in \mathcal{L}^\theta$. Now because x^* is also a complex-balanced point, we must have $A_k \psi(x^*) = 0$, or $\psi(x^*) = \sum_\theta \lambda_\theta p^\theta$ for some set $\{\lambda_\theta\}_{\theta=1,\ldots,\ell}$ of positive numbers and where $\{p^\theta\}_{\theta=1,\ldots,\ell}$ is the particular basis of $\ker A_k$ discussed in Theorem 4.9.3. So, this means for each $\theta = 1, \ldots, \ell$, $(x^{**})^{y_j} = \eta_\theta (x^*)^{y_j} = \eta_\theta \lambda_\theta p^\theta_{y_j}$ for all $y_j \in \mathcal{L}^\theta$. Hence, $\psi(x^{**}) = \sum_\theta \eta_\theta \lambda_\theta p^\theta$ and therefore $x^{**} \in Z_2$ must be a complex-balanced point. These arguments are easily reversed and so $Z_1 = Z_2$.

Remark 4.10.8

Although we can precisely describe the set of all interior complex-balanced points (if they exist) by the set Z_1, it remains to be unfolded whether such a mass-action network is even QTS. That is, how do we know that there are no other interior equilibrium points which are *not* complex-balanced? To do this, we need to take a look at QTD networks.

Remark 4.10.9

A QTD mass-action network is one which exhibits *both* normal statics and dynamics. Roughly speaking, condition (4.10) provides the negative semi-definiteness condition of a Lyapunov function,

and the "only if" condition in (4.10) ensures that all interior equilibria are precisely given by the set $\{x \in \mathbb{R}^m_+ : \ \ln x - \ln x^* \in D^\perp\}$. The reader is referred to [99] for details of the stability proof. Moreover, if one can find an $x^* \in \mathbb{R}^m_+$ satisfying the requirements of QTD, it can be shown that x^* is an interior equilibrium point [98-99]. And if those requirements are satisfied by one interior equilibrium point, then they are satisfied by all other interior equilibria [98-99]. Hence, like the QTS property, we can talk of a mass-action network which is QTD without respect to any particular point.

Remark 4.10.10

We defer until the next chapter that any complex-balanced point $x^* \in \mathbb{R}^m_+$ satisfies (4.10) (and also do not explain the QTD proof in [99]) since we would like to extend the stability results in [95] for mass-action networks which possess a complex-balanced point and which include certain state-dependent perturbations. Nonetheless, any mass-action network which contains at least one complex-balanced point must be a QTD mass-action network and therefore exhibits normal statics and dynamics. In particular, this ensures that not only do Z_1 and Z_2 coincide, but that there are no other interior equilibria which are not complex-balanced. In conclusion, any mass-action network which contains at least one complex-balanced has the property that in each positive stoichiometric class there exists one and only one interior equilibrium point, and that point is locally asymptotically stable with respect to its class (and globally if there are no boundary equilibria). Like before, we may talk of a complex-balanced mass-action network without respect to any particular point.

Remark 4.10.11

To show that there exists a complex-balanced point in any given weakly reversible we need only check the condition (4.9) in Theorem 4.9.7. This is what we will do for the BAD/tBID and un-catalyzed tBID/BAK networks. This is thoroughly pursued in Appendix B.

5 Stability of Complex-Balanced Mass-Action Networks under Perturbations

In this chapter we prove the global asymptotic stability of *any* complex-balanced network under state-dependent perturbations which preserve stoichiometric classes and satisfy a certain magnitude constraint. This is a novel result which generalizes the contributions made by Sontag in 2001 for deficiency-zero networks (which comprise a subset of complex-balanced networks) [92]. Our theoretical contributions in the study of chemical reaction networks can be summarized by Lemma 1 and Theorem 1 shown below.

We will look at equations of the form

$$\dot{x} = \bar{f}(x) \triangleq f(x) + g(x) \tag{5.1}$$

where $f(x) \triangleq \sum_{y_j \to y_i \in \mathcal{R}} k_{y_j \to y_i} x^{y_j} (y_i - y_j)$ is the vector field associated with a complex-balanced network and $g(x) \triangleq \sum_{y_j \to y_i \in \mathcal{R}} \Delta_{y_j \to y_i}(x)(y_i - y_j)$ is a locally Lipschitz vector field on $\mathbb{R}^m_{\geq 0}$ representing perturbations. The introduction of perturbations, of course, brings up the discussion of whether or not we are even dealing with a chemical reaction network anymore. Consequently, we will be introducing a few mild assumptions (A.1-A.3). In particular, we will be using the same type of class-preserving perturbations which were studied by Sontag in [92].

Lemma 1

Consider the perturbed system (5.1) and suppose that assumptions (A.1), (A.2), and the persistence property (A.3) (to be defined below) are satisfied. Let $S \bigcap \mathbb{R}^m_{\geq 0}$ be some positive stoichiometric class. Denote $x^* \in S \bigcap \mathbb{R}^m_+$ to be the unique interior equilibrium point of the complex-balanced mass-action network represented in (5.1) when $g \equiv 0$. Then, there exists a set of continuous functions $\{\delta^S_\theta\}_{\theta=1,\ldots,\ell}$, such that whenever $\sqrt{\sum_{y_j \to y_i \in \mathcal{R}^\theta} \Delta_{y_j \to y_i}(x)^2} \leq \delta^S_\theta(x)$ for all $x \in S \bigcap \mathbb{R}^m_+$ and for all θ, where $\mathcal{R}^\theta \triangleq \{y_j \to y_i : \ y_i, y_j \in \mathcal{L}^\theta\}$, then

$$\bar{f}(x) \cdot (\ln x - \ln x^*) < 0$$

for all $x \in S \bigcap \mathbb{R}^m_+$ such that $x \neq x^*$.

Theorem 1

Suppose that the conditions of Lemma 1 are satisfied, so that $\bar{f}(x) \cdot (\ln x - \ln x^*) < 0$ for all $x \in S \bigcap \mathbb{R}^m_+$ such that $x \neq x^*$. Then for each $\xi \in S \bigcap \mathbb{R}^m_{\geq 0}$ there exists a unique solution $x(\cdot)$ to (5.1) with $x(0) = \xi$, defined for all $t \geq 0$, and where

$$x \to \{x^*\} \bigcup E^*_0$$

where $E^*_0 \triangleq \{x \in \partial\mathbb{R}^m_{\geq 0} : \ \bar{f}(x) = 0\}$ is the set of boundary equilibria for (5.1). If, in addition, $E^*_0 = \phi$, then x^* is a globally asymptotically stable point relative to $S \bigcap \mathbb{R}^m_{\geq 0}$.

Lemma 1 and Theorem 1 proves stability and permits the study of robustness for certain perturbed chemical reaction networks, providing an upper bound on perturbations below which global asymptotic stability is guaranteed. In Chapter 6 we will apply our result to the BAD/tBID and tBID/BAK sub-networks. The global asymptotic stability of the complex-balanced BAD/tBID sub-network will follow immediately by setting all perturbations to zero. This is because $g \equiv 0$ will be assumed to be an admissible perturbation. On the other hand, we will apply the result to the un-catalyzed tBID/BAK network in the following sense: We treat the missing reaction of tBID catalyzing the activation of BAK as a perturbation to the un-catalyzed tBID/BAK network, an otherwise complex-balanced network. We then derive the upper bound as stipulated by our robust stability result. Further consideration of the upper bound will enable us to make definitive claims about the dynamic behavior of the full *catalyzed* network, without having to specify numerical values for the kinetic rate constants.

5.1 Definition of a Perturbed Complex-Balanced Network

Below, f will take the form of a mass-action network, defined earlier as (4.1), and g will be described by a collection of locally Lipschitz functions $\{\Delta_{y_j \to y_i} : \mathbb{R}^m_{\geq 0} \to \mathbb{R}_{\geq 0}\}$, one for each reaction $y_j \to y_i \in \mathcal{R}$, and where each function will enter into the perturbed differential equation as the product $\Delta_{y_j \to y_i}(x)(y_i - y_j)$.

Definition 5.1.1

We define our perturbed system,

$$\begin{aligned} \dot{x} = \bar{f}(x) &= f(x) + g(x) \\ &\triangleq \sum_{y_j \to y_i \in \mathcal{R}} k_{y_j \to y_i} x^{y_j} (y_i - y_j) \; + \sum_{y_j \to y_i \in \mathcal{R}} \Delta_{y_j \to y_i}(x)(y_i - y_j) \end{aligned} \tag{5.1}$$

with the following assumptions:

(A.1) $f : \mathbb{R}^m_{\geq 0} \to \mathbb{R}^m$ is a vector field induced by a complex-balanced mass-action network; and

(A.2) Each $\Delta_{y_j \to y_i} : \mathbb{R}^m_{\geq 0} \to \mathbb{R}_{\geq 0}$ is a locally Lipschitz vector field satisfying the following property: If there exists $k \in \{l : y_{lj} \neq 0\}$ such that $x_k = 0$, then $\Delta_{y_j \to y_i}(x) = 0$. (Physically, this means that the perturbation is zero whenever one or more of the reactant species' concentrations are zero.)

Similarly, each component in (5.1) may be expressed as

$$\begin{aligned} \dot{x}_k = \bar{f}_k(x) &= f_k(x) + g_k(x) \\ &\triangleq \sum_{y_j \to y_i \in \mathcal{R}} k_{y_j \to y_i} x^{y_j} (y_{ki} - y_{kj}) \; + \sum_{y_j \to y_i \in \mathcal{R}} \Delta_{y_j \to y_i}(x)(y_{ki} - y_{kj}) \end{aligned} \tag{5.2}$$

Remark 5.1.2

Because each $\Delta_{y_j \to y_i}(\cdot)$ is locally Lipschitz, $\bar{f}(\cdot)$ is locally Lipschitz, and so there exists a unique forward-evolving maximal solution $x(\cdot)$ with $x(0) \in \mathbb{R}^m_{\geq 0}$ and with maximal interval $[0, \sigma)$. (A.2) requires that the perturbation $\Delta_{y_j \to y_i}(\cdot)$, corresponding to the reaction $y_j \to y_i \in \mathcal{R}$, behaves like the monomial $x^{y_j} = x_1^{y_{1j}} x_2^{y_{2j}} \cdots x_m^{y_{mj}}$. That is, the perturbation is zero whenever one or more of the reactant species' concentrations are zero.

Remark 5.1.3

Of particular importance is to define perturbations which keep any solution of (5.1) within the non-negative orthant $\mathbb{R}^m_{\geq 0}$ as well as in the stoichiometric coset S. It follows from (A.2) that any solution cannot escape $\mathbb{R}^m_{\geq 0}$. To see this, suppose that $x_k = 0$ and consider the term

$$\Delta_{y_j \to y_i}(x)(y_{ki} - y_{kj}) = \Delta_{y_j \to y_i}(x) y_{ki} - \Delta_{y_j \to y_i}(x) y_{kj}$$

If $y_{kj} = 0$, then this term is nonnegative because $\Delta_{y_j \to y_i}(x) \geq 0$ and $y_{ki} \geq 0$. If $y_{kj} \neq 0$, then $k \in \{l : y_{lj} \neq 0\}$ and therefore $\Delta_{y_j \to y_i}(x) = 0$ since $x_k = 0$. Again, the term is non-negative. It follows that $x_k = 0$ implies $g_k(x) \geq 0$. Combining this with the fact that $x_k = 0$ implies $f_k(x) \geq 0$ (because $\mathbb{R}^m_{\geq 0}$ is forward-invariant for the differential equations induced from mass-action networks), it follows that $x_k = 0$ implies $\bar{f}_k(x) \geq 0$. The invariance of S is ensured by the fact that $\Delta_{y_j \to y_i}(x)(y_i - y_j)$ lies point-wise in $D = \text{span}\,\{y_i - y_j : y_j \to y_i \in \mathcal{R}\}$. In conclusion, (5.1) preserves the forward-invariance of the stoichiometric class $S \cap \mathbb{R}^m_{\geq 0}$.

Remark 5.1.4

Because we have $\bar{f}_k(x) \geq 0$ whenever $x_k = 0$, we can use the same proof as in [92] for our perturbed system to show that if $x(\cdot)$ is some forward maximal solution, with an initial condition such that $x_k(0) > 0$, then $x_k(t) > 0$ for all definable times $t \geq 0$. In other words, $\mathbb{R}_+$ is forward-invariant for each of the components described by (5.2). Naturally, this means $\mathbb{R}^m_+$ is forward-invariant for (5.1).

5.2 The Behavior of Complex-Balanced Networks Operating on the Boundary

Below we introduce a reformulation of (5.2) from [92] and derive a couple useful properties, whose proofs are based loosely on those used in [92]. These properties will enable us to better understand the significance and effects of boundary equilibria and boundary solutions of (5.1) which will be needed in the proof of Theorem 1.

The k^{th} component of $\bar{f}(x)$, that is $\bar{f}_k(x)$, satisfies $\bar{f}_k(x) = f_k(x) + g_k(x)$ where $f_k(x)$ is the k^{th} component of $f(x)$ and $g_k(x)$ is the k^{th} component of $g_k(x)$. According to [92],

$$\bar{f}_k(x) = \alpha_k(x)x_k + \beta_k(x) + g_k(x) \tag{5.3}$$

where $\alpha_k : \mathbb{R}^m_{\geq 0} \to \mathbb{R}$ and $\beta_k : \mathbb{R}^m_{\geq 0} \to \mathbb{R}$ are defined by

$$\alpha_k(x) \triangleq \sum_{j \in J_{k,1}} \left(\sum_{y_j \to y_i \in \mathcal{R}} k_{y_j \to y_i}(y_{ki} - y_{kj}) \right) x_1^{y_{1j}} x_2^{y_{2j}} \cdots x_k^{y_{kj}-1} \cdots x_m^{y_{mj}}$$

and

$$\beta_k(x) \triangleq \sum_{j \in J_{k,0}} \left(\sum_{y_j \to y_i \in \mathcal{R}} k_{y_j \to y_i} y_{ki} \right) x_1^{y_{1j}} x_2^{y_{2j}} \cdots x_m^{y_{mj}}$$

where $J_{k,1} \triangleq \{j : y_{kj} \neq 0\}$ indicates those complexes which contain at least one molecule of species k, and $J_{k,0} \triangleq \{j : y_{kj} = 0\}$ indicates those complexes which do not contain any number of molecules of species k. By partitioning the set of complexes $\mathcal{C}$ according to these sets, we are equivalently partitioning $\mathcal{R}$ into

1) All reactions such that the reactant complex is represented in $J_{k,1}$; and

2) All reactions such that the reactant complex is represented in $J_{k,0}$.

With this interpretation, $\alpha_k(x)$ and $\beta_k(x)$ have been defined as sums over the first and second set, respectively. As shown in (5.3), such definitions enable us to factor out an x_k from all those reaction rates which include this factor or a multiple thereof.

Lemma 5.2.1

Consider the perturbed system (5.1), along with (A.1) and (A.2). Suppose that for all $l \in S_j$, $x_l > 0$, where $S_j \triangleq \{k : y_{kj} \neq 0\}$. Then for each complex y_i such that $k_{y_j \to y_i} \neq 0$, we have the property that for all $k \in S_i$, either $x_k > 0$ or $\bar{f}_k(x) > 0$.

Proof:

Suppose we have a reaction $y_{\bar{j}} \to y_{\bar{i}}$ such that the above condition is satisfied. Let $k \in S_{\bar{i}}$ and suppose that $x_k = 0$. Since we know that $x_l \geq 0$ for any l by the forward-invariance of $\mathbb{R}^m_{\geq 0}$ for (5.1), it suffices to show that $\bar{f}_k(x) > 0$. By assumption and because $x_k = 0$, k cannot be an index which is in $S_{\bar{j}}$. That is, the complex $y_{\bar{j}}$ cannot contain the k^{th} species. In terms of the sets defined above this means $\bar{j} \in J_{k,0}$. So,

$$\begin{aligned} \bar{f}_k(x) &= \alpha_k(x)x_k + \beta_k(x) + g_k(x) \\ &= \beta_k(x) + g_k(x) \end{aligned}$$

$$= \sum_{j \in J_{k,0}} \left(\sum_{y_j \to y_i \in \mathcal{R}} k_{y_j \to y_i} y_{ki} \right) x_1^{y_{1j}} x_2^{y_{2j}} \cdots x_m^{y_{mj}} + g_k(x)$$

$$\geq \left(\sum_{y_{\bar{j}} \to y_i \in \mathcal{R}} k_{y_{\bar{j}} \to y_i} y_{ki} \right) x_1^{y_{1\bar{j}}} x_2^{y_{2\bar{j}}} \cdots x_m^{y_{m\bar{j}}} + g_k(x)$$

$$\geq k_{y_{\bar{j}} \to y_{\bar{i}}} y_{k\bar{i}} x_1^{y_{1\bar{j}}} x_2^{y_{2\bar{j}}} \cdots x_m^{y_{m\bar{j}}} + g_k(x)$$

where we have first discarded all members of $J_{k,0}$ except $\bar{j}$ and then, second, discarded all reactions except $y_{\bar{j}} \to y_{\bar{i}}$ itself. This can be done since every component of every complex is non-negative and $x^{y_j} \geq 0$ for any $y_j \in \mathcal{C}$. Note that $k_{y_{\bar{j}} \to y_{\bar{i}}} > 0$. Also note that because $k \in S_{\bar{i}}$ by assumption, we must have $y_{k\bar{i}} > 0$. Finally, because $x_l > 0$ for all $l \in S_{\bar{j}}$, we must have $x^{y_{\bar{j}}} = x_1^{y_{1\bar{j}}} x_2^{y_{2\bar{j}}} \cdots x_m^{y_{m\bar{j}}} > 0$. Hence,

$$\bar{f}_k(x) > g_k(x) \geq 0$$

since $g_k(x) \geq 0$ whenever $x_k = 0$ (see Remark 5.1.3).

□

Corollary 5.2.2

Consider the perturbed system (5.1), along with assumptions (A.1) and (A.2). Suppose that at time t^*, $x_l(t^*) > 0$ for all $l \in S_{j_0}$, where j_0 corresponds to some complex $y_{j_0} \in \mathcal{L}^\theta$. Then $x(t)^{y_j} > 0$ for all $y_j \in \mathcal{L}^\theta$ for $t > t^*$. (In other words, whatever species comprise one or more complexes in the linkage class $\mathcal{L}^\theta$, these species will have positive concentrations for all definable times $t > t^*$.)

Proof:

Consider any complex $y_j \in \mathcal{L}^\theta$ which is not y_{j_0}. Because the network is weakly reversible, there exists a finite sequence of complexes $\{y_{j_0}, y_{j_1}, ..., y_{j_N}\}$ in $\mathcal{L}^\theta$ with $y_{j_N} = y_j$ such that $y_{j_0} \to y_{j_1} \to \cdots \to y_{j_N}$. Application of Lemma 5.2.1 shows that either $x_k(t^*) > 0$ or $\bar{f}_k(x(t^*)) > 0$ for all $k \in S_{j_1}$. Consider one such $k \in S_{j_1}$. If $x_k(t^*) > 0$, then the invariance of $\mathbb{R}_+$ for (5.2) implies $x_k(t) > 0$ for $t > t^*$. In the other case if $\dot{x}_k(t^*) = \bar{f}_k(x(t^*)) > 0$, with $x_k(t^*) = 0$, then it follows that $x_k(t) > 0$ for $t - t^*$ small enough and so by $\mathbb{R}_+$-invariance again $x_k(t) > 0$ for $t > t^*$. So because $x_l(t) > 0$ for all $l \in S_{j_1}$ for $t > t^*$, we can continue this process to S_{j_2} (again applying Lemma 5.2.1), and then on up to $S_{j_N} = S_j$. Hence, $x_k(t) > 0$ for all $k \in S_j$ for $t > t^*$. Since y_j was any arbitrary complex in $\mathcal{L}^\theta$, this means $x(t)^{y_j} > 0$ for all $y_j \in \mathcal{L}^\theta$ for $t > t^*$.

□

Remark 5.2.3

What Corollary 5.2.2 roughly tells us is that if any monomial x^{y_j} is "on", that is if $\psi_{y_j}(x(t^*)) = x(t^*)^{y_j} > 0$ for some $y_j \in \mathcal{L}^\theta$ at time $t = t^*$, then every monomial in the linkage class $\mathcal{L}^\theta$ turns "on" for all definable times $t > t^*$.

5.3 Persistence Property

In deriving a result concerning the global asymptotical stability of (5.1), we will need some form of "persistence" preventing trajectories from remaining on the boundary $\partial\mathbb{R}^m_{\geq 0}$. In this instance, we presume that any trajectory of (5.1), initialized on the boundary but which are not equilibrium solutions, must immediately move into the interior $\mathbb{R}^m_+$ for greater times. More precisely, we require:

(A.3) Any forward maximal solution $x(\cdot)$ with $x(0) \in \partial\mathbb{R}^m_{\geq 0} \setminus E_0^*$ defined on the maximal interval $[0, \sigma)$ must be such that $x(t) \in \mathbb{R}^m_+$ for all $t \in (0, \sigma)$. Here $E_0^* \triangleq \{x \in \partial\mathbb{R}^m_{\geq 0} : \bar{f}(x) = 0\}$ is the set of boundary equilibrium points for the perturbed network defined in (5.1).

Remark 5.3.1

Assumption (A.3) will not preclude the consideration of boundary equilibria in Theorem 1; nor will it preclude the consideration of solutions initialized on the boundary; however, it will preclude consideration of forward solutions evolving nontrivially on the boundary for any length of time. Fortunately, the persistence assumption does not greatly hinder generality. As outlined in Appendix C it is shown that, in situations where the persistence property does not hold we can always decompose a perturbed network into two sub-networks, one which is a perturbed network satisfying the persistence property and another which has a trivial solution. Then, we may proceed as before, analyzing the first sub-network as one which satisfies (A.3). The disadvantage to this approach is of course that all various combinations of sub-networks must be investigated. Fortunately in the case of the BAD/tBID and catalyzed tBID/BAK networks, we do not even need to do this because (A.3) is already satisfied as long as the total concentrations (total BAD, total tBID, total Bcl-2, and total BAK) are all non-zero (this is also shown in Appendix C).

5.4 Lemma 1 and its Proof

To prove Lemma 1 we first need to slightly extend Lemma VIII.1 in [92]. The result is stated below, and proof is provided at the end of Appendix B.

Lemma 5.4.1

Consider any weakly-reversible mass-action network. Define for each linkage class the function

$$Q_\theta(\eta) \triangleq \sum_{y_j \to y_i \in \mathcal{R}^\theta} k_{y_j \to y_i} (\eta_{y_i} - \eta_{y_j})^2$$

for $\eta \in \mathbb{R}^{n_\theta}$, where $\mathcal{R}^\theta = \{y_j \to y_i : \ y_i, y_j \in \mathcal{L}^\theta\}$ and $n_\theta \geq 2$ is the total number of complexes in $\mathcal{L}^\theta$. Then, for each $\theta = 1, 2, ..., \ell$, there exists $\kappa_\theta > 0$ such that

$$Q_\theta \geq \frac{\kappa_\theta}{4n_\theta} \sum_{y_i, y_j \in \mathcal{L}^\theta} (\eta_{y_i} - \eta_{y_j})^2 \tag{5.4}$$

for all $\eta \in \mathbb{R}^{n_\theta}$.

Proof:
See Appendix B.

Lemma 1

Consider the perturbed system (5.1) and suppose that (A.1), (A.2), and the persistence property (A.3) are satisfied. Let $S \bigcap \mathbb{R}^m_{\geq 0}$ be some positive stoichiometric class. Denote $x^* \in S \bigcap \mathbb{R}^m_+$ to be the unique interior equilibrium point of the complex-balanced mass-action network when $g \equiv 0$. Then, there exists a set of continuous functions $\{\delta^S_\theta\}_{\theta=1,...,\ell}$, such that whenever $\sqrt{\sum_{y_j \to y_i \in \mathcal{R}^\theta} \Delta_{y_j \to y_i}(x)^2} \leq \delta^S_\theta(x)$ for all $x \in S \bigcap \mathbb{R}^m_+$ and all θ,

$$\bar{f}(x) \cdot (\ln x - \ln x^*) < 0$$

for all $x \in S \bigcap \mathbb{R}^m_+$ such that $x \neq x^*$.

Proof:
Note that

$$\bar{f}(x) \cdot (\ln x - \ln x^*) = (f(x) + g(x)) \cdot (\ln x - \ln x^*)$$

(here $\cdot$ represents the standard dot product)

We first consider $f(x) \cdot (\ln x - \ln x^*)$

$$\begin{aligned}
&= \sum_{\mathcal{R}} k_{y_j \to y_i} e^{y_j \cdot \ln x} (y_i \cdot (\ln x - \ln x^*) - y_j \cdot (\ln x - \ln x^*)) \\
&= \sum_{\mathcal{R}} k_{y_j \to y_i} e^{y_j \cdot \ln x} (q_i - q_j) \qquad \text{where} \quad q_i \triangleq y_i \cdot (\ln x - \ln x^*) \\
&= \sum_{\mathcal{R}} \left(k_{y_j \to y_i} e^{y_j \cdot \ln x} (q_i - q_j - e^{q_i - q_j} + 1) \right) + \boldsymbol{q}(x, x^*) \\
&= \sum_{\theta} \sum_{\mathcal{R}^\theta} \left(k_{y_j \to y_i} e^{y_j \cdot \ln x} (q_i - q_j - e^{q_i - q_j} + 1) \right) + \boldsymbol{q}(x, x^*) \\
&\leq -\sum_{\theta} \sum_{\mathcal{R}^\theta} \left[k_{y_j \to y_i} e^{y_j \cdot \ln x} \frac{(q_i - q_j)^2}{4 + (q_i - q_j)^2} \right] + \boldsymbol{q}(x, x^*)
\end{aligned} \tag{5.5}$$

where we have added and subtracted

$$q(x,x^*) \triangleq \sum_{\mathcal{R}} k_{y_j \to y_i} e^{y_j \cdot \ln x} (e^{q_i - q_j} - 1)$$

and made use of the fact that $1 + h - e^h \le -\frac{h^2}{4+h^2}$ for any $h \in \mathbb{R}$ (refer to [93]). In this case we used $h = q_i - q_j$. Again, we have also made use of the fact that $\mathcal{R} = \{y_j \to y_i : \ y_i, y_j \in \mathcal{C}\}$ can be partitioned into the sets $\mathcal{R}^\theta = \{y_j \to y_i : \ y_i, y_j \in \mathcal{L}^\theta\}$, for $\theta = 1, 2, ..., \ell$. Since (5.1) is assumed to be complex-balanced at $x = x^*$, it follows that

$$\begin{aligned}
&q(x,x^*) \\
&\quad = \sum_{\mathcal{R}} k_{y_j \to y_i} e^{y_j \cdot \ln x} (e^{q_i - q_j} - 1) \\
&\quad = \sum_{\mathcal{R}} k_{y_j \to y_i} e^{y_j \cdot \ln x^*} (e^{q_i} - e^{q_j}) \\
&\quad = \left[\sum_{\mathcal{R}} k_{y_j \to y_i} e^{y_j \cdot \ln x^*} (\omega_{y_i} - \omega_{y_j}) \right] \cdot \left[\sum_{y_h \in \mathcal{C}} e^{q_h} \omega_{y_h} \right] \\
&\quad = \left[A_k \psi(x^*) \right] \cdot \left[\sum_{y_h \in \mathcal{C}} e^{q_h} \omega_{y_h} \right] \\
&\quad = 0
\end{aligned}$$

Define

$$c_\theta(x) \triangleq \min_{y_j \to y_i \in R^\theta} e^{y_j \cdot \ln x}$$

$$\overline{\delta}_\theta(x,x^*) \triangleq \max_{y_j \to y_i \in \mathcal{R}^\theta} ((y_i - y_j) \cdot (\ln x - \ln x^*))^2$$

$$\delta_\theta(x,x^*) \triangleq \sum_{y_j \to y_i \in \mathcal{R}^\theta} ((y_i - y_j) \cdot (\ln x - \ln x^*))^2$$

$$\overline{\overline{\delta}}_\theta(x,x^*) \triangleq \sum_{y_i, y_j \in \mathcal{L}^\theta} ((y_i - y_j) \cdot (\ln x - \ln x^*))^2$$

Note that $((y_i - y_j) \cdot (\ln x - \ln x^*))^2 = (q_i - q_j)^2$. Continuing with the right-hand-side of (5.5), we find that

$$\begin{aligned}
&f(x) \cdot (\ln x - \ln x^*) \\
&\quad \le -\sum_\theta \sum_{\mathcal{R}^\theta} k_{y_j \to y_i} e^{y_j \cdot \ln x} \frac{(q_i - q_j)^2}{4 + (q_i - q_j)^2} \\
&\quad \le -\sum_\theta \frac{c_\theta(x)}{4 + \overline{\delta}_\theta(x,x^*)} \sum_{\mathcal{R}^\theta} k_{y_j \to y_i} (q_i - q_j)^2 \\
&\quad \le -\sum_\theta \frac{c_\theta(x)}{4 + \overline{\delta}_\theta(x,x^*)} \frac{\kappa_\theta}{4 n_\theta} \sum_{y_i, y_j \in \mathcal{L}^\theta} (q_i - q_j)^2 \\
&\quad \le -\sum_\theta \frac{\kappa_\theta}{4 n_\theta} \frac{c_\theta(x) \overline{\overline{\delta}}_\theta(x,x^*)}{4 + \overline{\delta}_\theta(x,x^*)}
\end{aligned} \tag{5.6}$$

where the last inequality is a result of Lemma 5.4.1. Because for each θ, $\kappa_\theta > 0$ and $c_\theta(x) = \min_{y_j \to y_i \in \mathcal{R}^\theta} x^{y_j} > 0$ whenever $x \in \mathbb{R}^m_+$, the right-hand-side of (5.6) is zero only when $\overline{\overline{\delta}}_\theta = 0$ for all θ. Suppose this is the case. That is, suppose the right-hand-side of (5.6) is zero for some $x \in S \bigcap \mathbb{R}^m_+$. From the definition of $\overline{\overline{\delta}}_\theta$ this means that $\ln x - \ln x^*$ is orthogonal to all $y_i - y_j$ such that $y_j \to y_i$. In other words, $\ln x - \ln x^* \in D^\perp$. But as discussed in Remark 4.10.6, the set $\{x \in \mathbb{R}^m_+ : \ln x - \ln x^* \in D^\perp\}$ meets each positive stoichiometric class in the interior at precisely one point. So since $x \in S \bigcap \mathbb{R}^m_+$ this means $x = x^*$.

We note the similarity of the negative-definiteness of (5.6) with respect to x^* and the quasi-thermodynamic condition in (4.10). In fact, this is why any complex-balanced network is QTD.

Now consider

$$
\begin{aligned}
& g(x) \cdot (\ln x - \ln x^*) \\
& \quad = \sum_{y_j \to y_i \in \mathcal{R}} \Delta_{y_j \to y_i}(x)(y_i \cdot (\ln x - \ln x^*) - y_j \cdot (\ln x - \ln x^*)) \\
& \quad = \sum_{\mathcal{R}} \Delta_{y_j \to y_i}(x)(q_i - q_j) \\
& \quad = \sum_{\theta} \sum_{\mathcal{R}^\theta} \Delta_{y_j \to y_i}(x)(q_i - q_j) \\
& \quad \le \sum_{\theta} \sqrt{\sum_{\mathcal{R}^\theta} \Delta_{y_j \to y_i}(x)^2} \sqrt{\sum_{\mathcal{R}^\theta} (q_i - q_j)^2} \text{ (by re-use of Cauchy-Schwartz inequality)}
\end{aligned}
$$

Combining our results, we see that

$$
\begin{aligned}
& \bar{f}(x) \cdot (\ln x - \ln x^*) \\
& \quad = (f(x) + g(x)) \cdot (\ln x - \ln x^*) \\
& \quad \le -\sum_{\theta} \left(\frac{\kappa_\theta}{4 n_\theta} \frac{c_\theta(x) \overline{\overline{\delta}}_\theta(x, x^*)}{4 + \overline{\delta}_\theta(x, x^*)} \right) + \sum_{\theta} \| \Delta(x) \|_{\mathcal{R}^\theta} \sqrt{\delta_\theta(x, x^*)}
\end{aligned}
\tag{5.7}
$$

where, in this case, $\| \Delta(x) \|_{\mathcal{R}^\theta} \triangleq \sqrt{\sum_{y_j \to y_i \in \mathcal{R}^\theta} \Delta_{y_j \to y_i}(x)^2}$ is the point-wise Euclidean norm of $\Delta(x)$ over the set of reactions $\mathcal{R}^\theta = \{y_j \to y_i : y_i, y_j \in \mathcal{L}^\theta\}$. We need the right-hand-side of (5.7) to be negative for all $x \in S \bigcap \mathbb{R}^m_+$ such that $x \neq x^*$. It is clear that there exists a set of continuous functions $\{\delta^S_\theta\}_{\theta = 1, \ldots, \ell}$, with $\delta^S_\theta : S \bigcap \mathbb{R}^m_+ \to \mathbb{R}_{\ge 0}$, which can be defined so that whenever $\| \Delta(x) \|_{\mathcal{R}^\theta} \le \delta^S_\theta(x)$ for all θ and all $x \in S \bigcap \mathbb{R}^m_+$, the right-hand-side of (5.7) is negative whenever $x \neq x^*$. For example, one could define the set $\{\delta^S_\theta\}_{\theta = 1, \ldots, \ell}$ by

$$
\delta^S_\theta(x) \triangleq \frac{N}{N+1} \frac{\kappa_\theta}{4 n_\theta} \frac{c_\theta(x) \sqrt{\delta_\theta(x)}}{4 + \delta_\theta(x)}
\tag{5.8}
$$

where N is some arbitrarily chosen large number. It is clear that each $\delta_\theta^S(\cdot)$ is well-defined, continuous, and non-negative for each value of $x \in S \bigcap \mathbb{R}_+^m$. To show that it works, we plug each $\delta_\theta^S(x)$ in (5.8) back into (5.7):

$$\begin{aligned}
&\bar{f}(x)\cdot(\ln x - \ln x^*) \\
&\quad \le -\sum_\theta \left(\frac{\kappa_\theta}{4n_\theta} \frac{c_\theta(x)\overline{\overline{\delta}}_\theta(x,x^*)}{4+\overline{\delta}_\theta(x,x^*)} \right) + \sum_\theta \left(\frac{N}{N+1} \frac{\kappa_\theta}{4n_\theta} \frac{c_\theta(x)\sqrt{\delta_\theta(x,x^*)}}{4+\delta_\theta(x,x^*)} \right) \sqrt{\delta_\theta(x,x^*)} \\
&\quad \le -\sum_\theta \left(\frac{1}{N+1} \frac{\kappa_\theta}{4n_\theta} \frac{c_\theta(x)\delta_\theta(x,x^*)}{4+\delta_\theta(x,x^*)} \right)
\end{aligned} \tag{5.9}$$

where we have made use of the fact that $\overline{\delta}_\theta(x,x^*) \le \delta_\theta(x,x^*) \le \overline{\overline{\delta}}_\theta(x,x^*)$. Moreover, using the same logic as we did for (5.6) (that x^* is unique) the right-hand-side of (5.9) must be negative for all $x \in S \bigcap \mathbb{R}_+^m$ such that $x \neq x^*$.

□

5.5 Theorem 1 and its Proof

Because of the persistence property (A.3), any forward maximal solution $x(\cdot)$ which does not belong to some positive stoichiometric class must necessarily be an equilibrium trajectory. In that case, $x(\cdot)$ is obviously defined for all time $t \ge 0$ and trivially we have $x(t) \equiv \xi \in E_0^*$. This is why Theorem 1 below considers stability relative to some *positive* stoichiometric class S. It shows that any forward trajectory in some positive stoichiometric class converges to the set $\{x^*\} \bigcup E_0^*$, where x^* is the unique interior equilibrium point associated with the complex-balanced mass-action network and E_0^* is the set of boundary equilibria for the perturbed system (which may or may not be equivalent to the set of boundary equilibria for the complex-balanced mass-action network). Nonetheless, we are able to describe forward trajectories initialized from *any* point in $\mathbb{R}_{\ge 0}^m$.

Theorem 1

Consider the perturbed system (5.1) and suppose that (A.1), (A.2), and the persistence property (A.3) are satisfied. Let $S \bigcap \mathbb{R}_{\ge 0}^m$ be some positive stoichiometric class. Denote $x^* \in S \bigcap \mathbb{R}_+^m$ to be the unique interior equilibrium point of the complex-balanced mass-action network when $g \equiv 0$. Suppose that the conditions of Lemma 1 are satisfied, so that $\bar{f}(x)\cdot(\ln x - \ln x^*) < 0$ for all $x \in S \bigcap \mathbb{R}_+^m$ such that $x \neq x^*$. Then for each $\xi \in S \bigcap \mathbb{R}_{\ge 0}^m$ there exists a unique solution $x(\cdot)$ to (5.1) with $x(0) = \xi$, defined for all $t \ge 0$, and where

$$x \to \{x^*\} \bigcup E_0^*$$

as $t \to \infty$. If, in addition, $E_0^* = \phi$, then x^* is a globally asymptotically stable point relative to $S \bigcap \mathbb{R}_{\ge 0}^m$.

Proof:
Define the Lyapunov function

$$V : \mathbb{R}^m_{\geq 0} \to \mathbb{R} \ : \ x \mapsto V(x)$$

according to the following two rules:

(1) If $x = (x_1, x_2, ..., x_m) \in \mathbb{R}^m_+$, then $V(x) = \sum_i V_i(x_i)$, where

$$V_i : \mathbb{R}_+ \to \mathbb{R} : \quad x_i \mapsto V_i(x_i) = x_i \ln x_i - x_i - x_i \ln x_i^* + x_i^*$$

(2) If $x \in \partial\mathbb{R}^m_{\geq 0}$, we extend for each k such that $x_k = 0$ the definition of $V_k(\cdot)$ to include the point $x_k = 0$ by defining $V_k(0) = x_k^*$ (permitting some abuse of notation).

Then we can say $V(x) = \sum_i V_i(x_i)$ for any $x = (x_1, x_2, ..., x_m) \in \mathbb{R}^m_{\geq 0}$. Note that each $V_i(\cdot)$ is continuously differentiable on $\mathbb{R}_+$, and each extended $V_i(\cdot)$ is continuous on $\mathbb{R}_{\geq 0}$ since $\lim_{x_i \to 0^+} V_i(x_i) = x_i^*$.

Since the natural logarithm $\ln(\cdot)$ is a strictly concave function, we have the well-known property regarding tangent and secant lines:

$$\ln x_i - \ln x_i^* \geq \frac{x_i - x_i^*}{x_i} \text{ for all } x_i \in \mathbb{R}_+ \text{ with equality if and only if } x_i = x_i^*$$

This implies that $V_i(x_i) = x_i \ln x_i - x_i - x_i \ln x_i^* + x_i^* \geq 0$ for all $x_i \in \mathbb{R}_+$ with equality if and only if $x_i = x_i^*$. Moreover, since $V_i(0) = x_i^* > 0$ for all i, we can conclude that

$$V(x) = \sum_i V_i(x_i) \geq 0 \quad \text{for all } x \in \mathbb{R}^m_{\geq 0} \text{ with equality if and only if } x = x^*$$

In particular, we have positive-definiteness of V in $S \bigcap \mathbb{R}^m_{\geq 0}$ relative to x^* (that is, $V(x^*) = 0$ and $V(x)$ positive elsewhere). Since $V(x)$ is continuous on $S \bigcap \mathbb{R}^m_{\geq 0}$ and $V_i \to \infty$ whenever $x_i \to \infty$, $\{x \in S \bigcap \mathbb{R}^m_{\geq 0} : \ V(x) \leq L\}$, for each $L > 0$, must be a compact subset of $S \bigcap \mathbb{R}^m_{\geq 0}$. In other words, V is proper in $S \bigcap \mathbb{R}^m_{\geq 0}$.

Let $x(\cdot)$ be any forward maximal solution with interval $[0, \sigma)$ and with $x(0) = \xi \in S \bigcap \mathbb{R}^m_{\geq 0}$. If $\xi \in E_0^*$ or $\xi = x^*$, then the trajectory is obviously defined for all $t \geq 0$ and converges trivially to $\{x^*\} \bigcup E_0^*$. So suppose $\xi \notin \{x^*\} \bigcup E_0^*$. Then, $x(t) \in S \bigcap \mathbb{R}^m_+$ for $t \in (0, \sigma)$, by (A.3) and invariance of $\mathbb{R}^m_+$ for (5.1).

Next consider the gradient of the Lyapunov function: $\nabla V(x) = \ln x - \ln x^*$ for $x \in \mathbb{R}^m_+$. Hence, the conclusions of Lemma 1 imply $\nabla V(x) \cdot \bar{f}(x) < 0$ for all $x \in S \bigcap \mathbb{R}^m_+$ such that $x \neq x^*$. This means that $\dot{V}(x(t)) = \nabla V(x(t)) \cdot \bar{f}(x(t)) \leq 0$ for all $t \in (0, \sigma)$ and therefore V is nonincreasing along the solution (in fact it is decreasing since $x(t) \neq x^*$ for any $t \in [0, \sigma)$, which is due to the fact that $\bar{f}(x)$ is locally Lipschitz at x^*). Nonetheless, this means that $x(\cdot)$ must remain in the compact set $\{x \in S \bigcap \mathbb{R}^m_{\geq 0} : \ V(x) \leq V(\xi)\}$. According to Proposition C.3.6 in [94], $x(\cdot)$ is defined for all time $t \geq 0$. Furthermore because $V(x(t))$ is nonincreasing and bounded below by zero, $V(x(t))$ must approach some finite limit as $t \to \infty$. So continuity and LaSalle's Invariance Principle imply that $x(t)$ must approach some invariant limit set, that is,

$$x(t) \to \Omega^+(\xi)$$

as $t \to \infty$, or, more precisely, $\Omega^+(\xi)$ is the forward ω-limit set of $x(\cdot)$. $\Omega^+(\xi)$ is a subset of $\{x \in S \bigcap \mathbb{R}^m_{\geq 0} : \ V(x) = a\}$, for some $a \geq 0$, since $S \bigcap \mathbb{R}^m_{\geq 0}$ is closed. Let $z(\cdot)$ be the forward solution with initial condition $\zeta \in \Omega^+(\xi)$ at time $t = 0$. If $\zeta \in \{x^*\} \bigcup E_0^*$, then, like before, we are done. So suppose not. Much like $x(\cdot)$, $z(\cdot)$ must be defined for all time $t \geq 0$ and furthermore $z(t) \in S \bigcap \mathbb{R}^m_+$ for all $t > 0$. Since $z(t) \neq x^*$ for any $t \geq 0$, $V(z(\cdot))$ must at some time be below a since $\dot{V}(z(t)) < 0$ for all $t > 0$. This contradicts the fact that $z(t) \in \{x \in S \bigcap \mathbb{R}^m_{\geq 0} : \ V(x) = a\}$ for all $t \geq 0$.

Therefore, $x \to \Omega^+(\xi) = \{x^*\} \bigcup E_0^*$ as $t \to \infty$.

□

Remark 5.5.1

Theorem 1 gives us global asymptotic stability of *any* appropriately-perturbed complex-balanced mass-action network as long as there are no boundary equilibria. We will see that both the BAD/tBID and the catalyzed tBID/BAK network do not possess any boundary equilibria as long as their total concentrations remain non-zero (i.e., $[\mathrm{BAD}_{\mathrm{total}}] > 0$, $[\mathrm{tBID}_{\mathrm{total}}] > 0$, $[\mathrm{BAK}_{\mathrm{total}}] > 0$, and $[\mathrm{Bcl\text{-}2}] > 0$). Proof is provided in Appendix C.

6 Application of Theorem 1 to the BAD/tBID and Catalyzed tBID/BAK Networks

Theorem 1 in Chapter 5 proves global asymptotic stability of complex-balanced mass-action networks as well as a way to measure robustness, providing an upper bound on perturbations below which Lyapunov stability is maintained. In this chapter we will use Theorem 1 to conclude global asymptotic stability of the complex-balanced BAD/tBID network as well as to derive under what conditions the complex-balanced *catalyzed* tBID/BAK sub-network is globally asymptotically stable. The former is a straightforward application of the stability result since there are no perturbations, that is, $g \equiv 0$. On the other hand, the latter network is a perturbed complex-balanced network, incorporating the missing tBID catalysis reaction as a perturbation to the *un-catalyzed* tBID/BAK network. As we shall see, the application of our theoretical results leads to a state-dependent condition, which if satisfied, ensures that the perturbed network, in this case the catalyzed tBID/BAK network, is globally asymptotically stable. In particular, the condition will reveal how large the catalysis reaction rate of tBID activating BAK can get before convergence to a non-apoptotic steady state is no longer ensured by Theorem 1. In fact, simulations will show that any catalysis reaction rate beyond this level will lead to polymerization of BAK, indicating that the magnitude constraint, in this case, is not conservative. Finally, through further consideration of the magnitude constraint, we will deduce a more satisfying and biologically-meaningful condition which ensures global convergence to a neighborhood of any "non-apoptotic" steady state. This will remove the ugliness of the state-dependent condition and give us a way to make logical hypotheses about how to design certain drug delivery systems.

The BAD/tBID network is re-illustrated in Fig. 6.1. The catalyzed tBID/BAK network, and how it is created, is illustrated in Fig. 6.2. We show the un-catalyzed tBID/BAK network being combined with its perturbation, the catalyzing reaction $\mathrm{BAK}_{\mathrm{inac}} + \mathrm{tBID} \rightarrow \mathrm{BAK} + \mathrm{tBID}$. Their combination now includes every reaction associated with the different states of tBID, BAK, and Bcl-2 which comprised our original network in Fig. 2.1. The full network is referred to as the catalyzed tBID/BAK network, and the robustness results in Chapter 5 will be used to study the full network. Looking back at equation (5.1), this means that f is the induced differential equations from the network shown at the top of Fig. 6.2 and g is the induced differential term derived from the network shown at the bottom of Fig. 6.2.

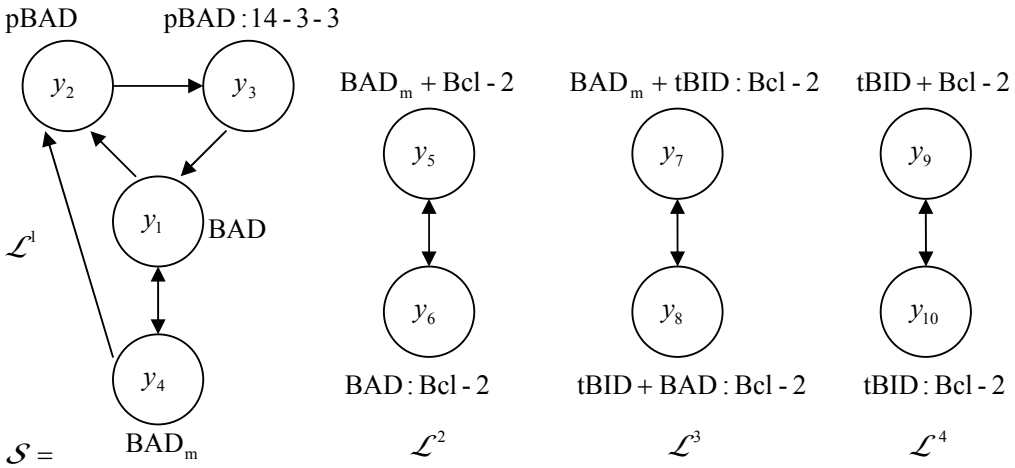

$\mathcal{S}$ =

$\{\text{BAD},\ \text{pBAD},\ \text{pBAD}:14-3-3,\ \text{BAD}_m,\ \text{BAD}:\text{Bcl}-2,\ \text{tBID},\ \text{tBID}:\text{Bcl}-2,\ \text{Bcl}-2\}$

$= \{1,\ 2,\ 3,\ 4,\ 5,\ 6,\ 7,\ 8\}$

FIGURE 6.1 BAD/tBID Chemical Reaction Network

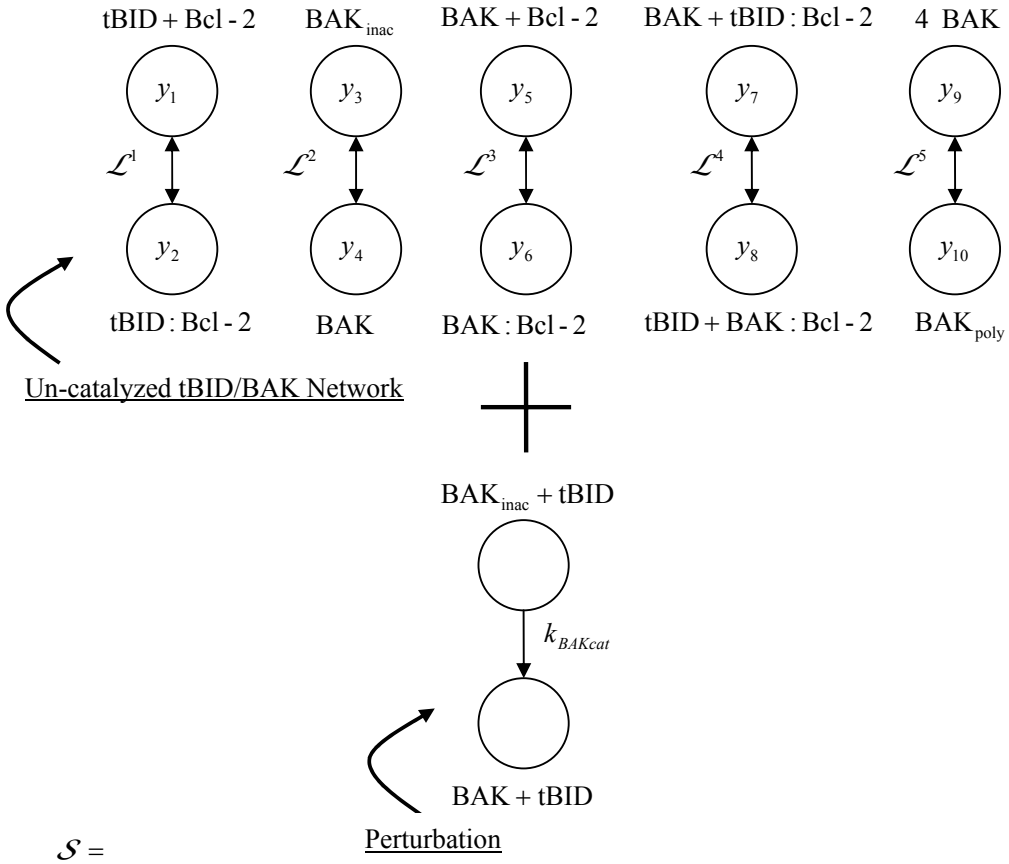

$\mathcal{S}$ =

$\{\text{Bcl}-2,\ \text{tBID},\ \text{tBID}:\text{Bcl}-2,\ \text{BAK}_{inac},\ \text{BAK},\ \text{BAK}:\text{Bcl}-2,\ \text{BAK}_{poly}\}$

$= \{1,\ 2,\ 3,\ 4,\ 5,\ 6,\ 7\}$

FIGURE 6.2 Creating the Catalyzed tBID/BAK Chemical Reaction Network

6.1 Applying the Stability Results to the BAD/tBID Network

For the BAD/tBID chemical reaction network, we label the species, complexes, and linkage classes according to how they are depicted in Fig. 6.1. Recall from Chapter 4 that a mass-action network may be represented in the form $\dot{x} = YA_k\psi(x)$. For the BAD/tBID network,

$$Y = \begin{bmatrix} 1 & 0 & 0 & 0 & 0 & 0 & 0 & 0 & 0 & 0 \\ 0 & 1 & 0 & 0 & 0 & 0 & 0 & 0 & 0 & 0 \\ 0 & 0 & 1 & 0 & 0 & 0 & 0 & 0 & 0 & 0 \\ 0 & 0 & 0 & 1 & 1 & 0 & 1 & 0 & 0 & 0 \\ 0 & 0 & 0 & 0 & 0 & 1 & 0 & 1 & 0 & 0 \\ 0 & 0 & 0 & 0 & 0 & 0 & 0 & 1 & 1 & 0 \\ 0 & 0 & 0 & 0 & 0 & 0 & 1 & 0 & 0 & 1 \\ 0 & 0 & 0 & 0 & 1 & 0 & 0 & 0 & 1 & 0 \end{bmatrix}$$

and

$$A_k = \begin{bmatrix} A_{k1} & 0 & 0 & 0 \\ 0 & A_{k2} & 0 & 0 \\ 0 & 0 & A_{k3} & 0 \\ 0 & 0 & 0 & A_{k4} \end{bmatrix}$$

where

$$A_{k1} = \begin{bmatrix} -k_{BADphos1} - \tau_{BAD}^{in} & 0 & k_{BADrel1} & \tau_{BAD}^{out} \\ k_{BADphos1} & -k_{BADseq} & 0 & k_{BADphos1} \\ 0 & k_{BADseq} & -k_{BADrel1} & 0 \\ \tau_{BAD}^{in} & 0 & 0 & -k_{BADphos1} - \tau_{BAD}^{out} \end{bmatrix}, \; A_{k2} = \begin{bmatrix} -k_{BAD:Bcl-2}^{a} & k_{BAD:Bcl-2}^{d} \\ k_{BAD:Bcl-2}^{a} & -k_{BAD:Bcl-2}^{d} \end{bmatrix},$$

$$A_{k3} = \begin{bmatrix} -k_{tBIDrel1} & k_{BADrel2} \\ k_{tBIDrel1} & -k_{BADrel2} \end{bmatrix}, \text{ and } A_{k4} = \begin{bmatrix} -k_{tBID:Bcl-2}^{a} & k_{tBID:Bcl-2}^{d} \\ k_{tBID:Bcl-2}^{a} & -k_{tBID:Bcl-2}^{d} \end{bmatrix}.$$

The BAD/tBID chemical reaction network depicted in Fig. 6.1 is clearly weakly reversible. To show complex-balancing, we must use Theorem 4.9.7. In Appendix B we show that the needed property of complex-balancing is satisfied in a region of parameter space (and further we show how this region can be expanded). In Appendix C, it is further shown that, as long as $[\text{BAD}_{\text{total}}] > 0$, $[\text{tBID}_{\text{total}}] > 0$, and $[\text{Bcl-2}_{\text{total}}] > 0$, the BAD/tBID mass-action network contains neither boundary equilibria nor trajectories evolving on the boundary. These properties are relegated to the appendices to conserve space and maintain the focus on the current topic. According to Theorem 1 (with $g \equiv 0$), for each positive stoichiometric class $S \cap \mathbb{R}^m_{\geq 0}$, there exists a unique steady state $x^* \in S \cap \mathbb{R}^m_+$ which is globally asymptotically stable relative to $S \cap \mathbb{R}^m_{\geq 0}$. In conclusion, given any initial condition in the non-negative orthant, the corresponding forward trajectory of the complex-balanced BAD/tBID network will be dynamically well-behaved and converge toward a unique and stable steady state. In

the next chapter, we will consider the biological importance of this result. Nonetheless, it is clear that chemical reaction network theory has bought us some information and mathematical sturdiness about the dynamic behavior of the interactions between BAD and tBID, which would be absent from numerical techniques alone.

6.2 Applying the Stability Results to the tBID/BAK Network

In this section, we formulate the catalyzed tBID/BAK network as a perturbed chemical reaction network using the terminology from Chapter 5. We then construct the robustness bound as was done in the proof of Lemma 1 in order to guarantee the conditions of Theorem 1.

The first step is to formulate the un-catalyzed tBID/BAK as a chemical reaction network. Again, we label the species, complexes, and linkage classes according to what is shown in Fig. 6.2. We have for the un-catalyzed chemical reaction network

$$Y = \begin{bmatrix} 1 & 0 & 0 & 0 & 1 & 0 & 0 & 0 & 0 & 0 \\ 1 & 0 & 0 & 0 & 0 & 0 & 0 & 1 & 0 & 0 \\ 0 & 1 & 0 & 0 & 0 & 0 & 1 & 0 & 0 & 0 \\ 0 & 0 & 1 & 0 & 1 & 0 & 0 & 0 & 0 & 0 \\ 0 & 0 & 0 & 1 & 0 & 0 & 1 & 0 & 4 & 0 \\ 0 & 0 & 0 & 0 & 0 & 1 & 0 & 1 & 0 & 0 \\ 0 & 0 & 0 & 0 & 0 & 0 & 0 & 0 & 0 & 1 \end{bmatrix}$$

and

$$A_k = \begin{bmatrix} A_{k1} & 0 & 0 & 0 & 0 \\ 0 & A_{k2} & 0 & 0 & 0 \\ 0 & 0 & A_{k3} & 0 & 0 \\ 0 & 0 & 0 & A_{k4} & 0 \\ 0 & 0 & 0 & 0 & A_{k5} \end{bmatrix}$$

where

$$A_{k1} = \begin{bmatrix} -k^a_{tBID:Bcl-2} & k^d_{tBID:Bcl-2} \\ k^a_{tBID:Bcl-2} & -k^d_{tBID:Bcl-2} \end{bmatrix}, \; A_{k2} = \begin{bmatrix} -k^{ac}_{BAK} & k^{inac}_{BAK} \\ k^{ac}_{BAK} & -k^{inac}_{BAK} \end{bmatrix}, \; A_{k3} = \begin{bmatrix} -k^a_{BAK:Bcl-2} & k^d_{BAK:Bcl-2} \\ k^a_{BAK:Bcl-2} & -k^d_{BAK:Bcl-2} \end{bmatrix},$$

$$A_{k4} = \begin{bmatrix} -k_{tBIDrel2} & k_{BAKrel1} \\ k_{tBIDrel2} & -k_{BAKrel1} \end{bmatrix}, \text{ and } A_{k5} = \begin{bmatrix} -k^a_{BAKpoly} & k^d_{BAKpoly} \\ k^a_{BAKpoly} & -k^d_{BAKpoly} \end{bmatrix}.$$

The un-catalyzed tBID/BAK chemical reaction network depicted at the top of Fig. 6.2 is clearly weakly reversible. To show complex-balancing, we must use Theorem 4.9.7. Again, this is shown in

Appendix B. In Appendix C, it is further shown that, as long as $[\text{tBID}_{\text{total}}] > 0$, $[\text{BAK}_{\text{total}}] > 0$, and $[\text{Bcl-2}_{\text{total}}] > 0$, the catalyzed tBID/BAK mass-action network contains neither boundary equilibria nor trajectories evolving on the boundary.

To study the full catalyzed tBID/BAK network, we associate the catalysis reaction $\text{BAK}_{\text{inac}} + \text{tBID} \to \text{BAK} + \text{tBID}$ with the perturbation g in (5.1). First, we introduce to the un-catalyzed tBID/BAK network the perturbation

$$g(x) \triangleq \Delta_{y_3 \to y_4}(x)(y_4 - y_3) \tag{6.1}$$

where $\Delta_{y_3 \to y_4}(x) = k_{BAKcat}[\text{BAK}_{\text{inac}}][\text{tBID}]$ is the reaction rate of the reaction $\text{BAK}_{\text{inac}} + \text{tBID} \to \text{BAK} + \text{tBID}$; and where the vector $y_4 - y_3$ is included because in the reaction $\text{BAK}_{\text{inac}} + \text{tBID} \to \text{BAK} + \text{tBID}$, 1 molecule of BAK_{inac} is exchanged for 1 molecule of BAK and no tBID is consumed. In this manner we are creating an admissible perturbation which satisfies assumption (A.2). Of course, we assume $\Delta_{y_j \to y_i}(x) \equiv 0$ for all $y_j \to y_i \in \mathcal{R} - \{y_3 \to y_4\}$, that is, we assume that all other perturbations are identically zero.

In the proof of Lemma 1, we were able to construct a magnitude constraint on the perturbations which ensured the negative-definiteness of the Lyapunov function used to prove Theorem 1. In a similar manner, we use (5.7) to derive a bound for the perturbation $\Delta_{y_3 \to y_4}(x)$. In particular, it can be shown that for the complex-balanced catalyzed tBID/BAK network if

$$k_{BAKcat}[\text{BAK}_{\text{inac}}][\text{tBID}] < \frac{1}{\sqrt{\delta_2(x)}} \sum_{\theta} \left(\frac{\kappa_\theta}{4n_\theta} \frac{c_\theta(x)\delta_\theta(x)}{4 + \delta_\theta(x)} \right) \tag{6.2}$$

for all $x \in S \bigcap \mathbb{R}^m_+$ such that $x \neq x^*$, then the negative-definite condition in (5.7) is satisfied, and the conditions of Theorem 1 are satisfied. Recall that

$\delta_\theta(x) \triangleq \sum_{y_j \to y_i \in \mathcal{R}^\theta} ((y_i - y_j) \cdot (\ln x - \ln x^*))^2$

$c_\theta(x) \triangleq \min_{y_j \to y_i \in \mathcal{R}^\theta} x^{y_j}$

κ_θ is the constant in Lemma 5.4.1, and

n_θ is the number of complexes in linkage class $\mathcal{L}^\theta$.

(Note that $\sqrt{\delta_2(x)}$ appears in the denominator of the right-hand-side of (6.2) since $y_3, y_4 \in \mathcal{L}^2$). So, if (6.2) is satisfied, then the conditions of Theorem 1 are satisfied, and therefore Theorem 1 tells us that x^* is globally asymptotically stable relative to $S \bigcap \mathbb{R}^m_{\geq 0}$. In fact, satisfaction of (6.2) applies to any positive stoichiometric class since the $\delta_\theta(\cdot)$'s can also be thought of as functions of the steady state x^*.

However, the unfortunate aspect of (6.2) is that even if the right-hand-side of (6.2) converges to zero as the system converges to the steady state x^*, the left-hand-side cannot do this (this is due to the fact that [tBID] and $[\text{BAK}_{\text{inac}}]$ must remain positive for all time because there are no boundary equilibria). However, what we can say is that if k_{BAKcat} is sufficiently small, then we can talk about convergence to a region of state space. That is, the only way that (6.2) is violated for sufficiently

small k_{BAKcat}, and hence when Theorem 1 is not applicable, is if the right-hand-side of (6.2) approaches zero. So, suppose the right-hand-side of (6.2), as a function of x, approaches zero. This can only happen if $x \to x^*$ or at least one component of x go to zero (that is, $x_k \to 0$ for some k). This can be seen as follows: If $\delta_2(x) \to 0$, then it is necessary that $\delta_\theta(x) \to 0$ or $c_\theta(x) \to 0$ for each $\theta \neq 2$. This must occur since otherwise the right-hand-side will explode. So we either have $x \to x^*$ (since $\delta_\theta(x) = 0$ for all θ if and only if $x = x^*$) or at least one $x_k \to 0$. If instead $\delta_2(x)$ does not get arbitrarily small, then the positive term $\frac{\kappa_2}{4n_2}\frac{c_2(x)\sqrt{\delta_2(x)}}{4+\delta_2(x)}$ in the right-hand-side of (6.2) can only go to zero if $c_2(x) \to 0$ or $\delta_2(x) \to \infty$ (this is because the positive function $\frac{\sqrt{h}}{4+h}$ for $h > 0$, converges to zero only if $h \to 0$ or $h \to \infty$). Because of conservation, both of these cases imply that at least one $x_k \to 0$. With this in mind, we can prove the following theorem.

Theorem 6.2.1

For all $\varepsilon > 0$ there exists $k_{BAKcat} > 0$ sufficiently small such that for any trajectory $x(\cdot)$, with $x(0) = \xi \in \mathbb{R}^m_{\geq 0}$, of the catalyzed tBID/BAK network,

$$| x(t) - x^* | < \varepsilon$$

for all time $t \geq T$, where $T > 0$.

Proof:

By the persistence property, it follows that $x(t) \in \mathbb{R}^m_+$ for all $t > 0$. Suppose that one of the components of $x(t)$ converges to zero, that is, suppose that the trajectory $x(\cdot)$ is such that $x_k(t) \to 0$ as $t \to \infty$. Note that we keep decreasing k_{BAKcat} so that the trajectory satisfies the conditions of Theorem 1 for any given interval $[0, \sigma)$ with $\sigma < \infty$. Since there are no boundary equilibria of the catalyzed tBID/BAK network and further because the network satisfies the persistence property (see Appendix C), we must have $\bar{f}_k(x(t)) \to \bar{f}_0 > 0$. This means that $\bar{f}_k(x(t))(\ln x_k(t) - \ln x_k^*) \to -\infty$, while for any other component of $x(t)$, say $x_l(t)$, which does not converge to zero, $\bar{f}_l(x(t))(\ln x_l(t) - \ln x_l^*)$ remains bounded (due to conservation and Lipschitz). So, $\dot{V}(x(t)) = \sum_i \bar{f}_i(x(t))(\ln x_i(t) - \ln x_i^*) \to -\infty$ as k_{BAKcat} is decreased to zero. But, for a sufficiently large interval $[0, \sigma)$, with $\sigma < \infty$, there exists a time $t_1 \in [0, \sigma)$ such that $x(t_1) \in \{x : V(x) \leq \min_i x_i^*\}$ since $\dot{V}(x(t))$ continues to grow more negatively. This contradicts the fact that each component of the Lyapunov function possesses the property that $\lim_{x_i \to 0^+} V_i(x_i) = x_i^*$ (see proof of Theorem 1). Hence, we cannot have both $x(t) \in \{x : V(x) \leq \min_i x_i^*\}$ for $t \geq t_1$ and some component $x_k(t) \to 0$ as $t \to \infty$. Therefore, the only way that (6.2) is violated for sufficiently small k_{BAKcat} is if $x \to x^*$.

Because $[\text{tBID}] \leq [\text{tBID}_{\text{total}}]$ and $[\text{BAK}_{\text{inac}}] \leq [\text{BAK}_{\text{total}}]$, this means that

$$k_{BAKcat} < \frac{1}{[\mathrm{BAK}_{\mathrm{total}}][\mathrm{tBID}_{\mathrm{total}}]\sqrt{\delta_2(x)}} \sum_{\theta} \left(\frac{\kappa_\theta}{4n_\theta} \frac{c_\theta(x)\delta_\theta(x)}{4+\delta_\theta(x)} \right)$$

defines a "region of violation" R_V which can be made sufficiently close to x^* by a sufficiently small choice of k_{BAKcat}. So choose $k_{BAKcat} > 0$ and $c_1 > 0$ such that $R_V \subset \{x:\ V(x) \le c_1\} \subset B_\varepsilon(x^*)$, where $B_\varepsilon(x^*)$ is the ε-neighborhood of x^*. Then for sufficiently small k_{BAKcat}, Theorem 1 tells us that any $x(\cdot)$, with $x(0) = \xi \in \mathbb{R}^m_{\ge 0}$, ends up in $\{x:\ V(x) \le c_1\}$ at some time $T > 0$. Moreover, it remains there for all $t \ge T$ because $\bar{f}(x) \cdot (\ln x - \ln x^*) < 0$ for any $x \notin R_V$ which is also on the boundary of the level set $\{x:\ V(x) \le c_1\}$, forcing the level set to be invariant.

Therefore, $x(t) \in B_\varepsilon(x^*)$ for all time $t \ge T$.

□

Remark 6.2.2

Theorem 6.2.1 demonstrates how the addition of the reaction $\mathrm{BAK}_{\mathrm{inac}} + \mathrm{tBID} \rightarrow \mathrm{BAK} + \mathrm{tBID}$ can be thought of as a "stable" network addition to the network which is the un-catalyzed tBID/BAK network. In other words, for sufficiently small $k_{BAKcat} > 0$, the impact of the catalysis reaction does not drastically change the behavior of the un-catalyzed tBID/BAK network. Moreover, this property is global, applying to any trajectory. Although this may appear to be a trivial result, adding in reactions, even when rate constants are set small, can significantly alter the behavior of any given network (refer to [95] for many examples).

6.3 Interpreting the State-Dependent Bound with Simulation

We would like to know if the right-hand-side of (6.2), as a dynamic perturbation, roughly approximates where the asymptotic behavior of the un-catalyzed network is deregulated when x^* is presumed to be a non-apoptotic steady state (that is, when there is no evidence of BAK activation or polymerization). We simulate a perturbed tBID/BAK network when the right-hand-side of (6.2) is substituted into the differential equations and another time when the right-hand-side, scaled by a factor of 3, is substituted. The results are illustrated in Figs. 6.3 and 6.4, respectively. The response in Fig. 6.3 is similar to the response of the un-catalyzed network when the perturbation is not included (data not shown). Nonetheless, this is evident by the negative-definiteness of $\dot{V}(x)$ and the small deviations in the different states of BAK. Hence, the dynamic perturbation caused by the right-hand-side of (6.2) is absorbed by the network and asymptotic behavior to the non-apoptotic steady state is retained.

The second case in Fig. 6.4, however, is significantly different. Here, we see the states of BAK converging to different levels and furthermore observe the polymerization of BAK. Moreover, the negative-definiteness of $\dot{V}(x)$ is clearly violated. Consequently, we conclude that the right-hand-side of (6.2) roughly approximates a dynamic perturbation which deregulates asymptotic stability of the un-catalyzed tBID/BAK network and, in addition, leads to BAK being triggered. Therefore, not only does the right-hand-side of (6.2) provide us with a sufficient condition but also roughly approximates a necessary condition for global asymptotic stability of the complex-balanced catalyzed tBID/BAK network.

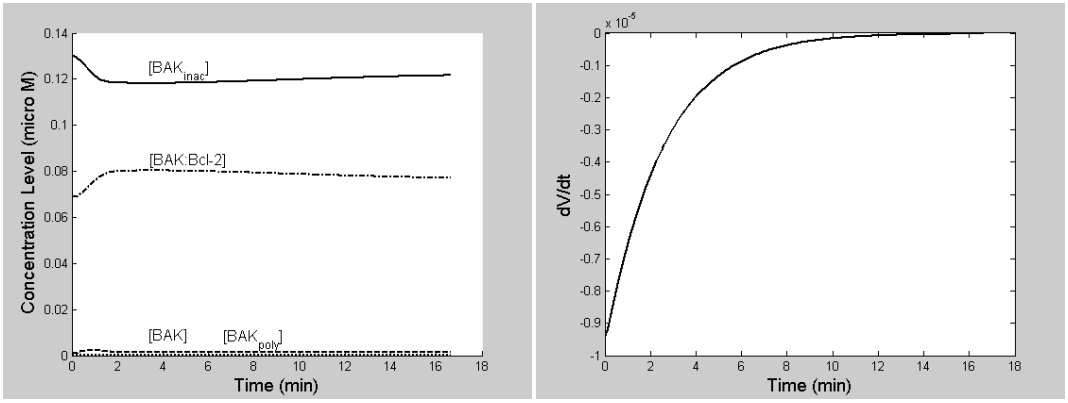

(a) **(b)**

FIGURE 6.3 Time simulations for when the right-hand-side of (6.2) is used to perturbed the un-catalyzed tBID/BAK network. **(a)** Showing the concentration levels of BAK_{inac}, BAK, BAK:Bcl-2, and BAK_{poly}; and **(b)** Showing the derivative of the Lyapunov function (defined in Chapter 5).

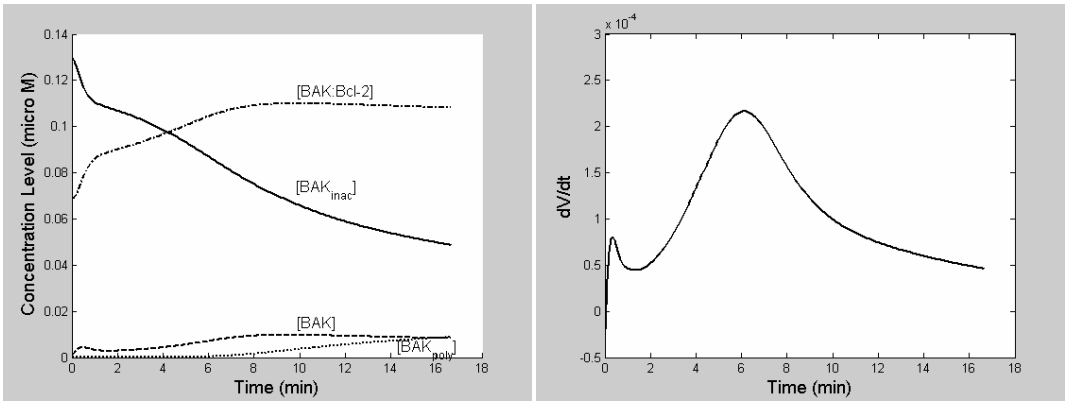

(a) **(b)**

FIGURE 6.4 Time simulations for when the right-hand-side of (6.2), scaled by a factor of 3, is used to perturbed the un-catalyzed tBID/BAK network. **(a)** Showing the concentration levels of BAK_{inac}, BAK, BAK:Bcl-2, and BAK_{poly}; and **(b)** Showing the derivative of the Lyapunov function (defined in Chapter 5).

6.4 Attaching Biological Meaning to the Results for the Catalyzed tBID/BAK Network

We attach biological meaning to the results of Theorem 6.2.1 by looking at steady states of the un-catalyzed network, depicted above as x^*, which are defined to be non-apoptotic. Although we no longer have asymptotic behavior to a *point*, we can talk of asymptotic behavior to a neighborhood of x^*, that is, a neighborhood of a non-apoptotic point -- a non-apoptotic region. This will enable us to make logical hypotheses about the design of certain drug delivery systems.

So suppose x^* is chosen to be a non-apoptotic steady state. Then, according to Theorem 6.2.1, for sufficiently small values of k_{BAKcat} (the kinetic rate constant associated with the catalysis reaction of tBID activating BAK), the catalyzed tBID/BAK network is guaranteed to evolve toward a non-apoptotic region. So, consider the hypothetical design of a drug delivery system, in particular, one

which works by re-regulating pathological deregulations of apoptosis. More specifically, suppose the goal of the design is to block the intrinsic pathway of apoptosis. Then, it may be worthwhile to identify or fabricate molecules which could be used as inhibitors to sufficiently lower the catalysis reaction rate of tBID activating BAK (or even the kinetic rate constant k_{BAKcat}). In this manner, if the reaction rate is decreased enough, then we would be ensured, at least mathematically, that the intrinsic pathway of apoptosis is shut off (through inhibition of BAK polymerization). Moreover, the design would be a logical one since we did not first specify rate constants and the mathematical conclusions are independent of the values of the other rate constants.

7 Conclusions

7.1 Initial Analysis of the BAD/tBID/BAK Network Using Simulation, Bifurcation Diagrams, and a Skeleton Model

We first selected specific rate constants for the BAD/tBID/BAK network and used computer-aided tools such as simulation, bifurcation analysis, and sensitivity analysis to provide us with an initial understanding of the BAD/tBID/BAK network. The study revealed and validated the experimentally-observed sensitization of BAD on the tBID-induction of BAK. The tBID-induction of BAK resembles a robust switch not unlike what is seen in many other cellular signaling pathways. The effect of BAD is one which sensitizes the switch from the activation of tBID to the activation of BAK. In particular, the total concentration of tBID triggers the activation of BAK in an all-or-none fashion, where the total concentration of BAD modulates the location of the triggering point.

We then derived an approximating model, known as the skeleton model, by stripping away the dynamics of BAK and making certain assumptions on the behavior of BAD. Ultimately, the skeleton model expressed the relationship among BAD, tBID, and BAK at an apoptotic triggering point as

$$[\mathrm{tBID}_{\mathrm{total}}] = [\mathrm{tBID}_{\mathrm{act}}] + \frac{[\mathrm{tBID}_{\mathrm{act}}]}{K_{D,tBID} + [\mathrm{tBID}_{\mathrm{act}}]}\left([\mathrm{Bcl\text{-}2}_{\mathrm{total}}] - \frac{1}{1+\alpha_2+(1+\alpha_1)\beta_2}[\mathrm{BAD}_{\mathrm{total}}] \right) \tag{7.1}$$

where $[\mathrm{BAD}_{\mathrm{total}}]$ and $[\mathrm{tBID}_{\mathrm{total}}]$ represent total concentration levels of BAD and tBID, respectively, and $[\mathrm{tBID}_{\mathrm{act}}]$ represents the (assumed constant) level of *free* tBID required to activate BAK. The remaining parameters are functions of rate constants only (see (3.5) for details).

The skeleton model in (7.1) approximates the behavior of the full BAD/tBID/BAK model accurately. Qualitatively, the skeleton model reveals two new facts about the BAD/tBID/BAK network: first, the impact of BAD on the tBID-induction of BAK is much like a titration process where the level of BAD:Bcl-2 reflects the amount of Bcl-2 which is sequestered away from tBID; and second, the level of BAD:Bcl-2, with respect to the total level of BAD, is a simple function of rate constants (phosphorylation, dephosphorylation, sequestration, and translocation rate constants).

Then, turning our attention to the novel kinetic modeling of BAD, we delineated differences between the two modes of phosphorylation of BAD (that is, phosphorylation of Bcl-2-bound BAD and phosphorylation of free unbound BAD). Not yet fully exhausting what the skeleton model could tell us, we combined the equation in (7.1) with "basal" or non-apoptotic steady state assumptions on the network. The assumptions are that $[\mathrm{BAD:Bcl\text{-}2}] << [\mathrm{BAD}_{\mathrm{total}}]$ and $[\mathrm{tBID}] << [\mathrm{tBID}_{\mathrm{total}}]$. In this manner we were able to derive an explicit constraint on the phosphorylation rate constants, necessary to maintain these conditions. In conclusion, what we found concerning the phosphorylation of BAD was that the Bcl-2-bound form of phosphorylation is independently more effective toward the removal of BAD from the mitochondria compared to the unbound form of phosphorylation, which seems to require cooperation from the other form of phosphorylation or a significant reduction in translocation. Interestingly, however, the unbound form of phosphorylation is more effective when the network is in transient. And finally, both modes work together synergistically to remove BAD from the mitochondria.

We then considered what our results about the phosphorylation of BAD meant, and in particular, what they meant in regards to the many experimental discrepancies. In general, we witnessed a potentially large deviation in the average removal of BAD from the mitochondria, depending on what mode(s) of phosphorylation were operating as well as the level of phosphatase present (that is, the

dephosphorylation rate). Moreover, there is no predefined mode or combination of modes of phosphorylation that is occurring in any given cell, since any given cell may either have Bcl-2 or Bcl-x_L expression (or both) (which determine if the phosphorylation-induced dissociation of BAD:Bcl-2 is possible). In conclusion, with such potentially large swings in the removal of mitochondrial BAD, experimental results could become unpredictable if the mode(s) and phosphatase level are not taken into account. As an example, we pointed out that Akt, a BAD kinase, could be mistaken as an inhibitor of apoptosis in one case and not in another merely from the variation as a result of the phosphatase level. Nonetheless, the abnormally high variation in regards to the removal of BAD could indicate why experimental data has come across unpredictable.

7.2 Proving the Stability of Perturbed Complex-Balanced Mass-Action Networks

In Chapter 5 we proved the global asymptotic stability of *any* complex-balanced network under state-dependent perturbations which preserve stoichiometric classes and satisfy a certain magnitude constraint. The result, stated as Lemma 1 and Theorem 1, extended the study of robustness of chemical reaction networks beyond zero-deficiency networks to any arbitrary deficiency network which is complex-balanced. Moreover, the proof of Lemma 1 provides a way to write out an explicit function for the magnitude constraint, which, though a function of states, possesses a nice form incorporating the graphical and stoichiometric properties of the unperturbed network.

Following along the same lines as in [92] we were able to describe the behavior of networks at boundary points (points where at least one state concentration level is zero) and not neglect the impact that such behaviors on the boundary can have on our theoretical results. In past years, much of chemical reaction network theory has been kept peripheral to boundary equilibria and boundary solutions. However, there are many instances where investigation of the boundary is warranted. For example, even the simple reaction network, $A \to B$, contains boundary equilibria. The stability and robustness results in Chapter 5 were derived with these issues in mind. For example, our stability result can be applied to networks which have initial conditions on the boundary or to networks which have boundary equilibria. Finally, in Appendix C, we showed how a network can be decomposed into more manageable sub-networks to deal with periodic orbits evolving on the boundary.

7.3 Applying Our Theoretical Results to the BAD/tBID and Catalyzed tBID/BAK Networks

Upon showing that a complex-balanced BAD/tBID network satisfies the requirements of Theorem 1, we were able to immediately conclude global asymptotic stability. In this case, we showed that for each positive stoichiometric class $S \bigcap \mathbb{R}^m_{\geq 0}$, there exists a unique steady state $x^* \in S \bigcap \mathbb{R}^m_+$ which is globally asymptotically stable relative to $S \bigcap \mathbb{R}^m_{\geq 0}$. In other words, for each values of $[\mathrm{BAD}_{\mathrm{total}}]$, $[\mathrm{tBID}_{\mathrm{total}}]$, and $[\mathrm{Bcl-2}_{\mathrm{total}}]$, all trajectories in the stoichiometric class converge to a unique and stable steady state. Furthermore, this rules out the possibility of any periodic orbits or chaotic behavior. Finally, we know that this stability comes with a certain degree of robustness, which, if desired, can be represented in an explicit form.

Upon showing that a complex-balanced un-catalyzed tBID/BAK network satisfies the requirements of Theorem 1, we made similar conclusions about the *catalyzed* tBID/BAK network, when the perturbation reaction upholds its magnitude constraint. The perturbation used in this paper was the catalyzing reaction of tBID activating BAK. Unfortunately, Theorem 1 could not apply

everywhere. However, we were still interested in knowing whether the addition of the reaction was a "stable" network addition, that is, whether the addition of a new reaction causes any drastic changes in behavior despite what we make the value of the rate constant. We found that the un-catalyzed tBID/BAK is stable in this sense if the rate constant is set sufficiently small.

More biologically meaningful, the conclusion above enables us to understand under what conditions the interactions between tBID and BAK are such that we would be left with a non-apoptotic response. With Theorem 6.2.1, we are able to definitively conclude that for sufficiently small values of k_{BAKcat} (the kinetic rate constant associated with the catalysis reaction of tBID activating BAK), the trajectory of the *catalyzed* tBID/BAK network is guaranteed to evolve toward a region which is local to the steady state of the un-catalyzed tBID/BAK network. And if the steady state of the un-catalyzed tBID/BAK network is one which could be considered "non-apoptotic", then we know that any trajectory of the *catalyzed* tBID/BAK network will be a "non-apoptotic" response.

7.4 Importance of the Results

What separates our work from many of the analyses of apoptotic pathways already studied is the novel inclusion of BAD. We showed how BAD acts as a sensitizer to the tBID-induction of BAK. We further showed that the sensitivity can be mediated by either of two experimentally-observed modes of phosphorylation of BAD which provide mediation in varying degrees, depending on whether these modes work together. The modeling of the phosphorylation of BAD is important since it helps clarify some of the discrepancies observed in experiments. In fact, our results suggest to experimenters whom are testing the BAD signaling response that not only should the kinase and phosphatase levels be measured (enzymes responsible for phosphorylation and dephosphorylation, respectively), the mode(s) of phosphorylation should be monitored (in particular, whether or not the Bcl-2-bound form of phosphorylation is taking place). In conclusion, our mathematical model of BAD provides a first attempt at matching a mathematical model with the experimental model of BAD, and provides some logical answers.

Our novel modeling of BAD is significant since, as a therapeutic target, BAD has the capacity to restore regulation of a cell's ability to respond appropriately to apoptotic stimuli. For example, a cancer cell is sometimes defined by an overexpression of Bcl-2 [10, 22] and hence the cell's appropriate apoptotic response is blocked. As we have seen, an abundance of Bcl-2 subverts the ability of the mitochondrial intrinsic pathway of apoptosis to be engaged. Recently, man-made BAD and BID peptides resembling their endogenous counterparts have been fabricated with the intent of delivering these peptidomimetics to tumor cells and restoring mitochondrial sensitivity with respect to apoptotic signaling [28, 54]. Unfortunately, targeting tumor cells and avoiding healthy cells is an ongoing challenge in the design of drug delivery systems. However, where BID (and other similar BH3-only) peptidomimetics would inadvertently lead to the destruction of healthy cells, BAD peptidomimetics would not, and may prove to be a more reliable therapeutic. This is because BAD generally does *not* have the capacity to trigger apoptosis; instead, BAD lowers the threshold at which cells respond to apoptotic stimuli. And since tumor cells have an increased threshold for apoptosis, BAD peptidomimetics could restore this threshold without actually triggering apoptosis. This would permit tumor and pre-cancerous cells to respond appropriately with apoptosis, while healthy cells would be less likely to die inappropriately.

Having proved the global asymptotic stability of any complex-balanced network under certain perturbations, we have contributed to the theory of chemical reaction networks. Unlike our initial analysis of the BAD/tBID/BAK pathway where we first selected rate constant values and then observed the static and dynamic properties, chemical reaction network theory provides a means to categorize static and dynamic properties as functions of the rate constants. This buys a mathematical sturdiness which would otherwise be absent from numerical analysis alone. That is, just because

certain behavior is observed for a specific set of rate constants does not mean it applies in general to all rate constants (or even to a neighborhood of parameter values). This is especially important when dealing with biological pathways where a lot of the time only qualitative data in the form of network structure and stoichiometry is available. Moreover, approaches with chemical reaction network theory prove to be more logical in making hypotheses toward future biological experimentation.

The complex-balanced BAD/tBID network is a good example of a network which is globally asymptotically stable, which can be stated without specifying rate constant values a priori. The un-catalyzed tBID/BAK network is a good example of a network which shows how the magnitude constraint on the perturbation level, which we derived, can be used to study the effects of dynamic perturbations, which in the case of the un-catalyzed tBID/BAK network, is a reaction. The magnitude constraint depends nicely on the original network's graphical and stoichiometric properties.

Basing hypotheses off of results from chemical reaction network theory could provide a more logical approach to designing therapeutics. The robustness result for the tBID/BAK network enables us to definitively conclude when we could expect to see a non-apoptotic response. Pathological deregulations which modulate the activation of tBID are known to be detrimental to a cell's survival. For example, SARS is caused by a virus which up-regulates the processing (and therefore activation) of tBID, inducing cell death in lung and intestinal tissue cells [9]. However, such deregulation of the cell's apoptosis machinery would be negated if the activation of tBID (or more generally the activation of BAK) is systematically blocked. One way an experimental biologist could test this is to identify molecules which inhibit the reaction rate of tBID activating BAK. Then, at least mathematically, one would be ensured that the polymerization of BAK would be blocked, and could hypothetically obstruct any pathological deregulation. This is a logical design since the design is based off of a general approach, not one from a specific set of rate constants which will invariably be uncertain and vary from cell to cell.

Toward a different end, the robustness result from Lemma 1 and Theorem 1 could be used to locate where (and in what manner) a disturbance undermines a network's stability. Moreover, the robustness result could be used to hypothesize new reactions or other unmodeled dynamics, in particular, if theoretical results do not align well with experimental data. The latter application illustrates again the importance of studying qualitative properties over quantitative properties since biological systems tend to be very uncertain systems, even structurally.

7.5 Future Work

The modeling of BAD is novel but many specifics were neglected to simplify the model and extract the overall mechanistic behavior of the two modes of phosphorylation. Future models for BAD should provide a means to differentiate among the three sites of phosphorylation, i.e., at Ser^{112}, Ser^{136}, and Ser^{155}. Such analysis could help distinguish once and for all whether cooperation between these sites is needed to engage the Bcl-2-bound form of phosphorylation, which is apparently a hot topic for experimenters looking at BAD.

As discussed in Appendix B, we suggested how one could look at stability and robustness of quasi-thermodynamic networks, more general than complex-balanced networks. Future work may include extension of our results to include quasi-thermodynamic networks or other networks. This would enable the development of an even bigger parameter space in which to conclude global asymptotic stability and robustness, such as for the BAD/tBID and tBID/BAK networks (some of this has already been undertaken in Appendix B). However, as also discussed in Appendix B, the stability of QTD leads to state-dependent issues and networks could potentially need to be handled in an ad hoc fashion (though, as shown in Appendix B, local stability results can still be concluded in the case of the BAD/tBID network). However, any given network may not be as simple as the BAD/tBID network.

On the other hand, general stability and robustness theory may more readily extend into a subset of deficiency-one networks (which may not necessarily be complex-balanced), in particular those studied by Feinberg, since properties of these networks are more numerous and available.

One of the reasons robustness of chemical reaction networks is so difficult to deal with is because parameter variations sometimes cause the steady state(s) to move and because robustness can lead to state-dependent conditions. However, as suggested in our work, analyzing convergence to neighborhoods is a possible way to study stability and robustness and lead to making better experimental hypotheses. Future work could include a conclusion like Theorem 6.2.1 which can be applied to any given network of a certain type as well as a way to find maximum rate constant values which lead to "acceptable" responses. To do this, one would need to estimate the smallest Lyapunov level set which encloses the region of violation in order to guarantee that trajectories of the perturbed system would evolve to (and stay within) the level set. Applied to the tBID/BAK network this would entail finding the largest k_{BAKcat} which can be tolerated before an "apoptotic" response is observed. Such estimates would undoubtedly be dependent on experimental observations in order to categorize regions which are "non-apoptotic" and "apoptotic", but theoretically it could be done.

A Appendix A

In this Appendix we first derive the full form of $r_{BAD:Bcl-2}$ which was stated in (3.5), and then prove the necessary constraint in (3.9) for when the BAD/tBID/BAK is operating under certain basal conditions as discussed in Chapter 3.

A.1 Derivation of BAD:Bcl-2 Ratio

Setting (Eqs. 2-3) in the full model to zero gives

$$\begin{aligned} k_{BADrel1}[\text{pBAD}:14\text{-}3\text{-}3] &= k_{BADseq}[\text{pBAD}] \\ &= k_{BADphos1}\left([\text{BAD}]+[\text{BAD}_\text{m}]\right)+k_{BADphos2}[\text{BAD}:\text{Bcl-}2] \end{aligned}$$

Substituting the result into (Eq. 1), and setting (Eq. 1) to zero, gives

$$\tau_{BAD}^{in}[\text{BAD}] = (\tau_{BAD}^{out} + k_{BADphos1})[\text{BAD}_\text{m}] + k_{BADphos2}[\text{BAD}:\text{Bcl-}2] \tag{A.1}$$

Conservation of BAD requires

$$\begin{aligned} [\text{BAD}_\text{total}] &= [\text{BAD}] + [\text{pBAD}] + [\text{pBAD}:14\text{-}3\text{-}3] + [\text{BAD}_\text{m}] + [\text{BAD}:\text{Bcl-}2] \\ &= [\text{BAD}] + \left(\frac{k_{BADphos1}}{k_{BADseq}} + \frac{k_{BADphos1}}{k_{BADrel1}}\right)[\text{BAD}] + \left(\frac{k_{BADphos1}}{k_{BADseq}} + \frac{k_{BADphos1}}{k_{BADrel1}}\right)[\text{BAD}_\text{m}] \\ &\quad + \left(\frac{k_{BADphos2}}{k_{BADseq}} + \frac{k_{BADphos2}}{k_{BADrel1}}\right)[\text{BAD}:\text{Bcl-}2] + [\text{BAD}_\text{m}] + [\text{BAD}:\text{Bcl-}2] \end{aligned}$$

Define

$$\alpha_1 \triangleq \frac{k_{BADphos1}}{k_{BADseq}} + \frac{k_{BADphos1}}{k_{BADrel1}}$$

$$\alpha_2 \triangleq \frac{k_{BADphos2}}{k_{BADseq}} + \frac{k_{BADphos2}}{k_{BADrel1}}$$

so that

$$\begin{aligned} [\text{BAD}_\text{total}] &= (1+\alpha_1)[\text{BAD}] + (1+\alpha_1)[\text{BAD}_\text{m}] + (1+\alpha_2)[\text{BAD}:\text{Bcl-}2] \\ &= (1+\alpha_1)\left(\frac{\tau_{BAD}^{out} + k_{BADphos1}}{\tau_{BAD}^{in}}[\text{BAD}_\text{m}] + \frac{k_{BADphos2}}{\tau_{BAD}^{in}}[\text{BAD}:\text{Bcl-}2]\right) \\ &\quad + (1+\alpha_1)[\text{BAD}_\text{m}] + (1+\alpha_2)[\text{BAD}:\text{Bcl-}2] \\ &= (1+\alpha_1)(1+\beta_1)[\text{BAD}_\text{m}] + (1+\alpha_2+(1+\alpha_1)\beta_2)[\text{BAD}:\text{Bcl-}2] \end{aligned}$$

where we have also defined

$$\beta_1 \triangleq \frac{\tau_{BAD}^{out} + k_{BADphos1}}{\tau_{BAD}^{in}}$$

$$\beta_2 \triangleq \frac{k_{BADphos2}}{\tau_{BAD}^{in}}$$

and substituted (A.1). Hence,

$$[\mathrm{BAD}_{\mathrm{total}}] = \Lambda_1[\mathrm{BAD}_{\mathrm{m}}] + \Lambda_2[\mathrm{BAD} : \mathrm{Bcl}\text{-}2] \tag{A.2}$$

where

$$\Lambda_1 \triangleq (1+\alpha_1)(1+\beta_1)$$
$$\Lambda_2 \triangleq (1+\alpha_2+(1+\alpha_1)\beta_2)$$

Setting (Eq. 4) to zero and substituting (A.1) again, we get

$$\begin{aligned} 0 = {} & (\tau_{BAD}^{out} + k_{BADphos1})[\mathrm{BAD}_{\mathrm{m}}] + k_{BADphos2}[\mathrm{BAD} : \mathrm{Bcl}\text{-}2] + k_{BAD:Bcl-2}^{d}[\mathrm{BAD} : \mathrm{Bcl}\text{-}2] \\ & + k_{BADrel2}[\mathrm{tBID}][\mathrm{BAD} : \mathrm{Bcl}\text{-}2] - k_{tBIDrel1}[\mathrm{BAD}_{\mathrm{m}}][\mathrm{tBID} : \mathrm{Bcl}\text{-}2] \\ & - (k_{BAD:Bcl-2}^{a}[\mathrm{Bcl}\text{-}2] + \tau_{BAD}^{out} + k_{BADphos1})[\mathrm{BAD}_{\mathrm{m}}] \end{aligned}$$

which, upon simplifying, is equivalent to

$$\begin{aligned} 0 = {} & \left(k_{BAD:Bcl-2}^{a}[\mathrm{Bcl}\text{-}2] + k_{tBIDrel1}[\mathrm{tBID} : \mathrm{Bcl}\text{-}2]\right)[\mathrm{BAD}_{\mathrm{m}}] \\ & - \left(k_{BADphos2} + k_{BAD:Bcl-2}^{d} + k_{BADrel2}[\mathrm{tBID}]\right)[\mathrm{BAD} : \mathrm{Bcl}\text{-}2] \end{aligned} \tag{A.3}$$

We consider (A.2) and (A.3) to be two equations in the two unknowns $[\mathrm{BAD}_{\mathrm{m}}]$ and $[\mathrm{BAD} : \mathrm{Bcl}\text{-}2]$. Solving for $[\mathrm{BAD}_{\mathrm{m}}]$ in (A.2) and substituting into (A.3), we obtain

$$\begin{aligned} & \left(k_{BAD:Bcl-2}^{a}[\mathrm{Bcl}\text{-}2] + k_{tBIDrel1}[\mathrm{tBID} : \mathrm{Bcl}\text{-}2]\right)\frac{[\mathrm{BAD}_{\mathrm{total}}]}{\Lambda_1} \\ & = \left(k_{BADphos2} + k_{BAD:Bcl-2}^{d} + k_{BADrel2}[\mathrm{tBID}] + \frac{\Lambda_2}{\Lambda_1}\left(k_{BAD:Bcl-2}^{a}[\mathrm{Bcl}\text{-}2] + k_{tBIDrel1}[\mathrm{tBID} : \mathrm{Bcl}\text{-}2]\right)\right) \\ & \quad \times [\mathrm{BAD} : \mathrm{Bcl}\text{-}2] \end{aligned}$$

Then solving for $\frac{[\mathrm{BAD} : \mathrm{Bcl}\text{-}2]}{[\mathrm{BAD}_{\mathrm{total}}]}$, we finally arrive to the full form of (3.5):

$$r_{BAD:Bcl-2} = \frac{1}{\Lambda_1\gamma + \Lambda_2} \tag{3.5}$$

where

$$\gamma \triangleq \frac{k_{BADphos2} + k_{BAD:Bcl-2}^{d} + k_{BADrel2}[\mathrm{tBID}]}{k_{BAD:Bcl-2}^{a}[\mathrm{Bcl}\text{-}2] + k_{tBIDrel1}[\mathrm{tBID} : \mathrm{Bcl}\text{-}2]}$$

A.2 Proof of Necessary Constraint on Kinetic Parameters Under Basal Conditions

Theorem A.2.1

If $[\text{BAD}:\text{Bcl-2}] << [\text{BAD}_{\text{total}}]$ and $[\text{tBID}] << [\text{tBID}_{\text{total}}]$ is satisfied at steady state, then, according to the skeleton model,

$$\alpha_2 + (1+\alpha_1)\beta_2 >> \max\left\{0,\ \frac{[\text{BAD}_{\text{total}}]}{[\text{Bcl-2}_{\text{total}}]} - 1\right\} \tag{3.9}$$

Proof:
According to the definition of $r_{BAD:Bcl-2}$, $[\text{BAD}:\text{Bcl-2}] << [\text{BAD}_{\text{total}}]$ is equivalent to $r_{BAD:Bcl-2} << 1$. Using the skeleton approximation for $r_{BAD:Bcl-2}$, that is, $r_{BAD:Bcl-2} = \dfrac{1}{1+\alpha_2+(1+\alpha_1)\beta_2}$, this means

$$\alpha_2 + (1+\alpha_1)\beta_2 >> 0 \tag{A.4}$$

Now consider the solution to the quadratic equation (3.2), which is also a defining characteristic of the skeleton model:

$$[\text{tBID}] = \frac{[\text{tBID}_{\text{total}}] - K_{D.tBID} - [\text{Bcl-2}_{\text{total}}] + \sqrt{([\text{tBID}_{\text{total}}] - K_{D.tBID} - [\text{Bcl-2}_{\text{total}}])^2 + 4K_{D.tBID}[\text{tBID}_{\text{total}}]}}{2}$$

Then $[\text{tBID}] << [\text{tBID}_{\text{total}}]$ implies

$$\sqrt{([\text{tBID}_{\text{total}}] - K_{D.tBID} - [\text{Bcl-2}_{\text{total}}])^2 + 4K_{D.tBID}[\text{tBID}_{\text{total}}]} << [\text{tBID}_{\text{total}}] + K_{D.tBID} + [\text{Bcl-2}_{\text{total}}]$$

which upon squaring both sides and simplifying, is equivalent to,

$$4\ [\text{tBID}_{\text{total}}][\text{Bcl-2}_{\text{total}}] >> 0$$

Since in the derivation of the skeleton model we assumed that $[\text{Bcl-2}_{\text{total}}]$ is replaced by $[\text{Bcl-2}_{\text{total}}] - [\text{BAD}:\text{Bcl-2}]$, this means that $4\ [\text{tBID}_{\text{total}}]([\text{Bcl-2}_{\text{total}}] - [\text{BAD}:\text{Bcl-2}]) >> 0$, that is,

$$[\text{Bcl-2}_{\text{total}}] >> [\text{BAD}:\text{Bcl-2}]$$

$$= r_{BAD:Bcl-2}[\text{BAD}_{\text{total}}]$$
$$= \frac{[\text{BAD}_{\text{total}}]}{1+\alpha_2+(1+\alpha_1)\beta_2}$$

that is,

$$\alpha_2 + (1+\alpha_1)\beta_2 >> \frac{[\text{BAD}_{\text{total}}]}{[\text{Bcl-2}_{\text{total}}]} - 1 \tag{A.5}$$

Combining (A.4) and (A.5) gives us the desired result.

□

B Appendix B

Appendix B includes the proof of Theorem 4.9.7 which provides a "rank" condition equivalent to guarantee the existence of a complex-balanced point for any given weakly reversible mass-action network. This proof is then applied to the BAD/tBID and un-catalyzed tBID/BAK networks to derive under what conditions these networks, when endowed with mass-action kinetics, are complex-balanced. We then discuss how such conditions can be relaxed in regards to our theoretical results in Chapter 5. Finally, we prove Lemma 5.4.1 (restated as Lemma B.2.1), which is needed to prove Lemma 1. The proof of Lemma 5.4.1 follows along the same lines as Lemma VIII.1 in [92].

B.1 Complex-balancing Property and Application to the BAD/tBID and Un-catalyzed tBID/BAK Networks

Theorem B.1.1

Consider any weakly-reversible mass-action network. Let $\{p^1, p^2, ..., p^\ell\} \subset \mathbb{R}^n_{\geq 0}$ be a basis for $\ker A_k$ which satisfies the following property: for each $\theta = 1, 2, ..., \ell$, $p^\theta_{y_j} > 0$ for all $y_j \in \mathcal{L}^\theta$ and $p^\theta_{y_j} = 0$ for all $y_j \notin \mathcal{L}^\theta$. Then, there exists an $x^* \in \mathbb{R}^m_+$ such that $\psi(x^*) \in \ker A_k$ if and only if

$$\ln\left(\sum_{\theta=1}^{\ell} p^\theta\right) \in \text{image} Y^T + \mathcal{U}$$

where Y^T is the transpose of Y and $\mathcal{U} \triangleq \text{sp}\{\omega_{\mathcal{L}^1}, \omega_{\mathcal{L}^2}, ..., \omega_{\mathcal{L}^\ell}\}$.

Proof:

The statement $\ln\left(\sum_{\theta=1}^{\ell} p^\theta\right) \in \text{image} Y^T + \mathcal{U}$ is equivalent to the following statement:

There exists a $z \in \mathbb{R}^m$ and $\xi_1, \xi_2, ..., \xi_\ell \in \mathbb{R}$ such that $\ln\left(\sum_{\theta} p^\theta\right) = Y^T z - \sum_{\theta} \xi_\theta \omega_{\mathcal{L}^\theta}$.

In turn, this statement is equivalent to:

There exists $x^* \in \mathbb{R}^m_+$ and $\lambda_1, \lambda_2, ..., \lambda_\ell \in \mathbb{R}_+$ such that $\ln\left(\sum_{\theta} p^\theta\right) = Y^T \ln x^* - \sum_{\theta} (\ln \lambda_\theta) \omega_{\mathcal{L}^\theta}$.

This can be done since any real number can be expressed as the natural logarithm of a positive number. In the situation that the last statement is satisfied,

$$Y^T \ln x^* = \ln\left(\sum_{\theta} p^\theta\right) + \sum_{\theta} (\ln \lambda_\theta) \omega_{\mathcal{L}^\theta}$$

$$= \ln\left(\sum_{\theta} \lambda_\theta p^\theta\right)$$

So because $Y^T \ln x^* = \ln \psi(x^*)$ and because the natural logarithm is strictly monotonic, the previous statement is equivalent to:

There exists $x^* \in \mathbb{R}_+^m$ and $\lambda_1,\ \lambda_2,\ ...,\ \lambda_\ell \in \mathbb{R}_+$ such that $\psi(x^*) = \sum_{\theta} \lambda_\theta p^\theta$.

In particular, $\ln\left(\sum_{\theta=1}^{\ell} p^\theta\right) \in \text{image} Y^T + \mathcal{U}$, which is equivalent to this final condition, implies that there exists an $x^* \in \mathbb{R}_+^m$ such that $\psi(x^*) \in \ker A_k$.

Conversely, if there exists an $x^* \in \mathbb{R}_+^m$ such that $\psi(x^*) \in \ker A_k$, then $\psi(x^*) = \sum_{\theta} \eta_\theta p^\theta$ for some $\eta_1,\ \eta_2,\ ...,\ \eta_\ell \in \mathbb{R}$. But these η_θ are necessarily positive since $\psi(x^*) \in \mathbb{R}_+^n$ for $x^* \in \mathbb{R}_+^m$ and the way the basis $\{p^\theta\}_{\theta=1,\ ...,\ \ell}$ has been chosen.

□

Theorem B.1.2

For a certain region of parameter space, the BAD/tBID network is complex-balanced.

Proof:

Let $g^*_{y_j} = g^*_j$, that is, let the j^{th} component of the vector g^* correspond to the $y_j{}^{\text{th}}$ complex. Then for the BAD/tBID network, the conditions $Yg^* = 0$ and $\sum_{y_j \in \mathcal{L}^\theta} g^*_{y_j} = 0$ from (4.4) and (4.5) are equivalent to

$$g^* = \alpha \begin{bmatrix} 0 & 0 & 0 & 0 & 1 & -1 & -1 & 1 & -1 & 1 \end{bmatrix}'$$

where $\alpha \in \mathbb{R}$. (In terms of deficiency, defined in [95], we are dealing with a deficiency-one mass-action network since $\dim(\ker Y \cap \text{span}\Delta) = 1$.) Because $\{g^* :\ \alpha \in \mathbb{R}\} = \ker Y \cap \text{span}\Delta$, $\{g^* :\ \alpha \in \mathbb{R}\}$ must be orthogonal to the orthogonal complement of $\ker Y \cap \text{span}\Delta$, which from [95], is shown to be $\text{image} Y^T + \mathcal{U}$. Therefore,

$$\ln\left(\sum_{\theta=1}^{\ell} p^\theta\right) \in \text{image} Y^T + \mathcal{U}$$

(the condition for the existence of complex-balanced points) if and only $\ln\left(\sum_{\theta=1}^{\ell} p^{\theta}\right)$ is orthogonal to every basis vector of $\{g^* :\ \alpha \in \mathbb{R}\}$. In other words, the BAD/tBID network is complex-balanced if and only if

$$\begin{bmatrix}\ln p^1 & \ln p^2 & \dots & \ln p^{\ell}\end{bmatrix}' \cdot \begin{bmatrix}0 & 0 & 0 & 0 & 1 & -1 & -1 & 1 & -1 & 1\end{bmatrix}' = 0 \tag{B.1}$$

Define $p^{\theta} \triangleq \begin{bmatrix}p_1^{\theta} & p_2^{\theta}\end{bmatrix}'$ for $\theta = 2,\ 3,\ 4$. Now, because A_k is block-diagonal, $A_{k\theta} p^{\theta} = 0$ for each $\theta = 2,\ 3,\ 4$, where the $A_{k\theta}$'s have been defined in Section 6.1. This means that (B.1) expands and simplifies to

$$\begin{bmatrix}\ln p^1 & \ln p^2 & \dots & \ln p^{\ell}\end{bmatrix}' \cdot \begin{bmatrix}0 & 0 & 0 & 0 & 1 & -1 & -1 & 1 & -1 & 1\end{bmatrix}'$$

$$\begin{aligned}
&= \ln p_1^2 - \ln p_2^2 - \ln p_1^3 + \ln p_2^3 - \ln p_1^4 + \ln p_2^4 \\
&= \ln\left(\frac{p_1^2 p_2^3 p_2^4}{p_2^2 p_1^3 p_1^4}\right) \\
&= \ln\left(\frac{k^d_{BAD:Bcl-2} k_{tBIDrel1} k^a_{tBID:Bcl-2}}{k^a_{BAD:Bcl-2} k_{BADrel2} k^d_{tBID:Bcl-2}}\right) \\
&= 0
\end{aligned}$$

So, as long as $\frac{k^d_{BAD:Bcl-2} k_{tBIDrel1} k^a_{tBID:Bcl-2}}{k^a_{BAD:Bcl-2} k_{BADrel2} k^d_{tBID:Bcl-2}} = 1$,

$$\ln\left(\sum_{\theta=1}^{\ell} p^{\theta}\right) \in \text{image} Y^T + \mathcal{U}$$

and the BAD/tBID network is complex-balanced (and hence QTD). Moreover, if $\frac{k^d_{BAD:Bcl-2} k_{tBIDrel1} k^a_{tBID:Bcl-2}}{k^a_{BAD:Bcl-2} k_{BADrel2} k^d_{tBID:Bcl-2}}$ is within a neighborhood of 1, then the mass-action network, though no longer complex-balanced, remains QTD (this can be seen by continuity of the steady states and (5.10)).

We can apply the results of Lemma 1 and Theorem 1 to certain mass-action networks which are not complex-balanced but are QTD. This will enable us to look at an even bigger region in the parameter space than that which produces complex-balancing. More precisely, as long as $q(x, x^*) \triangleq \sum_{\mathcal{R}} k_{y_j \to y_i} e^{y_j \cdot \ln x}(e^{q_i - q_j} - 1)$ in (5.10) is non-positive, then the results of Lemma 1 and Theorem 1 remain valid. Not surprisingly, [98] shows that $q(x, x^*) \le 0$ (with equality if and only if $\mu \in D^{\perp}$) is a sufficient condition for a mass-action network to be QTD. [98] further shows that $q(x, x^*) \le 0$ is equivalent to $\sum_{C} g^*_{y_j} x^{y_j} \le 0$. Applying this latter condition to the BAD/tBID network, and simplifying, we are left with the condition

$$\alpha\left([\text{tBID} : \text{Bcl - 2}] - [\text{BAD} : \text{Bcl - 2}]\right) \le 0$$

where

$$\begin{aligned}\alpha &= k^d_{BAD:Bcl-2}[\text{BAD} : \text{Bcl - 2}]^* - k^a_{BAD:Bcl-2}[\text{BAD}_\text{m}]^*[\text{Bcl - 2}]^* \\ &= k^a_{tBID:Bcl-2}[\text{tBID}]^*[\text{Bcl - 2}]^* - k^d_{tBID:Bcl-2}[\text{tBID} : \text{Bcl - 2}]^* \\ &= k_{tBIDrel1}[\text{BAD}_\text{m}]^*[\text{tBID} : \text{Bcl - 2}]^* - k_{BADrel2}[\text{tBID}]^*[\text{BAD} : \text{Bcl - 2}]^*\end{aligned}$$

and where the * superscript denotes steady state concentration levels, whenever $[\text{BAD}_{\text{total}}] << 1$, $[\text{tBID}_{\text{total}}] << 1$, and $[\text{Bcl - 2}_{\text{total}}] << 1$. For example, if $\alpha > 0$ then as long as $[\text{tBID} : \text{Bcl - 2}] \le [\text{BAD} : \text{Bcl - 2}]$, we are guaranteed a mass-action network which is QTD. In a sense we have traded off a kinetic rate constraint for a state space constraint. Practically, one would not deal with the above state-dependent constraint unless $\frac{k^d_{BAD:Bcl-2}k_{tBIDrel1}k^a_{tBID:Bcl-2}}{k^a_{BAD:Bcl-2}k_{BADrel2}k^d_{tBID:Bcl-2}}$ is far from unity. In that case, however, one could use the constraint to conclude local asymptotic stability. That is, if a steady state of the BAD/tBID network is such that $\alpha > 0$ and $[\text{tBID} : \text{Bcl - 2}]^* \le [\text{BAD} : \text{Bcl - 2}]^*$ (or $\alpha < 0$ and $[\text{BAD} : \text{Bcl - 2}]^* \le [\text{tBID} : \text{Bcl - 2}]^*$), then the corresponding steady state is locally asymptotically stable. This is because we may still apply the same Lyapunov function and show, at least locally, that its derivative is negative-definite sufficiently close to the steady state. Furthermore, using the Lyapunov function and the explicit formula above, one could infer a basin of attraction estimate. We leave this for future work.

Theorem B.1.3

For a certain region of parameter space, the un-catalyzed tBID/BAK network is complex-balanced.

Proof:
Similar to that in the proof of Theorem B.1.2, we have that

$$g^* = \alpha\begin{bmatrix}1 & -1 & 0 & 0 & -1 & 1 & 1 & -1 & 0 & 0\end{bmatrix}'$$

is orthogonal to $\ln\left(\sum_{\theta=1}^{\ell} p^\theta\right)$ if and only if the un-catalyzed tBID/BAK network is complex-balanced. In this case, we get

$$\begin{bmatrix}\ln p^1 & \ln p^2 & \dots & \ln p^\ell\end{bmatrix}' \cdot \begin{bmatrix}1 & -1 & 0 & 0 & -1 & 1 & 1 & -1 & 0 & 0\end{bmatrix}' = 0 \qquad \text{(B.2)}$$

Again, define $p^\theta \triangleq \begin{bmatrix}p_1^\theta & p_2^\theta\end{bmatrix}'$ for each θ (which can be done since there are two complexes in every linkage class). Similarly, (B.2) can be expanded and simplified to

$$\begin{bmatrix}\ln p^1 & \ln p^2 & \dots & \ln p^\ell\end{bmatrix} \cdot \begin{bmatrix}1 & -1 & 0 & 0 & -1 & 1 & 1 & -1 & 0 & 0\end{bmatrix}'$$

$$= \ln p_1^1 - \ln p_2^1 - \ln p_1^3 + \ln p_2^3 + \ln p_1^4 - \ln p_2^4$$

$$= \ln\left(\frac{p_1^1 p_2^3 p_1^4}{p_2^1 p_1^3 p_2^4}\right)$$
$$= \ln\left(\frac{k^d_{tBID:Bcl-2} k^a_{BAK:Bcl-2} k_{BAKrel1}}{k^a_{tBID:Bcl-2} k^d_{BAK:Bcl-2} k_{tBIDrel2}}\right)$$
$$= 0$$

So, as long as $\frac{k^d_{tBID:Bcl-2} k^a_{BAK:Bcl-2} k_{BAKrel1}}{k^a_{tBID:Bcl-2} k^d_{BAK:Bcl-2} k_{tBIDrel2}} = 1$, the un-catalyzed tBID/BAK network is complex-balanced. Again, if $\frac{k^d_{tBID:Bcl-2} k^a_{BAK:Bcl-2} k_{BAKrel1}}{k^a_{tBID:Bcl-2} k^d_{BAK:Bcl-2} k_{tBIDrel2}}$ is within a neighborhood of 1, then the mass-action network remains QTD. We can also consider further relaxation of this constraint much like we did for the BAD/tBID network (see discussion above).

B.2 Helpful Result for Lemma 1

Lemma B.2.1

Consider any weakly reversible mass-action network. Define for each linkage class the function

$$Q_\theta(\eta) \triangleq \sum_{y_j \to y_i \in \mathcal{R}^\theta} k_{y_j \to y_i} (\eta_{y_i} - \eta_{y_j})^2$$

for $\eta \in \mathbb{R}^{n_\theta}$, where $\mathcal{R}^\theta = \{y_j \to y_i : \ y_i, y_j \in \mathcal{L}^\theta\}$ and $n_\theta \geq 2$ is the total number of complexes in $\mathcal{L}^\theta$. Then for each $\theta = 1, 2, ..., \ell$, there exists $\kappa_\theta > 0$ such that

$$Q_\theta \geq \frac{\kappa_\theta}{4n_\theta} \sum_{y_i, y_j \in \mathcal{L}^\theta} (\eta_{y_i} - \eta_{y_j})^2$$

for all $\eta \in \mathbb{R}^{n_\theta}$.

Proof:

Consider a single linkage class $\mathcal{L}^\theta$. For convenience we re-label and re-order the complexes so that $\mathcal{L}^\theta = \{1, 2, ..., n_\theta\}$. Define

$$P_\theta(p_1, p_2, ..., p_{n_\theta}) \triangleq \sum_{\substack{j \to i \in \mathcal{R}^\theta \\ i,j \neq n_\theta}} k_{j \to i} (p_i - p_j)^2 + \sum_{\substack{j \to i \in \mathcal{R}^\theta \\ i = n_\theta}} k_{j \to i} p_j^2 + \sum_{\substack{j \to i \in \mathcal{R}^\theta \\ j = n_\theta}} k_{j \to i} p_i^2$$

Note that

$$Q_\theta(\eta_1, \eta_2, ..., \eta_{n_\theta}) = P_\theta(\eta_1 - \eta_{n_\theta}, \eta_2 - \eta_{n_\theta}, ..., \eta_{n_\theta - 1} - \eta_{n_\theta})$$

Clearly, $P_\theta \geq 0$ and $Q_\theta(\eta_1, \eta_2, ..., \eta_{n_\theta - 1}, 0) = P_\theta(\eta_1, \eta_2, ..., \eta_{n_\theta - 1})$. We wish to show that P_θ is positive definite. So we suppose that $\eta_{n_\theta} = 0$ and $Q_\theta(\eta_1, \eta_2, ..., \eta_{n_\theta - 1}, 0) = 0$. The latter implies that $\eta_i = \eta_j$ for each i, j such that $k_{j \to i} \neq 0$. Consider any complex $j_0 \in \mathcal{L}^\theta$ that is not n_θ. Since the network is weakly reversible, there exists an ordered set of indices from j_0 to n_θ, say

$\{j_0,\ j_1,\ ...,\ j_N\}$, where $j_N = n_\theta$, such that $j_0 \to j_1 \to \ ... \ \to j_N$. Hence, $0 = \eta_{n_\theta} = \eta_{j_N} = \eta_{j_{N-1}} = \ ... \ = \eta_{j_0}$. In particular, $\eta_{j_0} = 0$. Since j_0 could represent any complex in $\mathcal{L}^\theta$, it must be true for all complexes in $\mathcal{L}^\theta$. Hence, $\eta_1,\ \eta_2,\ ...,\ \eta_{n_\theta - 1} = 0$ whenever $P_\theta(\eta_1,\ \eta_2,\ ...,\ \eta_{n_\theta - 1}) = 0$. Therefore P_θ is positive definite. Because P_θ is positive definite, this means there exists a positive constant κ_θ such that

$$P_\theta(\eta_1,\ \eta_2,\ ...,\ \eta_{n_\theta - 1}) \geq \kappa_\theta \sum_{i=1}^{n_\theta - 1} \eta_i^2$$

for all $(\eta_1,\ \eta_2,\ ...,\ \eta_{n_\theta}) \in \mathbb{R}^{n_\theta}$, that is,

$$Q_\theta(\eta_1,\ \eta_2,\ ...,\ \eta_{n_\theta}) = P_\theta(\eta_1 - \eta_{n_\theta},\ \eta_2 - \eta_{n_\theta},\ ...,\ \eta_{n_\theta - 1} - \eta_{n_\theta}) \geq \kappa_\theta \sum_{i=1}^{n_\theta - 1} (\eta_i - \eta_{n_\theta})^2$$

Note that $(\eta_i - \eta_j)^2 \leq 2(\eta_i - \eta_{n_\theta})^2 + 2(\eta_j - \eta_{n_\theta})^2$

$$\Rightarrow \sum_{i=1}^{n_\theta} (\eta_i - \eta_j)^2 \leq 2\sum_{i=1}^{n_\theta} (\eta_i - \eta_{n_\theta})^2 + 2n_\theta(\eta_j - \eta_{n_\theta})^2$$

$$\Rightarrow \sum_{j=1}^{n_\theta}\sum_{i=1}^{n_\theta} (\eta_i - \eta_j)^2 \leq 2n_\theta \sum_{i=1}^{n_\theta} (\eta_i - \eta_{n_\theta})^2 + 2n_\theta \sum_{j=1}^{n_\theta} (\eta_j - \eta_{n_\theta})^2$$

$$\Rightarrow \sum_{j=1}^{n_\theta}\sum_{i=1}^{n_\theta} (\eta_i - \eta_j)^2 \leq 4n_\theta \sum_{i=1}^{n_\theta} (\eta_i - \eta_{n_\theta})^2$$

so

$$Q_\theta \geq \kappa_\theta \sum_{i=1}^{n_\theta - 1} (\eta_i - \eta_{n_\theta})^2 = \kappa_\theta \sum_{i=1}^{n_\theta} (\eta_i - \eta_{n_\theta})^2$$

$$\geq \frac{\kappa_\theta}{4n_\theta} \sum_{j=1}^{n_\theta}\sum_{i=1}^{n_\theta} (\eta_i - \eta_j)^2$$

In other words, in our usual notation where $\mathcal{L}^\theta = \{y_1,\ y_2,\ ...,\ y_{n_\theta}\}$

$$Q_\theta \geq \frac{\kappa_\theta}{4n_\theta} \sum_{y_i, y_j \in \mathcal{L}^\theta} (\eta_{y_i} - \eta_{y_j})^2$$

Moreover, this process can be repeated for each $\theta = 1,\ 2,\ ...,\ \ell$.

□

C Appendix C

In the first half of this Appendix, we study and discuss boundary solutions of complex-balanced mass-action networks. Complex-balanced networks which possess such behaviors can be decomposed into two sub-networks, one which is a perturbed network satisfying the persistence property and another which has a trivial solution. In the second half of this appendix, we prove that both the BAD/tBID and full tBID/BAK networks satisfy the persistence property as long as their total concentrations remain non-zero. Under the same conditions, we additionally show that both the BAD/tBID and the full tBID/BAK networks cannot possess boundary equilibria.

C.1 Decomposing Boundary-Evolving Mass-Action Networks into Two Sub-Networks

Suppose that we take a look at what happens when a perturbed complex-balanced network does not satisfy (A.3). So suppose there exists a maximal solution $x(\cdot)$ of (5.1), with $x(0) \in \partial\mathbb{R}^m_{\geq 0} \setminus E_0^*$, on some interval $[0,\sigma)$, and where $x(t) \in \partial\mathbb{R}^m_{\geq 0}$ for $t \in [0,T)$, for some $T \in (0,\sigma)$. Then there exists $\{k_1,\ k_2,\ ...,\ k_M\}$ such that $x_{k_1}(t) > 0,\ x_{k_2}(t) > 0,\ ...,\ x_{k_M}(t) > 0$ for all $t \in (0,T)$, and furthermore, there exists $\{k_{M+1},\ k_{M+2},\ ...,\ k_m\}$ such that $x_{k_{M+1}}(t) = x_{k_{M+2}}(t) = \cdots = x_{k_m}(t) = 0$ for all $t \in [0,T)$. This is due to the fact that $\mathbb{R}_+$ is forward-invariant for (5.2). For convenience, we reorder the species so that $x_1(t) > 0,\ x_2(t) > 0,\ ...,\ x_M(t) > 0$ for all $t \in (0,T)$ and $x_{M+1}(t) = x_{M+2}(t) = \cdots = x_m(t) = 0$ for all $t \in [0,T)$. (We also assume that we are not dealing with the trivial case $x(0) = 0$.)

Consider the union of linkage classes, denoted $\mathcal{C}_2$, where for each linkage class $\mathcal{L}^\theta \subset \mathcal{C}_2$, there exists $y_j \in \mathcal{L}^\theta$ and an index $k \in \{M+1,\ M+2,\ ...,\ m\}$ such that $k \in S_j$. In other words, consider all linkage classes which have at least one complex which contains one or more of the species $M+1,\ M+2,\ ...,\ m$ (which are those species that have concentrations identically zero on $[0,T)$).

We claim that $x(t)^{y_j} = 0$ for $t \in [0,T)$ and for all $y_j \in \mathcal{C}_2$ (of course this implies that all "total currents" in these linkage classes are zero). So, suppose not. Then there exists some complex $y_{\bar{j}}$ in some linkage class $\mathcal{L}^\theta \subset \mathcal{C}_2$ and at some time $t_1 \in (0,T)$ where $x(t_1)^{y_{\bar{j}}} > 0$. So $x_l(t_1) > 0$ for all $l \in S_{\bar{j}}$. According to Corollary 5.2.2, this means $x(t)^{y_j} > 0$ for all complexes $y_j \in \mathcal{L}^\theta$ for $t > t_1$. But this contradicts the fact that $\mathcal{L}^\theta \subset \mathcal{C}_2$, that is, the fact that $\mathcal{L}^\theta$ contains at least one complex which contains at least one of the species which is identically zero on the interval $[0,T)$. Therefore, $x(t)^{y_j} = 0$ for $t \in [0,T)$ and for all $y_j \in \mathcal{C}_2$. Furthermore, we must also have $\Delta_{y_j \to y_i}(x(t)) = 0$ for $t \in [0,T)$ and for all reactions in the set $\{y_j \to y_i :\ y_i, y_j \in \mathcal{C}_2\}$. This of course is a result of (A.2).

We partition $\mathcal{C}$ into two sets, $\mathcal{C}_2$ and $\mathcal{C}_1 \triangleq \mathcal{C} \setminus \mathcal{C}_2$. Note that $\mathcal{C}_1 \neq \phi$ since otherwise, $x(t)^{y_j} = 0$ for all $y_j \in \mathcal{C}$ for $t \in [0,T)$, and so, according to (5.1), $x(t)$ would be an equilibrium solution and necessarily $x(0) \in E_0^*$. This contradicts our assumption that $x(0) \notin E_0^*$.

Because in a sense we can segregate the set of species and complexes, we define the mass-action sub-network $\{\hat{\mathcal{S}},\ \hat{\mathcal{C}},\ \hat{\mathcal{R}},\ \hat{k}\}$ where $\hat{\mathcal{S}} \triangleq \{1,\ 2,\ ...,\ M\}$, $\hat{\mathcal{C}}$ is the set of complexes $\hat{y}_j$, one for each $y_j \in \mathcal{C}_1$, and such that $\hat{y}_{kj} = y_{kj}$ for $k = 1,\ 2,\ ...,\ M$, and $\hat{\mathcal{R}} \triangleq \{\hat{y}_j \to \hat{y}_i :\ \hat{y}_i, \hat{y}_j \in \hat{\mathcal{C}}\}$ and $\hat{k}$ are defined in the obvious manners. Defining $\hat{x} \triangleq [x_1 \quad x_2 \quad ... \quad x_M]'$, we must have

$$\dot{\hat{x}} = \sum_{\hat{y}_j \to \hat{y}_i \in \hat{\mathcal{R}}} \left(\hat{k}_{\hat{y}_j \to \hat{y}_i} \hat{x}^{\hat{y}_j} + \hat{\Delta}_{\hat{y}_j \to \hat{y}_i}(\hat{x})\right)(\hat{y}_i - \hat{y}_j) \tag{C.1}$$

for $t \in (0, T)$, which are the induced differential equations by the mass-action sub-network $\{\hat{\mathcal{S}},\ \hat{\mathcal{C}},\ \hat{\mathcal{R}},\ \hat{k}\}$. Here, $\hat{\Delta}_{\hat{y}_j \to \hat{y}_i} :\ \mathbb{R}^M_{\geq 0} \to \mathbb{R}_{\geq 0}$ is defined by $\hat{\Delta}_{\hat{y}_j \to \hat{y}_i}(\hat{x}) = \Delta_{y_j \to y_i}(x)\Big|_{x_{M+1} = \cdots = x_m = 0}$. Note that each $\hat{\Delta}_{\hat{y}_j \to \hat{y}_i}(\cdot)$ is locally Lipschitz and satisfies (A.2). Also note that (A.1) and (A.3) are satisfied by (C.1). The latter follows because we must have $x_1(t) > 0,\ x_2(t) > 0,\ ...,\ x_M(t) > 0$ for all $t \in (0, T)$.

The sub-network (C.1) is completely self-contained as a mass-action network and we can analyze its behavior independently, and further we have that (A.3) is satisfied. If it is not known a priori that boundary solutions exist, then the procedure above could be used as a starting point to prove or disprove their existence (we leave this for future work). However, for the BAD/tBID and catalyzed tBID/BAK networks, we need not be concerned with this since we can prove that no boundary solutions exist. This is undertaken in the next section.

C.2 Showing that the BAD/tBID and Catalyzed tBID/BAK Networks Have No Boundary Solutions

Theorem C.2.1

If $[\text{BAD}_{\text{total}}] > 0$, $[\text{tBID}_{\text{total}}] > 0$, and $[\text{Bcl-2}_{\text{total}}] > 0$, then any maximal solution $x(\cdot)$ of the BAD/tBID network, with initial time $t = 0$, must be in the positive orthant $\mathbb{R}^m_+$ for all definable times $t > 0$. In particular, this means that the BAD/tBID network has no boundary equilibria, that is, $E_0 = \phi$.

Proof:
Due to $\mathbb{R}^m_+$-invariance for (5.1), it suffices to consider only those maximal trajectories which emanate from the boundary $\partial\mathbb{R}^m_{\geq 0}$. So consider some maximal solution, defined on $[0, \sigma)$, which has been initialized on $\partial\mathbb{R}^m_{\geq 0}$. Suppose that the conditions of Theorem C.1 are satisfied. $[\text{BAD}_{\text{total}}] > 0$ implies that there exists at least one state of BAD which is positive at time $t = 0$. With this in mind, we consider the two following cases: **(i)** $[\text{BAD} : \text{Bcl-2}](0) > 0$ and **(ii)** $[\text{BAD} : \text{Bcl-2}](0) = 0$. For each of these cases, we show that all states of BAD and tBID (and free Bcl-2) must be positive for all $t \in (0, \sigma)$.

case (i) $[\text{BAD} : \text{Bcl-2}](0) > 0$

Due to $\mathbb{R}_+$-invariance for (5.2), it immediately follows $[\text{BAD}:\text{Bcl-2}](t)>0$ for all $t\in(0,\sigma)$. Because in the second linkage class we have $\text{BAD}:\text{Bcl-2}\leftrightarrow \text{BAD}_\text{m}+\text{Bcl-2}$, application of Corollary 5.2.2 at time $t=0$ means that $[\text{BAD}_\text{m}](t)>0$ and $[\text{Bcl-2}](t)>0$ for all $t\in(0,\sigma)$. Repeating this process for the first linkage class (since $\text{BAD}_\text{m}\to\text{BAD}$), it can be shown that all states of BAD are positive for $t\in(0,\sigma)$. The reason Corollary 5.2.2 applies for $t^*=0$ (and not at some greater time) is because for any chosen t in the interval $(0,\sigma)$, we can always find a smaller time $t_1<t$ such that $[\text{BAD}_\text{m}](t_1)>0$, which, through the application of Corollary 5.2.2 at time $t^*=t_1$ and to the first linkage class, forces the remaining states $[\text{BAD}]$, $[\text{pBAD}]$, and $[\text{pBAD}:14\text{-}3\text{-}3]$ to be positive at time t. .

We note the following property concerning the states of tBID (tBID and tBID:Bcl-2): If $[\text{tBID}_\text{total}]>0$, and if there is any material initialized in the Bcl-2-bound form, that is, $[\text{tBID}:\text{Bcl-2}](0)>0$, then through the application of Corollary 5.2.2, we can conclude that all states of tBID are positive for all $t\in(0,\sigma)$ as well as $[\text{Bcl-2}](t)>0$ for all $t\in(0,\sigma)$. .

Hence, case (i) is completed unless $[\text{tBID}:\text{Bcl-2}](0)=0$, that is, $[\text{tBID}](0)=[\text{tBID}_\text{total}]>0$. Of course, by invariance, this means $[\text{tBID}](t)>0$ for all $t\in(0,\sigma)$. But because we also have $[\text{Bcl-2}](t)>0$ for all $t\in(0,\sigma)$, application of Corollary 5.2.2 implies that $[\text{tBID}:\text{Bcl-2}](t)>0$ for all $t\in(0,\sigma)$.

case (ii) $[\text{BAD}:\text{Bcl-2}](0)=0$
Because there must exist BAD material initialized in at least one of the *other* states of BAD, by similar reasoning to that used in case (i), all *other* states of BAD must be positive for $t\in(0,\sigma)$. In particular, we must have $[\text{BAD}_\text{m}](t)>0$ for all $t\in(0,\sigma)$. This means that if $[\text{Bcl-2}](0)>0$, then $[\text{BAD}:\text{Bcl-2}](t)>0$ for all $t\in(0,\sigma)$ and we may proceed as in case (i). So suppose instead that $[\text{Bcl-2}](0)=0$. Because $[\text{Bcl-2}_\text{total}]>0$, this means that

$$\begin{aligned}0&<[\text{Bcl-2}_\text{total}]\\&=[\text{Bcl-2}](0)+[\text{BAD}:\text{Bcl-2}](0)+[\text{tBID}:\text{Bcl-2}](0)\\&=[\text{tBID}:\text{Bcl-2}](0)\end{aligned}$$

So because $[\text{tBID}:\text{Bcl-2}](0)>0$ all states of tBID are positive for all $t\in(0,\sigma)$ as well as $[\text{Bcl-2}](t)>0$ for all $t\in(0,\sigma)$. So because $[\text{BAD}_\text{m}](t)>0$ and $[\text{Bcl-2}](t)>0$ for $t\in(0,\sigma)$, $[\text{BAD}:\text{Bcl-2}](t)>0$ for all $t\in(0,\sigma)$.

□

Theorem C.2.2

If $[\text{tBID}_\text{total}]>0$, $[\text{BAK}_\text{total}]>0$, and $[\text{Bcl-2}_\text{total}]>0$, then any maximal solution $x(\cdot)$ of the catalyzed tBID/BAK network, with initial time $t=0$, must be in the positive orthant $\mathbb{R}_+^m$ for all definable times $t>0$. In particular, this means that the catalyzed tBID/BAK network has no boundary equilibria, that is, $E_0^*=\phi$.

Proof:
In a similar manner as was done for Theorem C.1, $[\text{BAK}_\text{total}]>0$ implies that there exists at least one state of BAK which is positive at time $t=0$. With this in mind, we consider the following two cases:

(i) $[\text{BAK} : \text{Bcl-2}](0) > 0$ and **(ii)** $[\text{BAK} : \text{Bcl-2}](0) = 0$. For each of these cases, we show that all states of tBID and BAK (and free Bcl-2) must be positive for all $t \in (0, \sigma)$.

case (i) $[\text{BAK} : \text{Bcl-2}](0) > 0$

Again, Corollary 5.2.2 implies that $[\text{BAK}](t) > 0$ and $[\text{Bcl-2}](t) > 0$ for all $t \in (0, \sigma)$, and repeating for the second and fifth linkage classes (since $\text{BAK} \to \text{BAK}_{\text{inac}}$ and $4\text{BAK} \to \text{BAK}_{\text{poly}}$), it is easily shown that all states of BAK are positive for $t \in (0, \sigma)$.

Like before, we still retain the property concerning the states of tBID (tBID and tBID:Bcl-2). Hence, case (i) is completed unless $[\text{tBID} : \text{Bcl-2}](0) = 0$, that is, $[\text{tBID}](0) = [\text{tBID}_{\text{total}}] > 0$. Of course, $[\text{tBID}](t) > 0$ for all $t \in (0, \sigma)$. But because $[\text{Bcl-2}](t) > 0$ for all $t \in (0, \sigma)$, it follows that $[\text{tBID} : \text{Bcl-2}](t) > 0$ for all $t \in (0, \sigma)$.

case (ii) $[\text{BAK} : \text{Bcl-2}](0) = 0$

Because there must exist BAK material initialized in at least one of the *other* states of BAK, by similar reasoning to that used in case (i), all *other* states of BAK must be positive for $t \in (0, \sigma)$. In particular, we must have $[\text{BAK}](t) > 0$ for all $t \in (0, \sigma)$. This means that if $[\text{Bcl-2}](0) > 0$, then $[\text{BAK} : \text{Bcl-2}](t) > 0$ for all $t \in (0, \sigma)$ and we may proceed as in case (i). So suppose instead that $[\text{Bcl-2}](0) = 0$. Because $[\text{Bcl-2}_{\text{total}}] > 0$, this means that

$$\begin{aligned} 0 &< [\text{Bcl-2}_{\text{total}}] \\ &= [\text{Bcl-2}](0) + [\text{tBID} : \text{Bcl-2}](0) + [\text{BAK} : \text{Bcl-2}](0) \\ &= [\text{tBID} : \text{Bcl-2}](0) \end{aligned}$$

So because $[\text{tBID} : \text{Bcl-2}](0) > 0$ all states of tBID are positive for all $t \in (0, \sigma)$ as well as $[\text{Bcl-2}](t) > 0$ for all $t \in (0, \sigma)$. So because $[\text{BAK}](t) > 0$ and $[\text{Bcl-2}](t) > 0$ for $t \in (0, \sigma)$, $[\text{BAK} : \text{Bcl-2}](t) > 0$ for all $t \in (0, \sigma)$.

□

D References

1. Shibasaki, F., Kondo, E., Akagi, T., and McKeon, F., *Suppression of signalling through transcription factor NF-AT by interactions between calcineurin and Bcl-2*. Nature, 1997. **386**: p. 728-731

2. Jambal, P., Masterson, S., Nesterova, A., Bouchard, R., Bergman, B., Hutton, J.C., Boxer, L.M., Reusch, J.E.-B., and Pugazhenthi, S., *Cytokine-mediated down-regulation of the transcription factor cAMP-response element-binding protein in pancreatic β-cells*. Journal of Biological Chemistry, 2003. **278**(25): p. 23055-23065.

3. Shinoda, S., Schindler, C.K., Quan-Lan, J., Saugstad, J.A., Taki, W., Simon, R.P., Henshall, D.C., *Interaction of 14-3-3 with Bid during seizure-induced neuronal death.* Journal of Neurochemistry, 2003. **86**: p. 460-469.

4. Won, J., Kim, D.Y., La, M., Kim, D., Meadows, G.G., and Joe, C.O. *Cleavage of 14-3-3 protein by caspase-3 facilitates Bad interaction with Bcl-x(L) during apoptosis*. Journal of Biological Chemistry, 2002. **278**(21): p. 19347-19351.

5. Kim, Y.M., Kim, T.H., Seol, D.W., Talanian, R.V., and Billiar, T.R., *Nitric oxide suppression of apoptosis occurs in association with an inhibition of Bcl-2 cleavage and cytochrome c release*. Journal of Biological Chemistry, 1998. **273**: p. 31437-31441.

6. Nicholson, D.W., *Caspase structure, proteolytic substrates, and function during apoptotic cell death*. Cell. Death Differ., 1999. **6**: p. 1028-1042.

7. Dillon, R.L., White, D.E., Muller, W.J., *The phosphatidyl inositol 3-kinase signaling network: implications for human breast cancer.* Oncogene, 2007. **26**: p. 1338-1345.

8. Testa, J.R., and Bellacosa A., *AKT plays a central role in tumorigenesis*. Proceedings of the National Academy of Sciences of USA, 2001. **98**(20): p. 10983-10985.

9. Law, P.T.W., Wong, C.-H., Au, T.C.C., Chuck, C.-P., Kong, S.-K., Chan, P.K.S., To, K.-F., Lo, A.W.I., Chan, J.Y.W., Suen, Y.-K., Chan, H.Y.E., Fung, K.-P., Waye, M.M.Y., Sung, J.J.Y., Lo, Y.M.D., and Tsui, S.K.W., *The 3a protein of severe acute respiratory syndrome-associated coronavirus induces apoptosis in Vero E6 cells*. Journal of General Virology, 2005. **86**: p. 1921-1930.

10. Fahy, B.N., Schlieman, M.G., Mortenson, M.M., Virudachalam, S., and Bold, R.J., *Targeting BCL-2 overexpression in various human malignancies through NF-κB inhibition by the proteasome inhibitor bortezomib*. Cancer Chemother. Pharmacol., 2005. **56**: p. 46-54.

11. DeLeo, F.R., *Modulation of phagocyte apoptosis by bacterial pathogens.* Apoptosis, 2004. **9**(4): p. 399-413.

12. James, E.R., Green, D.R., *Manipulation of apoptosis in the host-parasite interaction.* Trends In Parasitology, 2004. **20**(6): p. 280-287.

13. Yi, X., Yin, X.-M., and Dong, Z., *Inhibition of Bid-induced apoptosis by Bcl-2*. Journal of Biological Chemistry, 2003. **278**(19): p. 16992-16999.

14. Berthier, A., Lemaire-Ewing, S., Prunet, C., Monier, S., Athias, A., Bessede, G., Barros, J-P.P.d., Laubriet, A., Gambert, P., Lizard, G., and Neel, D., *Involvement of a calcium-dependent dephosphorylation of Bad associated with the localization of Trpc-1 within lipid rafts in 7-ketocholesterol-induced THP-1 cell apoptosis.* Cell Death and Differentiation, 2004. **11**: p. 897-905.

15. Saito, A. Hayashi, T., Okuno, S., Ferrand-Drake, M., and Chan, P.H., *Overexpression of copper/zinc superoxide dismutase in transgenic mice protects against neuronal cell death after transient focal ischemia by blocking activation of the Bad cell death signaling pathway*. Journal of Neuroscience, 2003. **23**(5): p. 1710-1718.

16. Saito, S., Hiroi Y., Zou, Y., Aikawa, R., Toko, H., Shibasaki, F., Yazaki, Y., Nagai, R., and Komuro I., *β-adrenergic pathway induces apoptosis through calcineurin activation in cardiac myocytes.* Journal of Biological Chemistry, 2000. **275**(44): p. 34528-34533.

17. Springer, J.E., Azbill, R.D., Nottingham, S.A., and Kennedy, S.E., *Calcineurin-mediated BAD dephosphorylation activates the caspase-3 apoptotic cascade in traumatic spinal cord injury.* Journal of Neuroscience, 2000. **20**(19): p. 7246-7251.

18. Li, H., Zhu, H., Xu, C.-j., and Yuan, J., *Cleavage of BID by caspase 8 mediates the mitochondrial damage in the Fas pathway of apoptosis*. Cell, 1998. **94**: p. 491-501.

19. Wei, M.C., Lindsten, T., Mootha, V.K., Weiler, S., Gross, A., Ashiya, M., Thompson, C.B., and Korsmeyer, S.J., *tBID, a membrane-targeted death ligand, oligomerizes BAK to release cytochrome c*. Genes and Development, 2000. **14**: p. 2060-2071.

20. Saito, M., Korsmeyer, S.J., and Schlesinger, P.H., *BAX-dependent transport of cytochrome c reconstituted in pure liposomes*. Nature Cell Biology, 2000. **2**: p. 553-555.

21. Hekman, M., Albert, S., Galmiche, A., Rennefahrt, U.E.E., Fueller, J., Fischer, A., Puehringer, D., Wiese, S., and Rapp, U.R., *Reversible membrane interaction of BAD requires two C-terminal lipid binding domains in conjunction with 14-3-3 protein binding*. Journal of Biological Chemistry, 2006. **281**(25): p. 17321-17336.

22. Adams, J.M., and Cory, S., *The Bcl-2 apoptotic switch in cancer development and therapy.* Oncogene, 2007. **26**: p. 1324-1337.

23. Letai, A., Bassik, M.C., Walensky, L.D., Sorcinelli, M.D., Weiler, and S., Korsmeyer, S.J., *Distinct BH3 domains either sensitize or activate mitochondrial apoptosis, serving as prototype cancer therapeutics*. Cancer Cell, 2002. **2**: p. 183-192.

24. Wang, K., Yin, X.-M., Chao, D.T., Milliman, C.L., and Korsmeyer, S.J., *BID: a novel BH3 domain-only death agonist*. Genes and Development, 1996. **10**: p. 2859-2869.

25. Cheng, E.H.-Y.A., Wei, M.C., Weiler, S., Flavell, R.A., Mak, T.W., Lindsten, T., and Korsmeyer, S.J., *BCL-2, BCL-X_L sequesters BH3 domain-only molecules preventing BAX- and BAK-mediated mitochondrial apoptosis*. Molecular Cell, 2001. **8**: p. 705-711.

26. Luo, X., Budihardjo, I., Zou, H., Slaughter, C., and Wang, X., *Bid, a Bcl2 interacting protein, mediates cytochrome c release from mitochondria in response to activation of cell surface death receptors*. Cell, 1998. **94**: p. 481-490.

27. Yang, E., Zha, J., Jockel, J., Boise, L.H., Thompson, C.B., and Korsmeyer, S.J., *Bad, a heterodimeric partner for Bcl-x_L and Bcl-2, displaces Bax and promotes cell death*. Cell, 1995. **80**: p. 285-291.

28. Goldsmith, K.C., Liu, X., Dam, V., Morgan, B.T., Shabbout, M., Cnaan, A., Letai A., Korsmeyer S.J., and Hogarty, M.D., *BH3 peptidomimetics potently activate apoptosis and demonstrate single agent efficacy in neuroblastoma.* Oncogene, 2006. **25**: p. 4525-4533.

29. Datta, S.R., Dudek, H., Tao, X., Masters, S., Fu, H., Gotoh, Y., and Greenberg, M.E., *Akt phosphorylation of BAD couples survival signals to the cell-intrinsic death machinery*. Cell, 1997. **91**: p. 231-241.

30. Tan, Y., Ruan, H., Demeter, M.R., and Comb, M.J., *$p90^{RSK}$ blocks Bad-mediated cell death via a protein kinase C-dependent pathway*. Journal of Biological Chemistry, 1999. **274**(49): p. 34859-34867.

31. Zhou, X.-M., Liu, Y., Payne, G., Lutz, R.J., and Chittenden, T., *Growth factors inactivate the cell death promoter BAD by phosphorylation of its BH3 domain on Ser^{155}*. Journal of Biological Chemistry, 2000. **275**(32): p. 25046-25051.

32. Peso, L.d., Gonzalez-Garcia, M., Page, C., Herrera, R., and Nunez, G., *Interleukin-3-induced*

phosphorylation of BAD through the protein kinase Akt. Science, 1997. **278**: p. 687-689.

33. Zha, J., Harada, H., Yang, E., Jockel, J., and Korsmeyer, S.J., *Serine phosphorylation of death agonist BAD in response to survival factor results in binding to 14-3-3 not BCL-X_L*. Cell, 1996. **87**: p. 619-628.

34. Wang H.-G., Pathan, N., Ethell, I.M., Krajewski, S., Yamaguchi, Y., Shibasaki, F., McKeon, F., Bobo, T., Franke, T.F., and Reed, J.C., *Ca^{2+}-induced apoptosis through calcineurin dephosphorylation of BAD*. Science, 1999. **284**: p. 339-343.

35. Ayllon, V., Martinez-A, C., Garcia, A., Cayla, X., and Rebollo, A., *Protein phosphatase 1α is a Ras-activated Bad phosphatase that regulates interleukin-2 deprivation-induced apoptosis*. EMBO Journal, 2000. **19**(10): p. 2237-2246.

36. Datta, S.R., Katsov, A., Hu, L., Petros, A., Fesik, S.W., Yaffe, M.B., and Greenberg, M.E., *14-3-3 proteins and survival kinases cooperate to inactivate BAD by BH3 domain phosphorylation*. Molecular Cell, 2000. **6**: p. 41-51.

37. Hirai, I., and Wang, H.-G., *Survival-factor-induced phosphorylation of Bad results in its dissociation from Bcl-x_L but not Bcl-2*. Biochem. J., 2001. **359**: p. 345-352.

38. Rapp, U.R., Fischer, A., Rennefahrt, U.E.E., Hekman, M., and Albert, S., *BAD association with membranes is regulated by Raf kinases and association with 14-3-3 proteins*. Advan. Enzyme Regul., 2007. **47**: p. 281-285.

39. Claerhout, S., Decraene, D., Laethem, A.V., Kelst, S.V., Agostinis, P., Garmyn, M., *AKT delays the early-activated apoptotic pathway in UVB-irradiated keratinocytes via BAD translocation.* Journal of Investigative Dermatology, 2007. **127**: p. 429-438.

40. Strasser, A., Huang, D.C., and Vaux, D.L., Biochim. Biophys. Acta, 1997. **1333**: F151-178.

41. Nechushtan, A., Smith, C.L., Lamensdorf, I., Yoon, S.-H., and Youle, R.J., *Bax and Bak coalesce into novel mitochondria-associated clusters during apoptosis*. Journal of Cell Biology, 2001. **153**(6): p. 1265-1276.

42. Oltvai, Z.N., Milliman, C.L., and Korsmeyer, S.J., *Bcl-2 heterodimerizes in vivo with a conserved homolog, Bax, that accelerates programmed cell death*. Cell, 1993. **74**: p. 609-619.

43. Sedlak, T.W., Oltvai, Z.N., Yang, E., Wang, K., Boise, L.H., Thompson, C.B., and Korsmeyer, S.J., *Multiple Bcl-2 family members demonstrate selective dimerizations with Bax*. Proc. Natl. Acad. Sci., 1995. **92**: p. 7834-7838.

44. Yin, X.M., Oltvai, Z.N., and Korsmeyer, S.J., *BH1 and BH2 domains of Bcl-2 are required for inhibition of apoptosis and heterodimerization with Bax*. Nature, 1994. **369**: p. 321-323.

45. Valentijn, A.J., Metcalfe, A.D., Kott, J., Streuli, C.H., and Gilmore, A.P., *Spatial and temporal changes in Bax subcellular localization during anoikis*. Journal of Cell Biology, 2003. **162**: p. 599-612.

46. Gilmore, A.P., Metcalfe, A.D., Romer, L.H., and Streuli, C.H., *Integrin-mediated survival signals regulate the apoptotic function of Bax through its conformation and subcellular localization*. Journal of Cell Biology, 2000. **149**: p. 431-445.

47. Antonsson, B., *Mitochondria and the Bcl-2 family proteins in apoptosis signaling pathways*. Molecular and Cellular Biochemistry, 2004. **256**/**257**: p. 141-155.

48. Obata, T., Yaffe, M.B., Leparc, G.G., Piro, E.T., Maegawa, H., Kashiwagi, A., Kikkawa, R., and Cantley, L.C., *Peptide and protein library screening defines optimal substrate motifs for AKT/PKB*. Journal of Biological Chemistry, 2000. **275**(46): p. 36108-36115.

49. Zhou G.-L., Zhuo Y., King, C.C., Fryer, B.H., Bokoch, G.M., and Field, J., *Akt phosphorylation of Serine 21 on Pak1 modulates Nck binding and cell migration*. Molecular and Cellular Biology, 2002. **23**(22): p. 8058-8069.

50. Deprez, J., Vertommen, D., Alessi, D.R., Hue, L., and Rider, M.H., *Phosphorylation and activation of heart 6-phosphofructo-2-kinase by protein kinase B and other protein kinases of the insulin signaling cascade*. Journal of Biological Chemistry, 1997. **272**(28): p. 17269-17275.

51. Liu Y., and Storm, D.R., *Dephosphorylation of neuromodulin by calcineurin*. Journal of Biological Chemistry, 1989. **264**(22): p. 12800-12804.

52. Wolff, D.J., and Sved, D.W., *The divalent cation dependence of bovine brain calmodulin-dependent phosphatase*. Journal of Biological Chemistry, 1985. **260**(7): p. 4195-4202.

53. Yaffe, M.B., Rittinger, K., Volinia, S., Caron, P.R., Aitken, A., Leffers, H., Gamblin, S.J., Smerdon, S.J., and Cantley, L.C., *The structural basis for 14-3-3:phosphopeptide binding specificity*. Cell, 1997. **91**: p. 961-971

54. Kuwana, T., Bouchier-Hayes, L., Chipuk, J.E., Bonzon, C., Sullivan, B.A., Green, D.R., and Newmeyer, D.D., *BH3 domains of BH3-only proteins differentially regulate Bax-mediated mitochondrial membrane permeabilization both directly and indirectly*. Molecular Cell, 2005. **17**: p. 525-535.

55. Nicholson, K.M., and Anderson, N.G., *The protein kinase B/Akt signalling pathway in human malignancy*. Cellular Signalling, 2002. **14**: p. 381-395.

56. Zdychova, J. and Komers, R., *Emerging role of Akt kinase/protein kinase B signaling in pathophysiology of diabetes and its complications*. Physiol. Res., 2005. **54**: p. 1-16.

57. Zou, R., and Ghosh, A., *Automated sensitivity analysis of stiff biochemical systems using a fourth-order adaptive step size Rosenbrock integration method*. IEE Proc.-Syst. Biol., 2006. **153**(2): p. 79-90.

58. Ghosh, A., Miller, D., Zou, R., Sokhansanj, H., and Kriete, A., *Integrated spatiotemporal model of cell signaling*, Foundations of Systems Biology in Engineering. (CA, 2005).

59. Ghosh, A., Miller, D., Zou, R., Sokhansanj, H., and Kriete, A., *Computational systems biology* in Ch. Spatio-Temporal Systems. (Elsevier Press, USA, 2005).

60. Ghosh, A., "http://bio.physics.drexel.edu/research.html", all information about CellSim can be found here (2005).

61. Eissing, T., Conzelmann, H., Gilles, E.D., Allgower, F., Bullinger, E., and Scheurich, P., *Bistability analyses of a caspase activation model for receptor-induced apoptosis*. Journal of Biological Chemistry, 2004. **279**(35): p. 36892-36897.

62. Legewie, S., Bluthgen, N., and Herzel, H., *Mathematical modeling identifies inhibitors of apoptosis as mediators of positive feedback and bistability*. PLoS Computational Biology, 2006. **2**(9): p. 1-13.

63. Leis, J.R., and Kramer, M.A., *Sensitivity analysis of systems of differential and algebraic equations*. Comput. Chem. Eng., 1985. **9:** p. 93-96.

64. Pant, D.K., and Ghosh, A., *Automated oncogene detection in complex protein networks, with applications to the MAPK signal transduction pathway*. Biophys. Chem., 2005. **113:** p. 275-288.

65. Eibing, T., Allgower, F., and Bullinger, E., *Robustness properties of apoptosis models with respect to parameter variations and intrinsic noise*. IEE Proc.-Syst. Biol, 2005. **152**(4): p. 221-228.

66. Anderson, D.F., Mattingly, J.C., Nijhout, H.F., and Reed, M.C., *Propagation of fluctuations in biochemical systems, I: linear SSC networks*. Bulletin of Mathematical Biology, 2007. **69**: p. 1791-1813.

67. Gillespie, D.T., *A general method for numerically simulating the stochastic time evolution of coupled chemical reactions*. J. Comput. Phys., 1976. **22**: p. 403-434.

68. Sontag, E.D., *For differential equations with r parameters, 2r + 1 experiments are enough for identification*.

J. Nonlinear Sci., 2002. **12:** p. 553-583

69. Kholodenko, B.N., Kiyatkin, A., Bruggeman, F., Sontag, E.D., Westerhoff, H., and Hock, J., *Untangling the wires: a novel strategy to trace functional interactions in signaling and gene networks*. Proc. Natl. Acad. Sci. USA., 2002. **99:** p. 12841-12846

70. Sontag, E.D., Kiyatkin, A., and Kholodenko, B.N., *Inferring dynamic architecture of cellular networks using time series of gene expression, protein and metabolic data*. Bioinformatics, 2004, in press.

71. Bastin, G., and Levine, J. *On state accessibility in reaction systems*. IEEE Transactions on Automatic Control, 1993. **38**(5)**:** p.733-742.

72. Golovchenko, E.N., Hanin, L.G., Kaufmann, S.H., Tyurin, K.V., Khanin, M.A., *Dynamics of granzyme B-induced apoptosis: mathematical modeling*. Mathematical Biosciences, 2008. **212**: p. 54-68.

73. Aldridge, B.B., Haller, G., Sorger, P.K., and Lauffenburger, D.A., *Direct Lyapunov exponent analysis enables parametric study of transient signaling governing cell behaviour*. IEE Proc.-Syst. Biol., 2006. **153**(6): p. 425-432.

74. Okazaki, N., Asano, R., Kinoshita, T., and Chuman, H., *Simple computational models of type I/type II cells in Fas signaling-induced apoptosis*. Journal of Theoretical Biology, 2008. **250**: p. 621-633.

75. Barkai, N., and Leibler, S., *Robustness in simple biochemical networks*. Nature, 1997. **387**: p. 913-917.

76. Bluthgen, N., and Herzel, H., *How robust are switches in intracellular signaling cascades?* Journal of Theoretical Biology, 2003. **225**: p. 293-300.

77. Goldbeter, A., and Koshland, Jr. D.E., *An amplified sensitivity arising from covalent modification in biological systems*. Proc. Natl. Acad. Sci. USA, 1981. **78**(11)**:** p. 6840-6844.

78. Kim, J., Bates, D.G., Postlethwaite, I., Ma, L., and Iglesias, P.A., *Robustness analysis of biochemical network models*. IEE Proc.-Syst. Biol., 2006. **153**(3): p. 96-104.

79. Sontag, E.D., *Some new directions in control theory inspired by systems biology*. Systems Biology, 2004. **1**(1): p. 9-18.

80. Sontag, E.D., *Asymptotic amplitudes and Cauchy gains: A small-gain principle and an application to inhibitory biological feedback*. Syst. Control Lett., 2002. **47:** p. 167-179.

81. Angeli, D., and Sontag, E.D., *Monotone control systems*. IEEE Trans. Autom. Control, 2003. **48:** p. 1684-1698.

82. Kholodenko, B.N., *Negative feedback and ultrasensitivity can bring about oscillations in the mitogen-activated protein kinase cascades*. Eur. J. Biochem, 2000. **267:** p. 1583-1588.

83. Shvartsman, S.Y., Wiley, H.S., and Lauffenburger, D.A., *Autocrine loop as a module for bidirectional and context-dependent cell signalling*. Preprint. MIT Chemical Engineering Department, 2000.

84. Ptashne, M., "A genetic switch: phage λ and higher organisms" (Cell Press and Blackwell Scientific Publications, Cambridge, MA, 1992).

85. Chen, C., Cui, J., Lu, H., Wang, R., Zhang, S., and Shen, P., *Modeling of the role of a Bax-activation switch in the mitochondrial apoptosis decision*. Biophysical Journal, 2007. **92**: p. 4304-4315.

86. Bagci, E.Z., Vodovotz, Y., Billiar, T.R., Ermentrout, G.B., and Bahar, I., *Bistability in apoptosis: roles of Bax, Bcl-2, and mitochondrial permeability transition pores*. Biophysical Journal, 2006. **90**: p. 1546-1559.

87. Hua, F., Cornejo, M.G., Cardone, M.H., Stokes, C.L., and Lauffenburger, D.A., *Effects of Bcl-2 levels on Fas signaling-induced caspase-3 activation: molecular genetic tests on computational model predictions*. Journal of Immunology, 2005. **175**: p.985-995.

88. Chaves, M., Sontag, E.D., *State-estimators for chemical reaction networks of Feinberg-Horn-Jackson zero deficiency type*. Eur. J. Control, 2002. **8**: p. 343-359.

89. Chaves, M., Sontag, E.D., Dinerstein, R.J., *Steady-states of receptor-ligand dynamics: a theoretical framework*. Journal of Theoretical Biology, 2004. **227**: p. 413-428.

90. Chaves, M., *Input-to-state stability of rate-controlled biochemical networks*. Siam J. Control Optim, 2005. **44**(2): p. 704-727.

91. Chaves, M., *Stability of rate-controlled zero-deficiency networks*. Proceedings of the 45th IEEE Conference on Decision & Control, 2006. p. 5766-5771.

92. Sontag, E.D., *Structure and stability of certain chemical networks and applications to the kinetic proofreading model of T-cell receptor signal transduction*. IEEE Transactions on Automatic Control, 2001. **46**(7): p. 1028-1047.

93. Sontag, E.D., *Correction to "structure and stability of certain chemical networks and applications to the kinetic proofreading model of T-cell receptor signal transduction*. IEEE Transactions on Automatic Control, 2002. **47**(4): p. 705.

94. Sontag, E.D., Mathematical Control Theory. (Springer, NJ, 1998)

95. Feinberg, M., *Lectures on chemical reaction networks*. Notes of lectures given at the Mathematics Research Centre, University of Wisconsin, in 1979.

96. Feinberg, M., *Chemical reaction network structure and the stability of complex isothermal reactors I. The deficiency zero and deficiency one theorems*. Chem. Eng. Sci., 1987. **42**(10): p. 2229-2268.

97. Feinberg, M., *The existence and uniqueness of steady states for a class of chemical reaction networks*. Arch. Rational Mech. Anal., 1995. **132**: p. 311-370.

98. Feinberg, M., *Mathematical aspects of mass action kinetics* in Chemical Reactor Theory: A Review (Prentice-Hall, Inc., NJ, 1977)

99. Horn, F.J.M., and Jackson, R., *General mass action kinetics*. Arch. Rational Mech. Anal., 1972. **47**: p. 81-116

100. Horn, F.J.M., *Necessary and sufficient conditions for complex balancing in chemical kinetics*. Arch. Rational Mech. Anal., 1972. **49**: p. 172-186.

101. Gunawardena, J., *Chemical reaction network theory for in-silico biologists*. Harvard University, 2003. p. 1-25.

102. Guberman, J.M., *Mass action reaction networks and the deficiency zero theorem*. Thesis: Harvard University, 2003. p. 1-45.